SOURCE-AND-SINK METHOD OF SOLUTION OF TWO AND THREE DIMENSIONAL STEFAN PROBLEMS

By

BONGJUN LI

A DISSERTATION PRESENTED TO THE GRADUATE SCHOOL
OF THE UNIVERSITY OF FLORIDA IN PARTIAL FULFILLMENT
OF THE REQUIREMENTS FOR THE DEGREE OF
DOCTOR OF PHILOSOPHY

UNIVERSITY OF FLORIDA

1993

TO MY WIFE YU LUO,
MY DAUGHTER ANGELA,
AND MY PARENTS.

ACKNOWLEDGEMENTS

I would like to express my sincere gratitude and appreciation to Dr. C. K. Hsieh, chairman of the supervisory committee, for his guidance and encouragement throughout my entire graduate study, especially for his patience in revising this manuscript. His enthusiasm and great scholarly attainments have contributed substantially to the quality of this work. I also want to extend my appreciation to Dr. Y. D. Goswami, co-chairman of the supervisory committee, for his continuous support, encouragement and guidance during the research. I would like to thank Dr. W. Shyy, Dr. J. F. Klausner, and Dr. R. Mei for serving on my supervisory committee and for their fruitful comments and suggestions.

I acknowledge my colleagues and fellow graduate students for their friendship and valuable help.

Finally, my deepest gratitude goes to my wife, Yu Lan, for her unselfish love, patience, and understanding, and to my parents for their love, encouragement and support.

TABLE OF CONTENTS

LIST OF TABLES

LIST OF FIGURES

NOMENCLATURE

A	Amplification factor, area
b	Thickness of TES containing wall
B,C	Constants
D	Constant, dimension of PCM in y direction
D_h	Hydraulic diameter
c	Specific heat
d	Weighting function, half width of channel
E	Energy
f	Friction factor
G	Green's function
g	Function defined in Eq. (3.110) etc
H	Dimension of PCM in z-direction
h	Convection heat transfer coefficient
k	Thermal conductivity
L	Latent heat
Nu	Nusselt number
n	Normal direction
J	Bessel function
Pe	Peclet number
Pr	Prandtl number
$\dot{Q}$	Volume flow rate

q	Heat flux
R	Radius
r	Coordinate in cylindrical and spherical systems
R'	Thermal resistance
Re	Reynolds number
S	interface position
Ste	Stefan number
T	Temperature
t	Time
U	Decomposed temperature, mean velocity
V	Decomposed temperature, velocity
W	PCM width
x,y,z	Coordinates in Cartesian system

Greek

α	Thermal diffusivity
β	Eigenvalues in the Green's function
δ	Dirac delta function
ϵ	Small constant
θ	Parameter in finite difference method
μ	Void fraction
Π	Function defined in Eq (3.86)
ρ	Density
τ	Dummy variable of time
Ω	Solution domain

Subscripts and Superscripts

b	Boundary value
cv	Control volume
f	Fluid
i	Boundary index, spatial index
j	Spatial index
l	Liquid phase
m	Melting point
n	Time level index
p	Phase regimes, PCM
s	Solid phase, interface position, sphere
w	Wall, shell

Abstract of Dissertation Presented to the Graduate School
of the University of Florida in Partial Fulfillment of the
Requirements for the Degree of Doctor of Philosophy

SOURCE-AND-SINK METHOD OF SOLUTION OF TWO AND THREE DIMENSIONAL STEFAN PROBLEMS

By

Hongjue Li

December 1993

Chairman: Dr. Cheng K. Hsieh
Cochairman: Dr. Yogi D. Goswami
Major Department: Mechanical Engineering

A source-and-sink method has been developed for the solution of conduction heat transfer with phase change in multiple dimensions. In this method, the heat transfer in one direction is decoupled from the other directions by changing the second partial differential in these directions where the phase change is less dominant to a finite difference form and solving the problem in the other directions with an analytical solution that accounts for the motion of the interface in a phase change problem. The solution developed in this work is thus independent of the equations used to represent the interface as well as the conditions imposed on the boundaries.

The method has been applied to the tracking of single, double, and coalescing interface fronts formed by different phases assuming

equal properties. The method has been demonstrated to be accurate, convergent, and stable by numerical computations as well as experimental measurements. The method has also been applied to the solution of conjugate heat transfer including convection in a fluid medium and conduction in the phase change material, a problem applicable to the analysis of latent heat thermal energy storage systems.

CHAPTER 1
INTRODUCTION

Phase change problems involving melting and freezing have found numerous applications in science and engineering. Phase-change processes are encountered in manufacturing and material processing, and in annealing and continuous casting. In the important area of food processing, phase change has been an integral part of a freezing and thawing process in which one substance can be separated from another by means of a phase change. The latent heat absorbed and released by a substance during a phase change also works favorably in energy storage. Since the latent heat is usually large for some substances, a small volume-to-energy ratio can be achieved. This makes the process particularly attractive for solar energy applications. Recently, with the increased use of lasers in industrial processes such as cutting, drilling, surface hardening and desalfication, the phase change has added another dimension to contemporary research.

Phase-change problems have been commonly referred to as a class of moving boundary problems. In contrast to many conventional physical problems in which the solutions are sought in a fixed domain, the phase change problems are solved in a variable domain

There are two phases in the medium which are separated by a phase-change interface. Under the continuous heat transfer with the surroundings through the boundary, this interface position can change with time. The interface position is unknown a *priori* and must be determined by solving nonlinear equations. The phase-change problems thus pose a real challenge for analysis.

Phase change problems that have been solved in the literature have often been treated with various degrees of simplification. Earliest phase-change analyses have been confined strictly to a heat diffusion study in a domain imposed with boundary conditions that are invariant with position and time. Later methods account for the property variations in different phase regions and for a medium imposed with time-variant conditions. While these are more realistic physically, they also add complexity to the analysis to the extent that these problems can no longer be solved exactly. Particularly noteworthy in the recent development of methods for the solution of phase change coupled with convection and radiation. These problems can only be solved numerically. These numerical methods have recently been further extended for the solution of phase change due to a moving heat front, a problem of great importance in welding and annealing. A detailed literature review is provided in Chapter 2.

Phase-change heat transfer problems can be classified according to the configuration and the formation of the interface in the medium. Thus, in some analyses, the phase change is assumed to occur at a distinct temperature which does not change with time. In such cases,

the solid and liquid regions are separated by a sharp front whose position can be determined rigorously. This permits the interface position to be verified experimentally. In some materials, however, the phase change occurs over a narrow temperature range. Then, the phase change takes place in a mushy zone where the phase change is smoothly dispersed. Probably most intriguing of all is the phase change in alloys. In the alloys, the phase change temperature is not distinct. There is a crystalline-like structure at the interface which is not necessarily smooth or even continuous. In practice, materials with crystalline structure and mushy zone can be analyzed more conveniently with computational approximations. This is not so, however, for a material with a distinct phase change temperature. The interface position in such a material must be determined more rigorously. This interface position can also serve as a basis for evaluation of the accuracy of the analysis.

Phase-change problems that have been solved in the literature are mostly for domains in one dimension. Solutions of two dimensional problems have rarely been attempted. Although an enthalpy method can be used to solve such problems conveniently, that method only works well if the phase change occurs in a mushy zone.

It is thus the purpose of this work to develop a hybrid scheme that employs a finite-difference method in one direction and a source-and-sink method in another direction. The former will be used in the direction where the phase change is less dominant, while the latter will be used in the other direction where the phase change interface

moves rapidly. The source-and-sink method is selected primarily for its convenience and accuracy as demonstrated in slight previous studies (see Usich, 1993; Usich and Choi, 1992a, 1992b; Choi and Usich, 1992; Choi, 1991). As will be shown, the source and sink method only requires one set of equations to solve for temperatures in 'all' phase regions. By contrast, it is necessary to use a set of equations for 'each' phase region in the traditional method of solution by the Neumann-Stefan formulation. The work involved in the solution can thus be reduced considerably for the source-and-sink method. In addition, in the traditional method of solution, the interface Stefan condition must be given as a separate condition, whereas in the source and sink method, this condition has been incorporated into the governing heat diffusion equations. The source and-sink method is thus highly efficient in the solution of the phase change problems.

In the present work, the source-and-sink method is subjected to a rigorous test for its feasibility for superpositions. The method is then used to develop strategies for the solution of the problems in Cartesian, cylindrical, and spherical coordinates. For problems in Cartesian coordinates, the method has been tested analytically for its accuracy for long-time solutions. An apparatus has also been built for experimentally testing its accuracy for short time solutions. In both efforts, the interface positions are used for comparison. Finally, the method has been applied for the analysis of two latent heat, thermal energy storage systems.

This dissertation is divided into six chapters. A brief literature review is provided in Chapter 2. Analytical methods that are related to the solution of phase change in multiple dimensions are compiled in Chapter 3. An experimental setup is described in Chapter 4. The analysis developed in this dissertation is used in a wide range of case studies and their results are presented in Chapter 5. Finally, conclusions and recommendations are given in Chapter 6 to close this dissertation. To facilitate use of the analysis developed in this work, computer programs written in FORTRAN language are compiled in the appendices. It is hoped that the insight gained from this study will contribute to the solution of phase change in multiple dimensions in the future.

CHAPTER 2
REVIEW OF LITERATURE

Study of phase-change problems dates back to 1831 when Lame and Clapeyron (see Rubinstein, 1971) first studied the thickness of the solid crust formed by cooling a liquid under a constant temperature condition. Ever since, the problems have drawn attention from various quarters, and today the phase-change principles have been greatly extended and applied to study various scientific phenomena. The phase-change problems have been studied for over one hundred and sixty years, and the phase change literature has spread over several disciplines. It is thus a daunting task even for a brief review in this chapter. Since the present work strictly deals with the development of a two dimensional, diffusion-driven, phase-change solution scheme that combines an analytical solution in one direction and a numerical solution in another direction, only mathematical methods for diffusion driven phase change are relevant here. It is thus the purpose of this chapter to provide a brief review of the mathematical techniques popular for the solution of phase-change problems by mechanical engineers; see a summary of methods diagramed in Figure 2.1. Interested readers are referred to books and monographs (e.g., Crank, 1984; Yao and Prusa, 1989) for a detailed treatise on the subject.

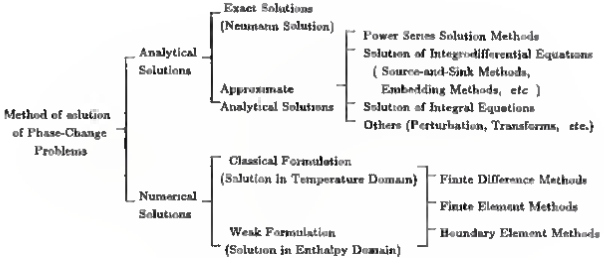

Figure 2 1 Solution methods of Stefan problems

2.1 Analytical Solutions of the Stefan Problems

2.1.1 Exact solutions

In the heat transfer literature, phase-change problems have often been referred to as Stefan problems in recognition of Stefan who first reported the solution of such problems in the open literature in 1889 (Carslaw and Jaeger, 1959). However, it has now been fully settled that the first exact solution of the problems was attributed to Neumann some thirty years earlier. Neumann's work was enunciated in a series of lecture notes that was complete in the sense that it provided derivation not only of the square root time law that governs the motion of the phase-change interface as predicted earlier by Lame and Clapeyron but also of the value of the proportionality constant which was missing in Lame and Clapeyron's work. Thus, for the first time in history, Neumann solved the Stefan problems completely.

Neumann's work is important for the fact that, despite innumerable efforts made by others in search of additional exact solutions after Neumann, Stefan problems that can be solved exactly today remain those that were originally solved by Neumann some one hundred and thirty years ago. Indeed, it has now been firmly established that, for a Stefan problem that can be solved exactly, the problem must be amenable to a similarity transformation. This limits the problems to be solved in an infinite domain, composed of a material of constant phase properties, and imposed with a constant temperature boundary condition.

2.1.2 Approximate analytical solutions

With the great limitations imposed by the exact solution, it is not surprising to see a wide range of approximate solutions developed and discussed in the literature. One of the early approximate methods expands the interface position and the temperature in the medium in terms of a power series or error and complementary error functions. These series are then substituted into the governing equations and boundary conditions to determine the coefficients in the series expansion. Tao used this method in a series of studies. He also extended the method for study of phase change imposed with arbitrary initial and boundary conditions (Tao, 1978, 1980, 1981).

Power series methods find great usefulness in the determination of short-time solutions. At short time, the series converge rapidly; only a few terms are thus sufficient for an accurate solution. However, at long time, more terms are necessary. The methods become tedious and the determination of the coefficients becomes time consuming. They lose their appeal.

Phase-change problems can also be solved by using integrodifferential equations. Lightfoot (1929) developed a moving heat source method for the solution of solidification imposed with a constant temperature boundary condition. In his method, liberation of latent heat due to solidification is taken as a moving heat source. The temperature in the medium is expressed in terms of a Green's function. Since Lightfoot used this method for solving a problem that is possible for an exact solution, the integrodifferential equations

obtained in his work can be solved by a similarity transformation. This leads to results expressed in error and complementary error functions (Crank, 1984). Thus, Lightfoot's integrodifferential solution effectively retrieves Neumann's exact solution.

Using a moving heat source front for solidification naturally leads to the use of a moving heat sink for melting. Lightfoot's method can thus be taken as a source-and-sink method. Chuang and Szekely (1971) have used this method in the development of a numerical scheme for the solution of Stefan problems. Recently, the source-and-sink method has been greatly extended for the solution of Stefan problems imposed with temperature and flux conditions that are either constant or variable with time (Haleh and Choi, 1982a,1982b; Choi and Haleh, 1982). In these efforts, the method has been shown to be highly accurate particularly for solution at long time. It has thus been used to assess the errors in some other solution methods frequently used in the literature. The method has also been applied to the solution of phase change subjected to cyclic temperature and flux conditions (Haleh and Choi, 1982a). In these problems, both melting and freezing fronts appear simultaneously in the medium. Recently, the source-and-sink method has been shown to be equivalent to the boundary element method (Haleh, 1983). This discovery carries promise of broadening the utility of both methods for the solution of heat transfer problems.

An important feature of the source-and-sink method is that the method uses only one set of equations to solve temperatures in 'all' phase regions. By contrast, in the nonconventional methods, one set of

equations is required to solve temperatures in each phase region. Furthermore, in the source-and-sink method, the interface flux condition has been incorporated into the governing equation. The number of equations solved in this method is thus far fewer than with the conventional methods. However, the method works best for a medium of constant and equal properties in different phase regions. For a medium with different property values, double sources and sinks or a combination of the source-and-sink and the boundary element can be used as suggested by Kuiodner (1956) and Haich (1953). However, the equations are lengthened considerably. The method loses its attractiveness.

Integrodifferential equations have also been used by Boley (1974) in the solution of Stefan problems. Following a different approach, Boley embedded the time-variant phase regions into a large domain enclosed by a fixed boundary. The problem can then be solved in a fixed domain. However, since the conditions imposed on the fixed boundary are intended to reproduce the conditions existing on the real physical boundaries including the interface, the conditions on the fixed boundary become unknown. In one case study, Boley (1974) introduced a fictitious flux condition at the fixed boundary. This results in the solution of a system of integrodifferential equations for the unknown flux and the interface position.

Stefan problems can also be solved by a heat balance integral method (Goodman, 1958). Essentially a branch of a large class that is commonly known as the method of weighted residuals, the heat integral

method is convenient to use particularly in the solution of phase change in a medium that is initially at the phase-change temperature (i.e., one-phase problem) and imposed with a time-invariant boundary condition. In this method, the governing equation is changed to an integral form and a trial function (usually polynomials) is used to represent the temperature of the medium. This temperature function is then substituted into the integral equation to solve for the relation of the interface position with time. Since the temperature function must be assumed *a priori*, the accuracy of the solution is related to the appropriateness of this function in the solution. Goodman and Shea (1960) and Yuan (1981) have also applied this method to solve phase change problems with two phase regions.

It has been widely accepted that, in the heat balance integral method, using a higher order polynomial for temperature in the trial function provides no assurance for improvement of accuracy in the solution (Goodman, 1964; Langford, 1973). However, a spatial subdivision has been found to be useful as reported by Noble (1975) and Bell (1978). Bell (1979) has further applied this method to the analysis of solidification around a cylindrical pipe by a Runge-Kutta numerical integration algorithm.

2.1.3 Other approximate solutions

Stefan problems can also be solved by using quasi-steady and quasi-stationary approximations. In the quasi-steady approximation, the unsteady terms in the governing equations are dropped. This

results in a temperature that is good for long-time solution. As for the quasi-stationary approximation, the interface velocity term in the governing equations and the interface condition are all discarded. As such, the interface is rendered stationary. Since the initial condition must still be satisfied, the temperature is good for short-time solution.

In the asymptotic method of solution, these quasi-steady and quasi-stationary limits are used for inner and outer expansions in the constructions of temperature and interface position. Duda and Vrentas (1968) have demonstrated that the quasi-stationary approximation is actually the zeroth order solution of a regular perturbation, which is, indeed, good for a short-time solution. On the other hand, Weinbaum and Jiji (1977) have shown that the lowest order term of a long-time perturbation actually leads to a quasi-steady limit and is thus good for a long-time solution. These perturbation methods work well for small Stefan numbers. Since the mathematics involved in the asymptotic solution is prohibitively tedious, the method is practically useful only for first-order approximations. Solomon (1978) developed an approximate solution for a phase change imposed with a constant heat flux condition. His method follows that of the integral method; however, the energy balance is not preserved in the solution.

Phase-change problems have also been solved by a Fourier transform (Ockendon, 1974). In this method, the Stefan problems are reduced to an initial-value problem. In a similar fashion, a Laplace transform can be used to change the problems into boundary-value

problems. While the transforms are relatively easy to apply, the inversion poses a problem. The inversion process often leads to the solution of integrodifferential equations.

2.1.4 Analytical solutions of two dimensional Stefan problems

Stefan problems that have been solved in the literature are mostly one dimensional. There has been a lack of solutions for two dimensional problems. Poots (1962) extended the heat balance integral method for the solution of phase change in a square prism imposed with a uniform temperature condition. He was able to show that his analytical results were in reasonable agreement with the numerical results obtained earlier by Allen and Severn (1962). Two dimensional Stefan problems can also be solved by using an embedding method as shown by Sikarski and Boley (1965). Following a totally different approach, Mathjea and Jiji (1971) were able to combine Lightfoot's moving heat source method and Patel's treatment of the interface condition (Patel, 1968). They developed an analytical solution for solidification in a two dimensional corner. Sadhia and Kreith (1973) followed essentially the same approach in the analysis of phase change in a planar wedge. In these efforts, the interface position must be assumed a function a *priori* and the constants in this function are determined by substituting the function into integrodifferential equations. The success of the method thus hinges on the use of the proper function in the early stage of solution.

2.2 Numerical Solutions of the Stefan Problem

It is expected that, in the numerical solution, the phase-change problem can be solved by using a finite difference method (FDM), a finite element method (FEM), and a boundary element method (BEM). It is noted that, in the study of heat diffusion without phase change, the problems are usually analyzed in a temperature domain. This is not so, however, for diffusion with phase change as in a Stefan problem. In the Stefan problem, because the phase change interface is unknown a priori and must be determined as a part of the solution, there is an alternative to the solution in the temperature domain: in fact, the problem can be solved more conveniently in an enthalpy domain. The former (solution in temperature domain) requires a classical formulation, while the latter (solution in enthalpy domain) requires a weak formulation. They are briefly reviewed in the sections that follow.

2.2.1 Classical formulation

In the classical formulation, temperature is targeted for solution. The governing equations, the initial and boundary conditions are all expressed in terms of temperature and they are used together in the solution of the interface position as well as the temperature in the medium. This method works well if the interface position is the focus of investigation. As such, the method is useful if the material has a distinct phase-change temperature.

In the solution of the phase change by a classical formulation, it is difficult to track the interface position. Since the predicted interface position may not fall on the grid lines initially set up in the solution, iteration is usually necessary which leads to complexity in the solution. A remedy to this is to use adaptive grids or transformation of variables. In these methods, the interface position is always tied to a grid line or is immobilized in the transformed domain. Furzeland (1980) has made an extensive study for comparisons of numerical methods. Some popular methods have been provided in works by Wilson *et al* (1978) and Crank (1981).

In the numerical solution by the FEM and FDM, the computational grids can be either fixed or time-variant. In the fixed grid method, an interpolation technique is usually necessary at each time step so that the interface positions can be determined accurately (Murray and Landis, 1959; Bostanglu, 1986; Hastaoglu and Bush, 1987). By contrast, in the variable grid method, the grid must be modified at each time step (Gupta and Kumar, 1980,1981). Bonnerot and Jamet (1981) solved a one dimensional Stefan problem by using a third-order accurate finite element method with an adaptive grid. In their work, the computational grid is re-constructed at the end of each time step and the results of the previous time step are mapped onto the new grid by interpolation. These methods are often referred to as front-tracking methods and have been used extensively in the numerical solution of phase-change problems.

An alternative to the fixed grid method is to introduce an appropriate set of space coordinates so that the governing equation and boundary conditions can be transformed from the physical domain to a computational domain. In the computational domain, the interface position rests on a grid line. This method fits into the category of front-fixing or boundary-fixing. Furzeland (1980) and Lacroix and Voller (1990) have made extensive studies for comparison of the fixed-grid method and the transformed-grid method. As expected, when the grid transformation is extended to the solution of phase change in two and three dimensions, the choice of the transformation coordinates, known as body-fitted coordinates, becomes particularly important. It is thus necessary that the interface front curve be smooth and continuous and the number of grid lines between the interface and the boundaries be fixed. Hsu *et al.* (1981) combined the transformation method with an energy conserving finite difference scheme in the analysis of freezing outside a cooled tube. Shyy *et al.* (1992) used body-fitted grids together with an adaptive grid technique in the solution of solidification in continuous casting. Additional numerical solutions by FEM and FEM have been documented in Eberkampf (1976), Saitoh (1978), Pham (1985) and Liang (1983), among others.

2.2.2 Weak formulation

In the weak formulation, the problem are solved in an enthalpy domain. Analogous to the Rankine Hugoniot equation in the shock-wave analysis, the weak formulation can be used to solve phase-change problems without searching for the exact position of the interface. It

in thus superior if the interface position is not targeted for investigation (Elliot and Ockendon 1982, Bouchuron and Smith 1985)

In the enthalpy method, the phase-change interface is determined a posteriori from the numerical solution carried out in a fixed domain. A survey of the recent developments of the enthalpy method has been given in Tanaka and Nakburn (1990) and a detailed formulation of the method can be found in Alexiades and Solomon (1993).

Although the enthalpy methods have been used in the solution of phase change in many engineering problems it is found that these methods work well if the phase change occurs over a mushy zone. For problems with a distinct phase-change temperature, the nonlinearity behavior of the enthalpy near the phase-change temperature presents great numerical difficulties which necessitate the application of an arbitrary smoothing function of the enthalpy (Goodrich, 1978) and suppression of the oscillations in the solution (Voller and Cross, 1983; Shamsundar, 1985, 1986). While these difficulties can be resolved by tracking the interface, it also complicates the solution. Most of all, it defeats the purpose of using the enthalpy method which is intended for bypassing the search for the interface in the first place (Yao and Prusa, 1989)

2.2.3 The boundary element method

Phase-change problems have recently been solved by a boundary element method (BEM) and a combination of BEM and FDM in the BEM, with the use of a time-dependent fundamental solution, only boundary

grids are required in the solution. O'Neill (1983) developed a noniterative boundary element analysis, which permitted the temperature gradients normal to the elements at the phase-change interface to be determined directly in the solution. Zabaras and Mukherjee (1987) developed an iterative implicit algorithm using BEM, which was shown to be free from major time-step limitations. Sadegh *et al.* (1987) applied BEM to the solution of solidification around a buried pipe in a semi-infinite medium with initial superheating. The planar boundary was thus initiated at the surface and propagated inward with time. The BEM has also been applied to the solution of solidification of metal casts in metal or sand molds (Hong *et al* 1984). This problem has also been solved by coupling the boundary element method and the finite difference method in a conjugate heat transfer analysis (Hong *et al* 1984). More recently, two and even three dimensional phase-change problems have been analyzed for laser heating, drilling, and cutting (see, for example Basu and Date, 1990 Sarler *et al* 1991 Reich *et al.* 1992). Reich (1993) showed that the BEM is closely related to the source-and-sink method and their unification is discussed in a great detail

CHAPTER 3
NUMERICAL ANALYSIS

In this chapter, the solution of Stefan problems by a source and sink method (SSM) is presented. To ensure both accuracy and efficiency, a superposition technique with a new time marching scheme is introduced. The validity of the superposition technique for the solution of nonlinear Stefan problems is verified. Finally, the SSM with superposition technique is extended to the solution of multi-dimensional Stefan problems.

3.1 Problem Formulation

3.1.1 Governing equations

Consider a phase-change process that is diffusion driven in a phase change material (PCM) having constant and equal properties in different phase regions. For such a process, the governing equations can be written as

$$\frac{1}{\alpha}\frac{\partial T_p(\vec{r},t)}{\partial t} = \nabla^2 T_p(\vec{r},t), \quad p = s, l, \quad t > t_0, \ \vec{r} \in \Omega \tag{3.1}$$

where the subscripts l and s denote the liquid phase region and solid-phase region, respectively.

The initial and boundary conditions are given as follows:

$$T(\vec{r},t_0) = T_0(\vec{r}) \tag{3.2}$$

$$k_i \frac{\partial T(\vec{r}_i,t)}{\partial n_{bi}} + h_i[T(\vec{r}_i,t) - T_\infty] = q_i, \quad i = 1,2, \tag{3.3}$$

where n_{bi} denotes the outward drawn normal of the ith boundary. For the sake of generality, the initial condition, Eq (3.2), starts at t_0. The boundary condition, Eq (3.3), is also general in that it reduces to the boundary condition of the first kind when k_i and q_i are taken to be zero; it reduces to the boundary condition of the second kind when h_i is taken to be zero.

In addition to the initial and boundary conditions, the interface between the liquid and solid regions is subjected to the temperature and flux conditions known as interface conditions, they are given by the following relations:

$$T_l(\vec{S},t) = T_s(\vec{S},t) = T_m \tag{3.4}$$

$$\frac{\partial T_s(\vec{S},t)}{\partial n} - \frac{\partial T_l(\vec{S},t)}{\partial n} = \frac{\rho L}{k} \frac{d\vec{S}(t)}{dt} \tag{3.5}$$

where n is in the normal direction of the interface. L is the latent heat of fusion ($L>0$ for freezing, $L<0$ for melting). Equation (3.5) is also known as the Stefan condition. It is this flux condition that makes the phase-change problem nonlinear.

3.1.2 Brief review of the SSM

To describe the source-and-sink method, a one dimensional Stefan problem is considered. In this method, the interface condition, Eq (3-5), is incorporated into the governing equation to form an equivalent problem (Hsieh and Choi, 1992a,1992b), which, in one dimensional Cartesian system takes the following form

$$\frac{1}{\alpha}\frac{\partial T}{\partial t}=\frac{\partial^2 T}{\partial x^2}+\frac{L}{k}\frac{dg}{dt}\delta(x-S(t)),\qquad t>t_0,\quad x\in\Omega \tag{3-6}$$

The corresponding initial , boundary, and interface conditions are given as follows

$$T(x,t_0)=T_0(x) \tag{3-7}$$

$$k_i\frac{\partial T(x_i,t)}{\partial n_{bi}}+h_i[T(x_i,t)-T_{\infty i}]=q_i \tag{3-8}$$

$$T(S,t)=T_m \tag{3-9}$$

The general solution of this problem can be expressed in terms of a Green's function as

$$\begin{aligned}T(x,t)=&\int_{\Omega}T_0(x')G(x,t\,|\,x',t_0)dx'\\&+\alpha\int_{\tau=t_0}^{t}\sum_{i=1}[BC_i]d\tau\\&+\frac{L}{k}\int_{\tau=t_0}^{t}\frac{dS(\tau)}{d\tau}G(x,t\,|\,S(\tau),\tau)d\tau\end{aligned} \tag{3-10}$$

In Eq.(3.10), the first term on the right hand side accounts for the contribution of the initial condition, the second term accounts for the boundary conditions, and the third term accounts for the motion of the interface. The expressions for [BC] in the second term vary with the specific condition imposed at the boundary and are listed in Table 3.1.

Table 3.1 Expressions to account for the effects of boundary conditions

Boundary conditions	Expressions for [BC] in Eq.(3.10)
$T(x_b,t) = T_b(t)$	$T_b(\tau)\frac{\partial G(x,t \mid x_b,\tau)}{\partial n_b}$
$\frac{\partial T(x_b,t)}{\partial n_b} = -\frac{q_b(t)}{k_b}$	$-\frac{q_b(\tau)}{k_b}G(x,t \mid x_b,\tau)$
$\frac{\partial T(x_b,t)}{\partial n_b} + \frac{h_b}{k_b}T(x_b,t) = \frac{1}{k_b}H_b(t)$	$\frac{H_b(\tau)}{k_b}G(x,t \mid x_b,\tau)$

Hsieh and Choi (1992a, 1992b) and Choi and Hsieh (1992) used the SSM to solve one dimensional Stefan problems in a semi-infinite domain. In the problems they solved, the medium was initially at a uniform temperature. The boundaries were imposed with constant or time variant temperature and flux conditions. To account for possible initial subcooling or superheating of the order, the solutions were divided into two stages: a pre-melt stage and a phase change stage. The solutions for these stages were then combined into a single equation as

$$T(x\ t) = T_0(x,t) + \bar{H}(t-t_0)\frac{k}{c}\int_{\tau=t_0}^{t} \frac{dS(\tau)}{d\tau} G(x\ t\,|\,S(\tau)\ \tau)d\tau \qquad (3\ 11)$$

where t_0 is the time when phase change took place, and $\bar{H}(t-t_0)$ is the Heaviside function given by

$$\bar{H}(t-t_0) = \begin{cases} 0 & \text{for } t < t_0 \\ 1 & \text{for } t \geq t_0 \end{cases}$$

Since the initial temperature was uniform, the first term on the right hand side of (3.11) could be expressed in a compact form as

$$T_0(x\ t) = \frac{\sqrt{\alpha}}{\sqrt{\pi}} \int_{\tau=t_0}^{t} \frac{E(\tau)}{(t-\tau)^{1/2}}\, e^{-\frac{x^2}{4\alpha(t-\tau)}} d\tau \qquad (3.12)$$

where

$$E(\tau) = \begin{cases} \frac{x}{2\alpha}\frac{T_b(\tau)}{\tau} & \text{for the first-kind boundary condition} \\ \frac{1}{\alpha} T_b(\tau) & \text{for the second kind boundary condition} \end{cases}$$

In practice, since the interface position is unknown *a priori*, Eq (3.11) must be solved numerically. In this effort, the entire time range is divided into small time intervals, Δt, over which numerical integration is performed as

$$\int_{\tau=t_0}^{t} F(\tau)d\tau = \sum_{n=1}^{N} \int_{t^{n-1}}^{t^n} F(\tau)d\tau \qquad (3\ 13)$$

where $t^N = t$ and $t^n = t_0 + (n-1)\Delta t$. One of the advantages of this numerical method is that its accuracy does not degrade with time. Large errors only occur over the first few time steps and they diminish rapidly with time. Accurate results can thus be obtained with this method. However, since the time integration always traces back to the initial condition at t_0, the effort of computation may be considerable particularly at long time.

3.1.3 Time marching method

Another approach to the solution of Eq (3.11) is the use of a time marching scheme. In this approach, the solution is expressed as

$$T(x\,t^{n+1}) = \int_{\Omega} T(x\,t^n) G(x\,t^{n+1} \mid x'\,t^n)\,dx'$$
$$+ \frac{\sqrt{\alpha}}{\sqrt{\pi}} \int_{\tau=t^n}^{t^{n+1}} \frac{E(\tau)}{(t^{n+1}-\tau)^{1/2}}\, e^{\frac{-x^2}{4\alpha(t^{n+1}-\tau)}}\,d\tau$$
$$+ \frac{L}{c} \int_{\tau=t^n}^{t^{n+1}} \frac{dS(\tau)}{d\tau} G(x\,t^{n+1} \mid S(\tau)\,\tau)\,d\tau \qquad (3.14)$$

The time integration is thus evaluated one step at a time, and the temperature evaluated at each time step serves as the initial condition for the succeeding time step and it moves on with time. For this method, a domain integral emerges as the first term on the right. In this term, the temperature at time t^n is $T(x\,t^n)$ which is nonuniform. A numerical integration must therefore be performed, giving rise to additional computational effort. It also degrades the accuracy, which

is particularly pronounced when the domain for integration extends to infinity

3.2 SSM With Superposition Techniques

To alleviate the problems stated in the preceding section, a superposition method with a new time marching scheme is developed. Before addressing this method, the validity of the superposition method for the solution of nonlinear Stefan problems is critically analyzed.

3.2.1 The validity of the superposition method

The superposition method has been widely used in the solution of linear boundary value problems. Although this method has also been applied to the solutions of nonlinear Stefan problems, its validity has never been established. For the case of derivation in what follows it is assumed that the domain is one dimensional. The PCM has constant and equal property values in different phase regions. Thus, the governing equations are all linear. The initial and boundary conditions are also linear if the radiation effect is incorporated into the convection effect by means of an overall heat transfer coefficient. The only nonlinear relation comes from the interface flux condition. It is thus necessary to decompose this condition if the superposition method is to be applied to the solution of the Stefan problem.

To start the derivation, a small constant ϵ is introduced such that, for a melting problem,

$$T_l(S,t)=T_l(S,t), \qquad T(S+\epsilon,t)-T_s(S,t) \tag{3.15}$$

As ϵ approaches zero,

$$\lim_{\epsilon\to 0} T(S\pm\epsilon,t)=T_m$$

By definition, the differential of T at x equal to S can be recast as

$$\left.\frac{dT}{dt}\right|_{x=S}=\left.\frac{\partial T(S\pm\epsilon,t)}{\partial x}\right|_{x=S}\left.\frac{dx}{dt}\right|_{x=S}+\left.\frac{\partial T(S\pm\epsilon,t)}{\partial t}\right|_{x=S}=0 \tag{3.16}$$

where, on the right hand side, the partial differentials are to be evaluated in the same phase region. That is to say, a $S+\epsilon$ in $\partial T/\partial x$ is to be followed by a $S+\epsilon$ in $\partial T/\partial t$. Then dS/dt can be expressed as

$$\frac{dS}{dt}=-\left.\frac{\partial T(S\pm\epsilon,t)/\partial t}{\partial T(S\pm\epsilon,t)/\partial x}\right|_{\epsilon\to 0} \tag{3.17}$$

Substituting (3.17) into (3.5) changes the interface condition to the following

$$\left[\frac{\partial T_s}{\partial x}-\frac{\partial T_l}{\partial x}\right]_{x=S}=-\frac{\rho|L|}{k}\left.\frac{\partial T(S\pm\epsilon,t)/\partial t}{\partial T(S\pm\epsilon,t)/\partial x}\right|_{\epsilon\to 0} \tag{3.18}$$

which is clearly nonlinear.

An alternative form of Eq. (3.17) can be derived by writing it in both solid and liquid regions and equating their results as

$$\left.\frac{dS}{dt}=\frac{\partial T(S+\epsilon,t)/\partial t}{\partial T(S+\epsilon,t)/\partial x}\right|_{\epsilon\to 0}=-\left.\frac{\partial T(S-\epsilon,t)/\partial t}{\partial T(S-\epsilon,t)/\partial x}\right|_{\epsilon\to 0} \tag{3.19}$$

which can be recast as

$$\left.\frac{\partial T(S-\epsilon,t)}{\partial x}\right|_{\epsilon\to 0} = \left\{\frac{\partial T(S-\epsilon,t)}{\partial t}\left[\frac{\partial T(S+\epsilon,t)/\partial x}{\partial T(S+\epsilon,t)/\partial t}\right]\right\}_{\epsilon\to 0} \tag{3.20}$$

Since for the Stefan problem

$$\left[\frac{\partial T(S+\epsilon,t)}{\partial x} - \frac{\partial T(S-\epsilon,t)}{\partial x}\right]_{\epsilon\to 0} \neq 0 \tag{3.21}$$

because of the flux jump at the interface, one can multiply the numerator and denominator of Eq (3.17) by the partial differential difference appearing on the left hand side of (3.21) as

$$\frac{dS}{dt} = -\left[\frac{\partial T(S+\epsilon,t)/\partial t}{\partial T(S+\epsilon,t)/\partial x}\,\frac{\partial T(S+\epsilon,t)/\partial x - \partial T(S-\epsilon,t)/\partial x}{\partial T(S+\epsilon,t)/\partial x - \partial T(S-\epsilon,t)/\partial x}\right]_{\epsilon\to 0} \tag{3.22}$$

Then, expanding the product in the numerator of the fractions in this equation and introducing (3.20) and canceling out terms enable the following relation to be derived

$$\frac{dS}{dt} = -\left.\frac{\partial T(S+\epsilon,t)/\partial t - \partial T(S-\epsilon,t)/\partial t}{\partial T(S+\epsilon,t)/\partial x - \partial T(S-\epsilon,t)/\partial x}\right|_{\epsilon\to 0} \tag{3.23}$$

Equation (3-18) can then be expressed as

$$\left[\frac{\partial T_g}{\partial x} - \frac{\partial T_l}{\partial x}\right]_{x=S} = -\frac{\rho L}{k}\left[\frac{\partial T(S+\epsilon,t)/\partial t - \partial T(S-\epsilon,t)/\partial t}{\partial T(S+\epsilon,t)/\partial x - \partial T(S-\epsilon,t)/\partial x}\right]_{\epsilon\to 0} \tag{3.24}$$

These equations will now be used to validate the use of the superposition principle in the solution. In this effort, the

temperature is decomposed into a linear part U and a nonlinear part V such that $T(x,t) = U(x,t) + V(x,t)$. For the diffusion problem solved, U is a smooth function of x and t. It thus has continuous first derivatives even at the interface, given by the relation

$$\frac{\partial U(S+\epsilon,t)}{\partial x} - \frac{\partial U(S-\epsilon,t)}{\partial x} = \frac{\partial U(S+\epsilon,t)}{\partial t} - \frac{\partial U(S-\epsilon,t)}{\partial t} = 0 \qquad \text{as } \epsilon \to 0 \tag{3.25}$$

Equations (3.23) and (3.24) can then be reduced to

$$\frac{dS}{dt} = -\left.\frac{\partial V(S+\epsilon,t)/\partial t - \partial V(S-\epsilon,t)/\partial t}{\partial V(S+\epsilon,t)/\partial x - \partial V(S-\epsilon,t)/\partial x}\right|_{\epsilon \to 0} \tag{3.26}$$

$$\left[\frac{\partial V_2}{\partial x} - \frac{\partial V_1}{\partial x}\right]_{x=S} = \frac{\rho_1 L_1}{k} \frac{dS(t)}{dt} \tag{3.27}$$

Equations (3.26) and (3.27) show clearly that U can be totally removed from the interface flux conditions; only the V problem has a nonlinear condition at the interface. The key point in the superposition method is that the U problem is linear and smooth at the interface, while the V problem is nonlinear which contains all the features characteristic of the Stefan problem.

It is noted that the derivation above can be easily extended to the solution of multi-dimensional Stefan problems. The derivation also illustrates well that the superposition principle is only valid for situations when the PCM has constant and equal properties in different regions.

3.2.2 Solution method

To describe the solution procedure, a general one dimensional Stefan problem is taken for analysis. For this problem, the governing equation is given by the relation

$$\frac{1}{\alpha}\frac{\partial T}{\partial t}=\frac{1}{x^d}\frac{\partial}{\partial x}\left(x^d\frac{\partial T}{\partial x}\right), \qquad t>t_0, \quad x\in\Omega \tag{3.28}$$

where x^d is the Sturm-Liouville weighting function, given as follows

$$d=\begin{cases}0 & \text{slab}\\ 1 & \text{cylinder}\\ 2 & \text{sphere}\end{cases}$$

The initial, boundary, and interface temperature and flux conditions are, respectively,

$$T(x\ t_0)=T_0(x) \tag{3.29}$$

$$k_i\frac{\partial T(x_i,t)}{\partial n_{bi}}+h_i[T(x_i,t)-T_\infty]=q_i \tag{3.30}$$

$$T(S\ t)=T_m \tag{3.31}$$

$$\left[\frac{\partial T_s}{\partial x}-\frac{\partial T_l}{\partial x}\right]_{x=S}=\frac{\rho|L|}{k}\frac{dS(t)}{dt} \tag{3.32}$$

Application of the superposition as described in the preceding section leads to the solution of two problems in which the linear problem $U(x,t)$ satisfies the following equations

$$\frac{1}{a}\frac{\partial U}{\partial t}=\frac{1}{x^d}\frac{\partial}{\partial x}\left(x^d\frac{\partial U}{\partial x}\right),\qquad t>t_0,\quad x\in\Omega \tag{3.33}$$

$$U(x,t_0)=T_0(x) \tag{3.34}$$

$$k_i\frac{\partial U_i}{\partial n_i}+h_i(U_i-T_{oi})=q_i \tag{3.35}$$

In this problem, Eq (3.25) is satisfied implicitly because of the smoothness of U

Correspondingly, the $V(x,t)$ problem satisfies the following relations

$$\frac{1}{a}\frac{\partial V}{\partial t}=\frac{1}{x^d}\frac{\partial}{\partial x}\left(x^d\frac{\partial V}{\partial x}\right),\qquad t>t_0,\qquad x\in\Omega \tag{3.36}$$

$$V(x,t_0)=0 \tag{3.37}$$

$$k_i\frac{\partial V_i}{\partial n_i}+h_iV_i=0 \tag{3.38}$$

$$V_f(S,t)=V_s(S,t)=T_m-U(S,t) \tag{3.39}$$

$$\left[\frac{\partial V_s}{\partial x}-\frac{\partial V_f}{\partial x}\right]_{x=S}=\frac{\rho|L|}{k}\frac{dS(x)}{dt} \tag{3.40}$$

The U-problem, being linear, can be solved exactly by established methods, such as separation of variables or integral transformations. However, these analytical solutions often lead to

infinite series of trigonometric or Bessel functions, which are slow to converge. In addition, the eigenvalues must often be found numerically. For these reasons, the analytical solutions may be impractical. Use will therefore be made of a numerical solution by a finite difference method (FDM) for the solution of the U-problem.

To solve the V problem, the source-and sink method is employed. Following Hsieh and Choi (1982a), the interface condition (3.40) is incorporated into the governing equation (3.36) to form an equivalent problem as follows

$$\frac{1}{\alpha}\frac{\partial V}{\partial t}=\frac{1}{x^d}\frac{\partial}{\partial x}\left(x^d\frac{\partial V}{\partial x}\right)+\frac{L_f}{\rho c}\frac{dS}{dt}\,\delta(x-S(t)),\quad t>t_0,\ x\in\Omega \tag{3.41}$$

This equation can be solved in terms of the Green's function. In this effort, since the initial and boundary conditions are all homogeneous (see Eqs (3.37) and (3.38)), the V problem can be solved as

$$V(x,t)=\frac{L_f}{\rho c}\int_{\tau=t_0}^{t}\frac{dS(\tau)}{d\tau}S^d(\tau)G(x,t|S(\tau),\tau)d\tau \tag{3.42}$$

Application of the interface condition, Eq (3.39), gives a relation

$$T_m-U(S,t)=\frac{L_f}{c}\int_{\tau=t_0}^{t}\frac{dS(\tau)}{d\tau}\,S^d(\tau)G(S(t),t|S(\tau),\tau)d\tau \tag{3.43}$$

which is to be solved implicitly for the interface position in this effort, it is noted that, if S is located at a grid point, $U(S,t)$ can be directly obtained from the finite difference solution. Otherwise, a cubic spline will be used to determine U at point S.

The solution procedure can now be stated as follows. For each time step after phase change, the T-problem is decomposed into a U-problem and a V-problem. The U-problem satisfies the nonhomogeneous initial and boundary conditions (see Eqs (3.33) through (3.35)), while the V-problem satisfies homogeneous initial and boundary conditions together with interface conditions (see Eqs (3.36) through (3.40)). In the solution, it is convenient to use (3.41) as the governing equation for the V problem, which incorporates (3.36) and (3.40), a reduction of one equation. Then the U-problem is solved first by FDM. The V problem is solved next by SSM. These solutions are then superimposed and this is done for each time step. In this method, the temperature evaluated at the new time level will be used as the initial condition for the U-problem at the next time level and it moves incrementally with time until the desired time is reached. A summary of the procedure can be given as follows:

(1) Start from an initial condition $T_0(x)$ and set $n=1$,

(2) Set $t_0=t^n, t=t^{n+1}$ and solve Eq (3.33) for $U(x,t^{n+1})$,

(3) Solve Eq (3.43) for $S(t^{n+1})$,

(4) Calculate $V(x,t^{n+1})$ from Eq (3.42),

(5) Find $T(x,t^{n+1})=U(x,t^{n+1})+V(x,t^{n+1})$,

(6) Set $T_0(x)=T(x,t^{n+1})$, $n=n+1$, and repeat (2) to (6).

An important feature in this solution method is that the integral in $V(x,t)$ (see Eq (3.42)) is evaluated one step at a time and

the V-problem always starts with homogeneous initial and boundary conditions. No domain integration is thus involved. Since a time marching scheme is employed, the method is equally efficient and accurate for short time as well as for long time.

In the numerical evaluation of the integrals in Eqs. (3.42) and (3.43), a multi-point Gauss Quadrature formula is used. With sufficiently small time steps, the interface velocity can be approximated as

$$\frac{dS(\tau)}{d\tau} \simeq \frac{S(t^{n+1}) - S(t^n)}{\Delta t} \tag{3.44}$$

where $t^n \leq \tau < t^{n+1}$ and $\Delta t = t^{n+1} - t^n$. Then, only one unknown $S(t^{n+1})$ appears in Eq. (3.43). This unknown can be found by using a root-finding method. To insure a fast and convergent solution of this method, a conjugate Newton-Raphson and bisection method is employed. It is expected that, for problems imposed with a sudden change of temperature at the boundary, the interface velocity $\frac{dS}{dt}$ tends to be infinity at time equal to t_0. A large error may thus result if a finite and constant velocity is assumed in the first time step (see also Hsieh and Chen, 1982a). To reduce this error, a slow-start procedure is used in which the time step is treated as a variable. It starts with a very small value and increases gradually with time until it reaches a preset upper bound. In this way, the errors can be reduced considerably.

3.3 Solutions of One dimensional Stefan Problems

The analysis given in the preceding section will now be used to solve one dimensional Stefan problem examples in Cartesian, cylindrical, and spherical systems. For the examples in Cartesian system, both semi-infinite and finite domain (plan slab) will be solved, whereas in the cylindrical and spherical systems, only finite domain of the cylinders and spheres will be considered. For these examples, the governing equation, initial, boundary, and interface conditions have been given as Eqs (3.28) through (3.32). The U and V problems are formulated as Eqs (3.33) through (3.40). The V problem has been solved using the equivalent problem (3.41) with the result given as (3.42). The interface position is to be solved using (3.43). Solutions for these examples are now compiled in the subsections that follow.

3.3.1 Solutions in one dimensional Cartesian system

U-problem

The governing equation for the U-problem in a Cartesian system can be obtained from Eq (3.33) by setting d equal to zero. To ensure numerical stability for all time steps, an implicit finite difference method is used with the results given as follows:

$$-\theta_x U_{j-1}^{n+1} + (1+2\theta_x) U_j^{n+1} - \theta_x U_{j+1}^{n+1} = U_j^n \tag{3.45a}$$

or

$$\tfrac{1}{2}\theta_x U_{j-1}^{n+1} + (1+\theta_x) U_j^{n+1} - \tfrac{1}{2}\theta_x U_{j+1}^{n+1} = \tfrac{1}{2}\theta_x U_{j-1}^n + (1-\theta_x) U_j^n + \tfrac{1}{2}\theta_x U_{j+1}^n \tag{3.45b}$$

where $\theta_x = \alpha \Delta t / \Delta x^2$. Here, the superscript n refers to the time level and

the subscript j refers to the nodal point location. Thus

$$U_j^n = U(x_j t^n), \qquad U_{j\pm1}^{n+1} = U(x \pm \Delta x, t^{n+1})$$

Notice that Eq. (3.45a) is second-order accurate in space and first order accurate in time and is often referred to as the simple implicit method. Equation (3.45b), however, is second-order accurate in both space and time and is commonly known as the Crank-Nicolson method. Both methods have been well established and are unconditionally stable for all time steps. These equations can be solved by using a tridiagonal system of linear algebraic equations with a simple forward- and backward-substitution, an efficient numerical procedure.

V-problem

The solution of the V-problem can be directly obtained from Eq. (3.42) by setting d to zero. For simplicity sake, let t^n be t_0 and t^{n+1} be t_1. Thus at the end of the first time step,

$$V(x, t^{n+1}) = V(x, t_1) = \frac{L}{\tau} \int_{\tau=t_0}^{t_1} \frac{\partial S(\tau)}{\partial \tau} G(x, t_1 | S(\tau), \tau) d\tau \tag{3.46}$$

For the PCM in a semi-infinite domain, the Green's function is given by

$$G(x, t_1 | x', \tau) = \frac{1}{\sqrt{4\pi\alpha(t_1 - \tau)}} \left\{ e^{\frac{-|x-x'|^2}{4\alpha(t_1-\tau)}} \pm e^{\frac{-(x+x')^2}{4\alpha(t_1-\tau)}} \right\} \tag{3.47}$$

where the plus (+) and minus (-) signs inside the brackets are to be used for flux (second-kind) and temperature (first-kind) conditions at the boundary, respectively.

A close examination of the Green's function in (3.47) reveals that a singularity is located at $\tau = t_1$. This singularity may degrade the accuracy of the numerical integration and can be resolved by introducing a transformation

$$\eta = \sqrt{4\alpha(t_1 - \tau)} \tag{3.48}$$

so that Eq. (3.46) is changed to

$$V(x,t_1) = \frac{I}{c}\frac{dS}{dt}\int_{\eta=0}^{\sqrt{4\alpha\Delta t}} \frac{1}{2\sqrt{\pi}\alpha}\left[e^{-\frac{(x-S)^2}{\eta^2}} \pm e^{-\frac{-(x+S)^2}{\eta^2}}\right] d\eta \tag{3.49}$$

For the PCM is a finite domain, such as a plan slab ($0 \le x \le H$), the Green's function varies with the boundary conditions. For a temperature condition imposed at $x = 0$, the Green's function is independent of the condition at $x = H$ and can be derived as

$$G(x,t\,|\,x',\tau) = \sum_{n=1}^{\infty}\frac{2}{H} e^{-\alpha\beta_n^2(t-\tau)}\sin(\beta_n x)\sin(\beta_n x') \tag{3.50}$$

However,

$$\beta_n = \begin{cases} \dfrac{n\pi}{H}, & \text{for a temperature condition at } x = H, \\ \dfrac{(2n-1)\pi}{2H}, & \text{for a flux condition at } x = H \end{cases}$$

On the other hand, for a flux condition imposed at $x = 0$, the Green's function is given by

$$G(x\ t|x'\ \tau)=C_n+\sum_{n=1}^{\infty}\frac{2}{H}\ e^{-\alpha\beta_n^2(t\ \tau)}\cos(\beta_n x)\cos(\beta_n x') \qquad 3.5$$

where

$$\beta_n=\begin{cases}\dfrac{(2n-1)\pi}{2H}, & \text{for a temperature condition at } x=H\\[2ex] \dfrac{n\pi}{H}, & \text{for a finx condition at } x=H\end{cases}$$

and

$$C_n=\begin{cases}0, & \text{for a temperature condition at } x=H\\[2ex] \dfrac{1}{H}, & \text{for a flux condition at } x=H\end{cases}$$

In practice, when the Green's functions are substituted into Eq. (3.46), a tedious and time consuming algorithm will be necessary to evaluate the integral because of the repetitive computation of the infinite series. However, by assuming a constant interface velocity from t_0 to t_1, Eq. (3.46) can be simplified to the following forms (see Appendix A for derivation):

$$V(x,t_1)=\frac{2L}{Hc}\sum_{n=1}^{\infty}B_n(t_1)\sin(\beta_n x) \qquad (3.52)$$

for a temperature condition imposed at $x=0$, and

$$V(x,t_1)=C_o\frac{L}{c}\frac{dS}{dt}\Delta t+\frac{2L}{Hc}\sum_{n=1}^{\infty}C_n(t_1)\cos(\beta_n x) \qquad (3.53)$$

for a flux condition imposed at $x=0$. In these equations

$$B_n(t_1)=\frac{v}{(\alpha\beta_n^2)^2+(\beta_n v)^2}\left\{(\alpha\beta_n^2)\sin(\beta_n S_1)-(\beta_n v)\cos(\beta_n S_1)\right.$$

$$\left.-e^{-\alpha\beta_n^2\Delta t}\left[(\alpha\beta_n^2)\sin(\beta_n S_0)-(\beta_n v)\cos(\beta_n S_0)\right]\right\} \qquad (3\text{-}54)$$

and

$$C_n(t_1)=\frac{v}{(\alpha\beta_n^2)^2+(\beta_n v)^2}\left\{(\alpha\beta_n^2)\cos(\beta_n S_1)+(\beta_n v)\sin(\beta_n S_1)\right.$$

$$\left.-e^{-\alpha\beta_n^2\Delta t}\left[(\alpha\beta_n^2)\cos(\beta_n S_0)+(\beta_n v)\sin(\beta_n S_0)\right]\right\} \qquad (3\text{-}55)$$

Here, in both equations, $S_0=S(t_0)$, $S_1=S(t_1)$, and $v=dS/dt$.

3.3.2 Solutions in cylindrical coordinate system

U problem

The governing equation for the U problem in a cylindrical system can be obtained from Eq. (3.33) by setting d equal to unity. An implicit finite difference solution for this problem can be derived as

$$(\theta_x-\theta'_x)U_{j-1}^{n+1}+(1+2\theta_x)U_j^{n+1}-(\theta_x+\theta'_x)U_{j+1}^{n+1}=U_j^n, \qquad \text{if } x\neq 0 \qquad (3\text{-}56)$$

and

$$(1+4\theta_x)U_j^{n+1}-4\theta_x U_{j+1}^{n+1}=U_j^n, \qquad \text{if } x=0 \qquad (3\text{-}57)$$

Here, $\theta'_x=\alpha\Delta t/(2x\Delta x)$ and θ_x has been defined previously. These equations can then be solved by using the same tridiagonal solver mentioned previously.

V-problem:

The solution of the *V*-problem can be obtained by setting d equal to unity in Eq. (3.42). Then,

$$V(x,t_1)=\frac{1}{c}\int_{\tau=t_1}^{1}\frac{dS(\tau)}{d\tau}S(\tau)G(x,t_1|S(\tau),\tau)d\tau \qquad (3.58)$$

The Green's function for a solid cylinder ($0\le x\le R_c$) with a temperature condition imposed on the boundary at R_c is given by the relation

$$G(x\,t_1|x',\tau)=\frac{2}{R_c^2}\sum_{n=1}^{\infty}e^{-\alpha\beta_n^2(t_1-\tau)}\frac{J_0(\beta_n x')}{J_1^2(\beta_n R_c)}J_0(\beta_n x) \qquad (3.59)$$

where J_0 and J_1 are Bessel functions of the first kind of order zero and one, respectively. The eigenvalues β_n are roots of

$$J_0(\beta_n R)=0 \qquad n=1,2,3 \qquad (3.60)$$

3.3.3 Solutions in spherical coordinate system

U-problem

The governing equation for the *U* problem in a spherical system can be obtained from Eq. (3.33) by setting d equal to two. An implicit finite difference solution for such a problem can be derived as

$$-(\theta_x-2\theta'_x)U_{j-1}^{n+1}+(1+2\theta'_x)U_j^{n+1}-(\theta_x+2\theta'_x)U_{j+1}^{n+1}=U_j^n, \quad \text{if } x\neq 0 \qquad (3.61)$$

and

$$(1+6\theta'_x)U_1^{n+1}-6\theta'_xU_{j+1}^{n+1}=U_j^n, \quad \text{if } x=0 \qquad (3.62)$$

where θ_g and θ'_g have been defined previously. These equations can also be solved by using the tridiagonal solver.

V-problem

For a problem in spherical system, the solution of V can be obtained directly from Eq (3.42) by setting δ equal to two. This gives

$$V(x,t_1)=\frac{t_1}{\int_{\tau=t_0}}\frac{dS(\tau)}{d\tau}S^2(\tau)G(x,t_1|S(\tau),\tau)d\tau \qquad (3.63)$$

The Green's function for a solid sphere ($0\le r\le R_g$) is

$$G(x,t_1|x'\tau)=\frac{1}{xx'}\sum_{n=1}^{\infty}\frac{1}{N}e^{-\alpha\beta_n^2(t_1-\tau)}\sin(\beta_n x')\sin(\beta_n x) \qquad (3.64)$$

For a temperature condition imposed on the spherical surface,

$$\frac{1}{N}=\frac{2}{R_g} \qquad \beta_n=\frac{n\pi}{R_g} \qquad (3.65)$$

On the other hand, for a mixed condition imposed on the surface,

$$\frac{1}{N}=\frac{2(\beta_n^2+K^2)}{R_g(\beta_n^2+K^2)+K} \qquad (3.66)$$

where β_ns are roots of

$$\beta_n\cot(\beta_n R_g)+K=0 \qquad (3.67)$$

and $K=\frac{h}{k}-\frac{1}{R_g}$

The solution for the V-problem can also be simplified to the following form (see Appendix B for derivation):

$$V(x,t_1)=\frac{L}{2x}\sum_{n=1}^{\infty}\frac{D_n(t_1)}{N}\sin(\beta_n x) \tag{3.68}$$

where

$$D_n(t_1)=\frac{v}{(\alpha\beta_n^2)^2+(\beta_n v)^2}\left\{\alpha\beta_n^2\left[S_1\sin(\beta_n S_1)-S_{n\ell}e^{-\alpha\beta_n^2\Delta t}\sin(\beta_n S_n)\right]\right.$$
$$\left.-(\beta_n v)\left[S_1\cos(\beta_n S_1)-S_{n\ell}e^{-\alpha\beta_n^2\Delta t}\cos(\beta_n S_n)\right]\right\}$$
$$-\frac{v^2}{[(\alpha\beta_n^2)^2+(\beta_n v)^2]^2}\left\{\left[(\alpha\beta_n^2)^2-(\beta_n v)^2\right]\left[\sin(\beta_n S_1)-e^{-\alpha\beta_n^2\Delta t}\sin(\beta_n S_n)\right]\right.$$
$$\left.-2\alpha\beta_n^2 v\left[\cos(\beta_n S_1)-e^{-\alpha\beta_n^2\Delta t}\cos(\beta_n S_n)\right]\right\} \tag{3.69}$$

3.3.4 Multiple Interfaces

The method developed above can also be applied to the solution of problems involving multiple interfaces. In this case, the solution of the U-problem remains unchanged. However, the solution of the V-problem can be obtained by using multiple sources and sinks. The equivalent governing equation for this problem is

$$\frac{1}{\alpha}\frac{\partial V}{\partial t}=\frac{1}{x^2}\frac{\partial}{\partial x}\left(x^2\frac{\partial V}{\partial x}\right)+\sum_{p=1}^{M}\frac{L}{\Delta t}\frac{dS_p}{dt}\,\delta(x-S_p(t)) \tag{3.70}$$

where M is the number of interfaces. The general solution of this equation is

$$V(x,t_1) = \sum_{p=1}^{M} \frac{k}{\ell} \int_{\tau=t_0}^{t_1} \frac{dS_p(\tau)}{d\tau} S_p^d(\tau) G(x,t_1|S_p(\tau),\tau)\,d\tau \tag{3.71}$$

Here, the interface positions are determined by solving the following nonlinear equations simultaneously

$$\begin{aligned}
T_m - U(S_1,t_1) &= \sum_{p=1}^{M} \frac{k}{\ell} \int_{\tau=t_0}^{t_1} \frac{dS_p(\tau)}{d\tau} S_p^d(\tau) G(S_1,t_1|S_p(\tau),\tau)\,d\tau \\
T_m - U(S_2,t_1) &= \sum_{p=1}^{M} \frac{k}{\ell} \int_{\tau=t_0}^{t_1} \frac{dS_p(\tau)}{d\tau} S_p^d(\tau) G(S_2,t_1|S_p(\tau),\tau)\,d\tau \\
&\vdots \\
T_m - U(S_M,t_1) &= \sum_{p=1}^{M} \frac{k}{\ell} \int_{\tau=t_0}^{t_1} \frac{dS_p(\tau)}{d\tau} S_p^d(\tau) G(S_M,t_1|S_p(\tau),\tau)\,d\tau
\end{aligned} \tag{3.72}$$

3.3.5 Stability analysis

Stability and convergency are essential to numerical solutions. For most problems, the stability and convergency tests are limited to the analysis of linear equations, which, hopefully, provides trends for the projection of nonlinear equations. An alternative to this approach is the use of a numerical experiment. In this subsection, the stability of the linearized Stefan problem in one dimensional Cartesian system will be analyzed. Numerical tests for stability will be relegated to Chapter 5 where concrete examples will be examined.

Following the Von Neumann stability analysis, a small disturbance of T is defined at time level n so that

$$T^n = \bar{T}^n + \epsilon^n \tag{3.73}$$

where the bar denotes the exact solution and ϵ is the disturbance. In the superposition method, the temperature at a new time level $n+1$ can be decomposed as

$$T^{n+1} = U^{n+1} + V^{n+1} \tag{3.74}$$

Then, the disturbance at the new time level becomes

$$\epsilon^{n+1} = \epsilon_1^{n+1} + \epsilon_2^{n+1} \tag{3.75}$$

where ϵ_1 comes from U and ϵ_2 comes from V. As for the present work, the solution of U is obtained by using a finite difference method. Thus,

$$\epsilon_1^{n+1} = \frac{\epsilon^n}{1+2\theta(1-\cos\lambda)} \tag{3.76a}$$

if the simple implicit method (3.45a) is used, and

$$\epsilon_1^{n+1} = \frac{1-\theta(1-\cos\lambda)}{1+\theta(1-\cos\lambda)}\,\epsilon^n \tag{3.76b}$$

if the Crank-Nicolson method (3.45b) is used (Andersen *et al.* 1984). Here, in both equations λ is the phase angle.

As for V and S, Eq (3.41) must be first linearized so that the Dirac delta function $\delta(x-S)$ can be treated as constant. Then, if V and S are represented as

$$V=\bar{V}+\epsilon_2, \quad S=\bar{S}+\gamma \tag{3.77}$$

The disturbance ϵ_2 must satisfy the following equation

$$\frac{1}{U}\frac{\partial \epsilon_2}{\partial t}=\frac{\partial^2 \epsilon_2}{\partial x^2}+\frac{I_0}{dc}\frac{d\gamma}{dt}\,\delta(x-S) \tag{3.78}$$

which is of the same form as (3.41). The disturbance ϵ_2 can then be expressed in terms of γ, the deviation in the interface position, as

$$\epsilon_2=\frac{I_0}{C}\int_{\tau=1}^{t_1}\frac{d\gamma}{d\tau}G(x,t_1|S(\tau),\tau)\,d\tau \tag{3.79}$$

As discussed previously for small Δt, $d\gamma/d\tau$ can be treated as constant; it can thus be taken out of the integral as

$$\epsilon_2=\frac{I_0}{C}\frac{d\gamma}{dt}\int_{\tau=1}^{t_1} G(x,t_1|S(\tau),\tau)\,d\tau \tag{3.80}$$

It is noted that, in this work, the V problem has been solved by using a homogeneous initial conditions, the disturbance in V thus will not accumulate. However, the disturbance in U can be transferred to V through S which is solved using Eq (3.43).

It is clear that, at the interface,

$$V(\bar{S}, t_1) = T_m - U(\bar{S}, t_1) \tag{3.81}$$

Hence

$$\epsilon_2|_{x=\bar{S}} = -\epsilon_1 \tag{3.82}$$

Introduction of (3.82) into (3.80) yields

$$-\epsilon_1 = \frac{L}{c}\frac{d\gamma}{dt}\int_{\tau=t_0}^{t_1} G(\bar{S}, t_1 | S(\tau), \tau)\, d\tau \tag{3.83}$$

or

$$\frac{d\gamma}{dt} = \frac{-\epsilon_1}{\frac{L}{c}\int_{\tau=t_0}^{t_1} G(\bar{S}, t_1 | S(\tau), \tau)\, d\tau} \tag{3.84}$$

So that Eq. (3.80) can be written as

$$\epsilon_2 = -\Pi\epsilon_1 \tag{3.85}$$

Π is defined as

$$\Pi = \frac{\int_{\tau=t_0}^{t_1} G(x, t_1 | S(\tau), \tau)\, d\tau}{\int_{\tau=t_0}^{t_1} G(\bar{S}, t_1 | S(\tau), \tau)\, d\tau} \tag{3.86}$$

The disturbance at the new time level can then be expressed as

$$\epsilon^{n+1} = \frac{(1-\Pi)\,\epsilon^n}{\left[1+2\theta(1-\cos\lambda)\right]} \tag{3.87a}$$

for the simple implicit method, and

$$\epsilon^{n+1} = \frac{1-\theta(1-\cos\lambda)}{1+\theta(1-\cos\lambda)}(1-\Pi)\epsilon^n \tag{3.87b}$$

for the Crank-Nicolson method. Clearly, the amplification factor, defined as the ratio of ϵ^{n+1} and ϵ^n, can be related to Π as

$$A = \left|\frac{\epsilon^{n+1}}{\epsilon^n}\right| = \left|\frac{(1-\Pi)}{[1+2\theta(1-\cos\lambda)]}\right| \tag{3.88a}$$

and

$$A = \left|\frac{1-\theta(1-\cos\lambda)}{1+\theta(1-\cos\lambda)}(1-\Pi)\right| \tag{3.88b}$$

for Eqs (3.45a) and (3.45b), respectively.

Since

$$\left|\frac{1}{1+2\theta(1-\cos\lambda)}\right| \leq 1, \qquad \left|\frac{1-\theta(1-\cos\lambda)}{1+\theta(1-\cos\lambda)}\right| \leq 1$$

for all θ and λ, the stability condition hinges on the value of $|1-\Pi|$. A Π versus x plot is thus given in Figure 3.1. It is found that the integration of the Green's function in the numerator of Eq. (3.86) peaks at $x=\hat{S}+\gamma$. If $\gamma=0$, the denominator of Eq. (3.88) is maximized so that Π is always less than or equal to one. On the other hand, if γ is not equal to zero but remains small, Π is peaked at a value that is slightly greater than one. However, it is independent of the time step. In any case, the condition of $|1-\Pi|\leq 1$ is met. It can thus be

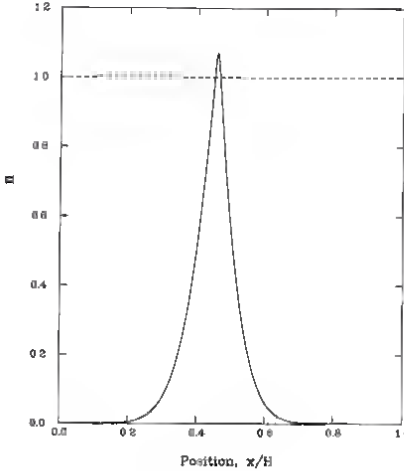

Figure 3.1 H versus x plot

concluded that the amplification A can never be greater than one providing assurance of an unconditionally stable solution.

When a numerical scheme is developed for the solution of the Stefan problem it is necessary that the numerical solution converges to the true solution. For numerical solutions using finite difference methods, convergence analysis is usually accomplished through the application of the fundamental equivalence theorem of Lax. According to this theorem, a numerical scheme is considered to be convergent if and only if the scheme is stable and consistent. In the superposition method the U problem is solved by a finite difference method, while as the V-problem is solved by an analytical method. The numerical scheme will be stable and consistent if both the U- and the V-problems are stable and consistent. It has been well established that the finite-difference equations, (3.45), for the U problem are consistent with their differential-equation counterpart in (3.33). The solution of the V-problem is exact up to Eq (3.43). In (3.44), the velocity of the interface is approximated as a finite-difference. It is obvious that this equation is also consistent. Thus the entire solution of the T problem is consistent with the original governing equations. As it is also stable for all time steps, convergence is thus assured.

It should be noted that the above analyses have been carried out on the basis of linearized equations. The nonlinearity effects remain to be investigated. One will thus be made of numerical experiment later to test the stability (Chapter 5).

3.4 Extension to Multi-Dimensional Stefan Problems

The analyses developed above for the solution of one dimensional Stefan problems will now be extended to the solution of multi-dimensional Stefan problems. Again, the phase change is considered to be diffusion driven in a PCM having constant and equal properties in different phase regions.

3.4.1 Solutions in two dimensional Cartesian systems

For phase change in a two dimensional Cartesian system, the governing equation, initial, and boundary conditions are, respectively,

$$\frac{1}{\alpha}\frac{\partial T}{\partial t}=\frac{\partial^2 T}{\partial x^2}+\frac{\partial^2 T}{\partial y^2} \qquad t>t_0, \quad (x,y)\in\Omega \tag{3-89}$$

$$T(x,y,t_0)=T_0(x,y) \tag{3-90}$$

$$k_i\frac{\partial T_{bi}}{\partial n_{bi}}+h_i[T_{bi}-T_\infty]=q_i, \qquad i=1,2, \ldots \tag{3-91}$$

Following Fotel (1968) the interface position (Figure 3.2) can be expressed in the y direction as

$$S=S(x,t) \tag{3-92}$$

Then the interface temperature and flux conditions become

$$T_l(x,S,t)=T_s(x,S,t)=T_m \tag{3-93}$$

$$\left[1+\left(\frac{\partial S}{\partial x}\right)^2\right]\left[\frac{\partial T_s(x,S,t)}{\partial y}-\frac{\partial T_l(x,S,t)}{\partial y}\right]=\frac{\rho L}{k}\frac{\partial S(x,t)}{\partial t} \tag{3-94}$$

The governing equation for the equivalent problem becomes

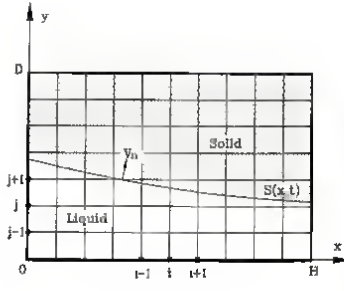

Figure 3.2 System analyzed is a two dimensional Cartesian coordinate system

$$\frac{1}{\alpha}\frac{\partial T}{\partial t} = \frac{\partial^2 T}{\partial x^2} + \frac{\partial^2 T}{\partial y^2} + \frac{L}{\alpha c}\frac{\partial y}{\partial t}\,\delta(y - S(x,t)) \tag{3 95}$$

Applicatien of the superpositien method

$$T(x,y,t) = U(x,y,t) + V(x\,y,t) \tag{3 96}$$

leads to the solution of two problems, for which the U-problea satisfies

$$\frac{1}{\alpha}\frac{\partial U}{\partial t} = \frac{\partial^2 U}{\partial x^2} + \frac{\partial^2 U}{\partial y^2}, \qquad t > t_0\,, \quad (x\,y) \in \Omega \tag{3 97}$$

$$U(x\,y,t_0) = T_0(x\,y) \tag{3 98}$$

$$k_i \frac{\partial U_{bi}}{\partial n_{bi}} + h_i[U_{bi} - T_\infty] = q_i, \qquad i=1,2, \tag{3 99}$$

For the V problea, the governing equatien is

$$\frac{1}{\alpha}\frac{\partial V}{\partial t} = \frac{\partial^2 V}{\partial x^2} + \frac{\partial^2 V}{\partial y^2} + \frac{L}{\alpha c}\frac{\partial y}{\partial t}\,\delta(y - S(x,t)), \quad t > t_0, \ (x\,y) \in \Omega \tag{3-100}$$

The initial, boundary, and interface conditions for the V-problem are

$$V(x\,y,t_0) = 0 \tag{3-101}$$

$$k_i \frac{\partial V_{bi}}{\partial n_{bi}} + h_i V_{bi} = 0, \qquad i=1,2, \tag{3 102}$$

$$V_i(x,S,t) = V_s(x,S,t) = T_m - U(x\,S,t) \tag{3 103}$$

As discussed previously in Section 3 2 2, the U-problem can be solved by FDM For a two dimensional problem, it can be solved efficiently by an alternating direction implicit (ADI) method which has been established to be unconditionally stable for all time steps. In this method, the temperature in x- and y-directions are calculated alternately The finite differences equations are

$$-\theta_x U^{n+1}_{i-1,j} + (1+2\theta_x) U^{n+1/2}_{i,j} - \theta_x U^{n+1/2}_{i+1,j} = \theta_y U^{n}_{i,j-1} + (1-2\theta_y) U^{n}_{i,j} + \theta_y U^{n}_{i,j+1}$$

$$-\theta_y U^{n+1}_{i,j-1} + (1+2\theta_y) U^{n+1}_{i,j} - \theta_y U^{n+1}_{i,j+1} = \theta_x U^{n+1/2}_{i-1,j} + (1-2\theta_x) U^{n+1/2}_{i,j} + \theta_x U^{n+1/2}_{i+1,j} \tag{3 104}$$

where $\theta_x = \frac{\alpha \Delta t}{2\Delta x^2}$ and $\theta_y = \frac{\alpha \Delta t}{2\Delta y^2}$ These finite difference equations can be solved by using two tridiagonal systems of linear algebraic equations by means of an efficient tridiagonal solver.

The solution of the V-problem can be expressed again in terms of a Green's function as

$$V(x,y,t_1) = \frac{1}{c} \int_{\tau=1_0}^{1_1} d\tau \int_{x'=0}^{H} \frac{\partial S}{\partial \tau} G(x,y,t_1 \mid x', S(x',\tau), \tau) dx' \tag{3 105}$$

The interface position curve $S(x,t_1)$ is then determined implicitly by the following equation

$$T_m - U(x, S, t_1) = \frac{1}{c} \int_{\tau=1_0}^{1_1} d\tau \int_{x'=0}^{H} \frac{\partial S}{\partial \tau} G(x, S, t_1 \mid x', S(x',\tau), \tau) dx' \tag{3 106}$$

In this effort, since the interface S is a function of both x and t, Eq. (3.106) can not be solved directly for S. The difficulty lies in the fact that a two dimensional searching for the position is necessary if this position is to be found iteratively. Alternatively, an assumption of the S function to represent the interface position will be necessary if this position is to be found analytically. Moreover, in the analytical solution, the accuracy of the result depends greatly on the fitness of the function that is initially assumed for approximation. In any event, the interface position can not be determined easily.

To overcome these problems, a new approach is developed by splitting the two dimensional problem into an array of transversely related one dimensional problems. In this approach, the second partial differential of V with x in (3.100) is changed to a finite difference as

$$\frac{\partial^2 V(x,y,t)}{\partial x^2} = \frac{V(x+\Delta x, y, t) - 2V(x,y,t) + V(x-\Delta x, y, t)}{\Delta x^2} \qquad (3.107)$$

Then, by indexing x position with subscript i so that $V(x,y,t)$ is changed to $V_i(y,t)$ and $V(x \pm \Delta x, y, t)$ to $V_{i \pm 1}(y,t)$, Eq. (3.100) can be re-written as follows

$$\frac{1}{\alpha}\frac{\partial V_i(y,t)}{\partial t} = \frac{\partial^2 V_i(y,t)}{\partial y^2} + \frac{V_{i+1}(y,t) - 2V_i(y,t) + V_{i-1}(y,t)}{\Delta x^2}$$

$$+ \frac{L}{\alpha c} \frac{\partial y}{\partial t}\, \delta(y - S_i(t)), \qquad i = 1, 2, \ldots \qquad (3.108)$$

Equation (3.108) represents a group of piecewisely related one dimensional problems which can be solved by means of the Green's function using a time marching scheme. In this effort, the last two terms on the right hand side of Eq. (3.108) can be collectively taken as source terms. Then with the help of zero initial condition and homogeneous boundary conditions imposed in the V-problem, the solution of V can be written as

$$V_i(y,t_1) = \frac{E}{\rho}\int_{\tau=t_0}^{t_1} \frac{\partial S_i}{\partial \tau} G_i(y,t_1|S_i,\tau)d\tau + n\int_{\tau=t_0}^{t_1} d\tau \int_{y=0}^{D} g_i(y',\tau) G_i(y,t_1|y',\tau)dy \qquad (3.109)$$

where

$$g_i(y',\tau) = \frac{V_{i+1}(y',\tau) - 2V_i(y',\tau) + V_{i-1}(y',\tau)}{\Delta x^2} \qquad (3.110)$$

It is still not possible to solve Eq (3.110) because of the function $g_i(y,t)$ which depends on $V_i(y,t)$. Some additional work is necessary, and one way to do it is to expand g about t_0 as

$$g_i(y,\tau) = g_i(y,t_0) + \frac{\partial g_i(y,t_0)}{\partial t}(\tau - t_0) + \cdots, \qquad t_0 \le \tau \le t_1 \qquad (3.111)$$

If higher order terms are neglected, then g can be expressed as

$$g_i(y,\tau) = g_i(y,t_0) + \frac{\partial g_i(y,t_0)}{\partial t}(\tau - t_0) \qquad (3.112)$$

Using Eqs (3.101) and (3.110) permits the first term on the right hand side of this equation to drop out. As for the second term, it can be shown from (3.110) that

$$\frac{\partial g_i(y,t_0)}{\partial t}=\frac{1}{\Delta z^2}\left[\frac{\partial V_{i+1}(y,t_0)}{\partial t}-2\frac{\partial V_i(y,t_0)}{\partial t}+\frac{\partial V_{i-1}(y,t_0)}{\partial t}\right] \tag{3.113}$$

Then with the help of the initial condition given as (3.101), Eq. (3.100) can be used to re-write (3.113) as

$$\frac{\partial g_i(y,t_0)}{\partial t}=\frac{k}{c\Delta z^2}\left\{\frac{\partial y}{\partial t}\delta(y-S_{i+1})-2\frac{\partial y}{\partial t}\delta(y\ S_i)+\frac{\partial y}{\partial t}\delta(y-S_{i-1})\right\}_{t=t_0} \tag{3.114}$$

It thus follows that

$$V_i(y,t_1)=\frac{k}{c}\int_{\tau=t_0}^{t_1}\frac{\partial S_i}{\partial\tau}G_i(y,t_1|S_i,\tau)d\tau$$

$$+\frac{gL}{c\Delta z^2}\left(w_{i+1}-2w_i+w_{i-1}\right) \tag{3.115}$$

where

$$w_\kappa=\int_{\tau=t_0}^{t_1}(\tau-t_0)\frac{\partial S_\kappa(t_0)}{\partial t}G_i(y,t_1|S_\kappa(t_0),\tau)d\tau \qquad \kappa=i,i\pm1 \tag{3.116}$$

In practice, a first-order approximation is sufficiently accurate to solve the problem at hand. For the first-order approximation

$$g_i(y,\tau)\simeq g_i(y,t_0) \tag{3.117}$$

Then, from (3.101),

$$g_i(y'\ r) \equiv 0 \tag{3.118}$$

and V can be obtained by solving a simple equation as

$$V_i(y,t_i) = \frac{L}{\alpha}\int_{r=l_0}^{l_1} \frac{\partial S_i}{\partial r}\, G_i(y,t_1|S_i,r)\mathrm{d}r \tag{3.119}$$

3.4.2 Solutions in cylindrical coordinate systems

The governing equation for heat diffusion in a two dimensional cylindrical system can be written as follows

$$\frac{1}{\alpha}\frac{\partial T}{\partial t} = \frac{\partial^2 T}{\partial z^2} + \frac{1}{r}\frac{\partial}{\partial r}\left(r\frac{\partial T}{\partial r}\right), \quad t > t_0, \quad (z,r) \in \Omega \tag{3.120}$$

As in always the case, appropriate initial and boundary conditions as well as the interface conditions must be specified. For the phase change in cylindrical coordinates, two types of the interface motion will be addressed—the phase-change interface may be moving in z-direction (Figure 3.3), and the phase change interface may be moving in r-direction (Figure 3.4).

In the former, the interface position may be expressed as

$$S = S(r,t) \tag{3.121}$$

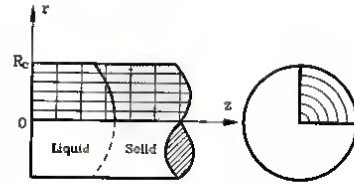

Figure 3.3 System analyzed in cylindrical coordinates: Interface moves in r-direction

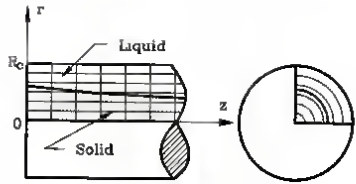

Figure 3.4 System analyzed in cylindrical coordinates: Interface moves in r-direction

Then, the interface conditions are written as

$$T(S(z,t),r,t)=T_m \tag{3.122}$$

$$\left[1+\left(\frac{\partial S}{\partial r}\right)^2\right]\left[\frac{\partial T_s}{\partial z}-\frac{\partial T_l}{\partial z}\right]_{z=S}=\frac{\rho|L|}{k}\frac{\partial S(r,t)}{\partial t} \tag{3.123}$$

In the latter, the interface position may be expressed as

$$S=S(z,t) \tag{3.124}$$

Then, the interface conditions are given by

$$T(z,S(z,t),t)=T_m \tag{3.125}$$

$$\left[1+\left(\frac{\partial S}{\partial z}\right)^2\right]\left[\frac{\partial T_s}{\partial r}-\frac{\partial T_l}{\partial r}\right]_{r=S}=\frac{\rho|L|}{k}\frac{\partial S(z,t)}{\partial t} \tag{3.126}$$

In the method of superposition, the temperature is decomposed as

$$T(z,r,t)=U(z,r,t)+V(z,r,t) \tag{3.127}$$

Here, the U-problem satisfies the same governing equations for T as in Eq (3.120), and the nonhomogeneous boundary and initial conditions. This problem can be solved by a finite difference method as

$$U_{i,j}^{n+1}-U_{i,j}^{n}=2\theta_z^2(U_{i+1,j}-2U_{i,j}+U_{i-1,j})$$
$$+\theta_r^2(U_{i,j+1}-U_{i,j-1})+2\theta_r(U_{i,j+1}-2U_{i,j}+U_{i,j-1}) \tag{3.128}$$

where $\theta_z=\frac{\alpha\Delta t}{2\Delta z^2}$, $\theta_r^2=\frac{\alpha\Delta t}{2r\Delta r}$ and $\theta_r=\frac{\alpha\Delta t}{2\Delta r^2}$

Equation (3.128) can be solved either by an explicit method by setting $U = U^n$ on the right hand side, or by an implicit method by setting $U = U^{n+1}$ on the same side. In any event, the solution is routine.

The V-problem can be solved by the Green's function method. Again, the interface flux condition is incorporated into the governing equation. Thus, for the case of interface moving in the z-direction, the governing equation becomes

$$\frac{1}{\alpha}\frac{\partial V}{\partial t} - \frac{\partial^2 V}{\partial z^2} + \frac{1}{r}\frac{\partial}{\partial r}\left(r\frac{\partial V}{\partial r}\right) + \frac{L}{k}\frac{\partial z}{\partial t}\,\delta(z - S(r,t)) \tag{3.129}$$

The governing equation is split into two directions, where a finite difference method is used in the r-direction. This reduces the V equation to the following

$$\frac{1}{\alpha}\frac{\partial V_j}{\partial t} - \frac{\partial^2 V_j}{\partial z^2} + \frac{L}{k}\frac{\partial z}{\partial t}\,\delta(z - S_j(t)) + g_j(z,t) \tag{3.130}$$

where

$$g_j(z,t) = \begin{cases} \dfrac{V_{j+1} - V_{j-1}}{2r\Delta r} + \dfrac{V_{j+1} - 2V_j + V_{j-1}}{\Delta r^2}, & \text{for } r \neq 0 \\ \dfrac{4(V_{j+1} - V_j)}{\Delta r^2}, & \text{for } r = 0 \end{cases} \tag{3.131}$$

As described in Section 3.4.1, the first-order approximation of g_j leads to a very simple approximation as

$$g_j(z,r) \simeq g_j(z,t_0) = 0 \tag{3.132}$$

The V problem can be solved as

$$V_j(z,t_1)=\frac{L}{c}\int_{\tau=t_0}^{t_1}\frac{\partial S_j}{\partial\tau}\,G_j(z,t_1|S_j,\tau)\mathrm{d}\tau \tag{3.133}$$

Similarly, the second-order approximation of g_j results in the following solution

$$V_j(z,t_1)=\frac{L}{c}\int_{\tau=t_0}^{t_1}\frac{\partial S_j}{\partial\tau}\,G_j(z,t_1|S_j,\tau)\mathrm{d}\tau+W_j \tag{3.134}$$

where

$$W_j=\begin{cases}\dfrac{w_{j+1}-w_{j-1}}{2r\Delta r}+\dfrac{w_{j+1}-2w_j+w_{j-1}}{\Delta r^2}, & \text{for } r\neq 0\\[2ex] \dfrac{4(w_{j+1}-w_j)}{\Delta r^2}, & \text{for } r=0\end{cases} \tag{3.135}$$

and

$$w_\kappa=\int_{\tau=t_0}^{t_1}(\tau-t_0)\frac{\partial S_\kappa(t_0)}{\partial t}G_j(z,t_1|S_\kappa(t_0),\tau)\mathrm{d}\tau,\quad \kappa=j\,j\pm1 \tag{3.136}$$

For the case of the interface moving in the r-direction, the governing equation of the equivalent problem is given by

$$\frac{1}{\alpha}\frac{\partial V}{\partial t}=\frac{\partial^2 V}{\partial z^2}+\frac{1}{r}\frac{\partial}{\partial r}\left(r\frac{\partial V}{\partial r}\right)+\frac{L}{kc}\frac{\partial\Gamma}{\partial t}\,\delta(r-S(z,t)) \tag{3.137}$$

Again, the governing equation is split into two directions, this time, a finite difference method is used in the z-direction. The V equation becomes

$$\frac{1}{\alpha}\frac{\partial V_i(r,t)}{\partial t} = \frac{1}{r}\frac{\partial}{\partial r}\left[r\frac{\partial V_i(r,t)}{\partial r}\right] + \frac{f}{\pi r}\frac{\partial r}{\partial t}\,\delta(r - S_i(t)) + g_i(r,t) \qquad (3\text{-}138)$$

where

$$g_i(r,t) = \frac{V_{i+1}(r,t) - 2V_i(r,t) + V_{i-1}(r,t)}{\Delta z^2} \qquad (3\text{-}139)$$

The first order accurate solution of the V_i problems is readily obtained as

$$V_i(r,t_1) = \frac{f}{\pi}\int_{\tau=1_0}^{1_1}\frac{\partial S_i}{\partial \tau}S_i(\tau)G_i(r,t_1|S_i,\tau)d\tau \qquad (3\text{-}140)$$

and the second-order accurate solution can be derived as

$$V_i(r,t_1) = \frac{f}{\pi}\int_{\tau=1_0}^{1_1}\frac{\partial S_i}{\partial \tau}S_i(\tau)G_i(r,t_1|S_i,\tau)d\tau + \frac{\alpha I_0}{c\Delta z^2}\left(w_{i+1} - 2w_i + w_{i-1}\right) \qquad (3\text{-}141)$$

where

$$w_\alpha = \int_{\tau=1_0}^{1_1}(\tau - 1_0)\frac{\partial S_\alpha(t_0)}{\partial t}S_\alpha(t_0)G_i(r,t_1|S_\alpha(t_0),\tau)d\tau$$

$$\alpha = i,\ i\pm 1 \qquad (3\text{-}142)$$

3.4.3 Solutions in three dimensional Cartesian systems

The governing equation of a Stefan problem in a three dimensional Cartesian system takes the form

$$\frac{1}{\alpha}\frac{\partial T}{\partial t}=\frac{\partial^2 T}{\partial x^2}+\frac{\partial^2 T}{\partial y^2}+\frac{\partial^2 T}{\partial z^2}\ , \quad t>t_0, \quad (x,y,z)\in\Omega \tag{3.143}$$

The interface position is expressed as

$$S=S(x,y,t)$$

Then, the interface condition can be written as (Patel,1968)

$$\left[1+\left(\frac{\partial S}{\partial x}\right)^2+\left(\frac{\partial S}{\partial y}\right)^2\right]\left[\frac{\partial T_s}{\partial z}-\frac{\partial T_l}{\partial z}\right]=\frac{\rho|L|}{k}\ \frac{\partial S}{\partial t} \tag{3.144}$$

With the use of the superposition method, the temperature is decomposed as

$$T(x,y,t)=U(x,y,z,t)+V(x,y,z,t) \tag{3.145}$$

in which the U-problem satisfies a governing equation that is of the same form as (3.143) and relevant nonhomogeneous initial and boundary conditions. The finite difference equation for the U-problem can be derived as

$$\begin{aligned}U_{i,j,k}^{n+1}-U_{i,j,k}^{n}=&2\theta_x(U_{i+1,j,k}-2U_{i,j,k}+U_{i-1,j,k})\\&+2\theta_y(U_{i,j+1,k}-2U_{i,j,k}+U_{i,j-1,k})\\&+2\theta_z(U_{i,j,k+1}-2U_{i,j,k}+U_{i,j,k-1})\end{aligned} \tag{3.146}$$

where ϑ_x, ϑ_y, and ϑ_z have been defined previously. This equation can be solved by using an iteration procedure such as Gauss-Seidel and SOR method, or by a modified ADI method.

Again, the V-problem can be solved by a Green's function method. In this method, the equivalent problem can be written as

$$\frac{1}{a}\frac{\partial V}{\partial t} = \frac{\partial^2 V}{\partial x^2} + \frac{\partial^2 V}{\partial y^2} + \frac{\partial^2 V}{\partial z^2} + \frac{L}{ak}\frac{\partial z}{\partial l}\,\delta(z-S) \tag{3 147}$$

Then, by using a finite difference method in both x- and y-directions, Eq. (3-147) can be re-written as

$$\frac{1}{a}\frac{\partial V_{i,j}}{\partial t} - \frac{\partial^2 V_{i,j}}{\partial z^2} + \frac{L}{ak}\frac{\partial z}{\partial l}\,\delta(z-S) + g_{i,j}(z,t) \tag{3.148}$$

where

$$g_{i,j}(z,t) = \frac{V_{i+1,j} - 2V_{i,j} + V_{i-1,j}}{\Delta x^2} + \frac{V_{i,j+1} - 2V_{i,j} + V_{i,j-1}}{\Delta y^2} \tag{3 149}$$

With the help of the homogeneous initial condition for the V-problem, the first-order accurate approximation of $g_{i,j}$ leads to a very simple relation as

$$g_{i,j}(z,\tau) = g_{i,j}(z,t_n) = 0 \tag{3 150}$$

and the solution of the V-problem follows as

$$V_{i,j}(z,t_1) = \frac{L}{k}\int_{\tau=t_n}^{t_1} \frac{\partial S_{i,j}}{\partial \tau}\, G_{i,j}(z,t_1|S_{i,j},\tau)\,d\tau \tag{3 151}$$

In a similar fashion (see Section 3.4.1), the second order accurate approximation of $g_{i,j}$ leads to a solution as

$$V_{i,j}(z,t_1) = \frac{1}{\beta}\int_{\tau=t_0}^{t_1} \frac{\partial S_{i,j}}{\partial \tau} G_{i,j}(z,t_1|S_{i,j},\tau)\,d\tau$$

$$+ \frac{\alpha L}{c\Delta z^2}\left(w_{i+1,j} - 2w_{i,j} + w_{i-1,j}\right)$$

$$+ \frac{\alpha L}{c\Delta z^2}\left(w_{i,j+1} - 2w_{i,j} + w_{i,j-1}\right) \qquad (3.152)$$

where

$$w_{m,n} = \int_{\tau=t_0}^{t_1} (\tau - t_0)\frac{\partial S_{m,n}(t_0)}{\partial t} G_{i,j}(z,t_1|S_{m,n}(t_0),\tau)\,d\tau$$

$$m = i,\ i\pm 1, \quad n = j, j\pm 1 \qquad (3.153)$$

3.4.4 Stability analysis

For multi dimensional problems, the explicit treatment of the second partial differential may impose additional constraints on the stability of the solution. Due to the difficulties associated with the nonlinearity of the problem, the stability can not be tested by simple analysis. However, some comments can be made as follows.

It is well known that the solution of U is unconditionally stable. As for the V, since it always starts with a homogeneous initial condition, the disturbance (error) of V will not accumulate-

The only source of error that may be brought into the V-problem is $U(\vec{S}(t)$ which is used to find the interface position. In this connection, because of the use of the Green's functions, disturbance in the integrand will not be magnified but will be suppressed. On the other hand, the disturbance in the V solution can still be brought to the U-problem through the superposition principle. However, this disturbance can still be suppressed by the ADI method in the solution for the temperature in the succeeding time step. It is thus expected that any disturbance will not grow in the solution, and, as a result, the method is unconditionally stable. It is noted that the discussion above is not meant to be rigorous. Numerical experiments for a two dimensional problem (See Chapter 5) will be provided later for tests.

3.5 Applications to Latent Heat Thermal Energy Storage Systems

For the phase change problems solved in the preceding sections by the source-and-sink method, the boundary conditions have been applied directly to the phase change material. In practice, the phase change material may be heated or cooled by a fluid which is in motion itself, a conjugate heat transfer problem thus results. In this problem, the fluid temperature is only given at the inlet. Both the wall and the fluid exit temperature are unknown.

Two conjugate heat transfer problems will be solved in Sections 3.5 and 3.6. Analysis for fluid flow in a straight parallel channel of phase change material will be studied first. Results for a sample study for this problem will be given in Chapter 5.

3.5.1 Problem formulation

A thermal energy storage (TES) unit is sketched in Figure 3.5. This unit can be modeled for analysis as shown in Figure 3.6. It consists of a straight parallel channel surrounded by PCM. Heat transfer fluid (HTF) is forced to flow through the channel and it exchanges heat with the PCM. It is a time-dependent phase-change problem combined with conjugate forced convection. The governing equations for the forced convection in the HTF and the heat diffusion in the PCM must be solved simultaneously. The solution for heat transfer in the PCM has been covered in the previous sections. Only the convection problem and the matching method need be described in this section.

Analysis of forced convection for channel flow can be accomplished by solving the Navier-Stokes equations and the energy equation. However, a direct numerical simulation of the Navier-Stokes equations is time consuming. In addition, for a conjugate problem, an iteration is necessary to satisfy the boundary condition at the fluid/PCM interface, which further adds to the complexity of the solution. An alternative approach is taken that uses empirical correlations for the treatment of the heat transfer at the fluid side. This permits the use of convective heat transfer coefficient. While the accuracy of the method depends on the accuracy of the empirical correlations, the uncertainty is comparable with that introduced in the turbulence model. With this effort, the fluid temperature in the channel can be modeled as a function of position and time and analyzed by solving the following equations:

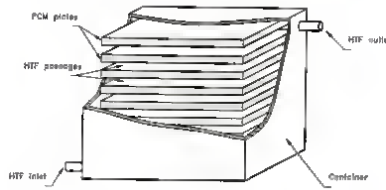

Figure 3.5 A schematic drawing for thermal energy storage unit

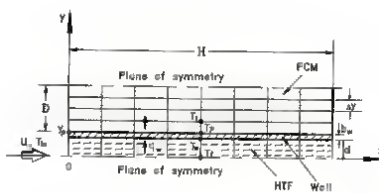

Figure 3.6 Simplified system for analysis

$$\frac{\partial T_f}{\partial t} + U\frac{\partial T_f}{\partial z} + \frac{h(T_f - T_w)}{\rho_f c_f d} = 0 \qquad (3.154)$$

At the inlet,

$$T_f(0,t) = T_{in}(t) \qquad (3.155)$$

In these equations, T_f is the mixed mean temperature of the fluid, U is the mean velocity, h is the convective heat transfer coefficient, d is the half width of the channel, and ρ_f and c_f are the density and the specific heat of the fluid, respectively. In the formulations above, the Peclet number is taken to be large, so that the heat diffusing in the z direction can be neglected.

In the conjugate problem Eq. (3.154) is to be solved in conjunction with the phase-change problem whose solution has been given previously. If the heat conduction in the axial direction in the channel wall and the heat storage in the wall are negligibly small, heat transfer by convection from the fluid to the wall must be equal to the heat that is supplied to the PCM through its lower boundary. Hence,

$$h(T_f - T_w) = -k\left.\frac{\partial T}{\partial y}\right|_{y=y_p} = q_w \qquad (3.156)$$

where y_p is the lower boundary of the PCM (see Figure 3.6). Using an electric analogy, the temperature at this boundary can be related to the temperature at the inner surface of the channel wall by the relation

$$T_c = T_w - b_w q_w / k_w \qquad (3.157)$$

where b_w and k_w are the thickness and the conductivity of the wall, respectively.

The heat transfer coefficient h is taken from the literature. In this regard, the Nusselt number for a fully developed laminar flow varies from 7.54 for constant wall temperature to 8.24 for constant wall heat flux condition (Kays and Crawford, 1980). There is a lack of correlation for turbulent flow in a straight channel. Use is thus made of an empirical equation developed by Gnielinski (1976) as

$$Nu_D = \frac{(f/8)(Re_D - 1000)Pr}{1 + 12.7(f/8)^{1/2}(Pr^{2/3} - 1)} \qquad (3.158)$$

where f is the friction factor, which is related to the Reynolds number as

$$f = [0.79\ln(Re_D) - 1.64]^{-2} \qquad (3.159)$$

In these equations, both the Nusselt number and the Reynolds number are defined as

$$Nu_D = \frac{hD_h}{k_f}, \qquad Re_D = \frac{UD_h}{\nu} \qquad (3.160)$$

where D_h is the hydraulic diameter of the channel. It is noted that Eq. (3.158) is strictly valid for a circular pipe with any condition (constant wall temperature or flux) imposed on the boundary. The

Prandtl number is in the range of 0.5 to 2,000, while the Reynolds number is in the range of 2,300 to 5×10^6. It is adopted for one is the straight channel by redefining the dimensionless numbers in terms of D_h as shown in (3.160)

3.5.2 Solution method

In the conjugate problem, the heat flux at the channel wall and the temperature in the PCM and the fluid are all unknown. To satisfy the matching condition (3.156) it is necessary to use an iteration. However, as discussed by Baroczi and Pagliarini (1985), even for a simple steady state conjugate problem without phase change, instabilities may be encountered during the iteration process. Convergent results can only be obtained if the initial guesses are sufficiently close to the true values.

To alleviate these problems, the heat flux in the third term in (3.154) is re-written in terms of T_1, the temperature at the first grid point above the boundary of the PCM at y_p (Figure 3.6). Thus,

$$h(T_f - T_w) = \frac{T_f - T_1}{R''} \tag{3.161}$$

where R'' represents the overall thermal resistance per unit area,

$$R'' = \frac{1}{h} + \frac{b_w}{k_w} + \frac{\Delta y}{k_p} \tag{3.162}$$

It is noted that, in the numerical solution, if the interface position

S is less than Δy, which is the grid spacing in y direction, then the T_1 in Eq. (3.161) is replaced by T_∞, the phase-change temperature, and the Δy is changed to S.

The energy equation (3.154) can then be written as

$$\frac{\partial T_f}{\partial t}+U\frac{\partial T_f}{\partial x}+\frac{T_f-T_1}{\rho_f c_f R''_f}=0 \tag{3.163}$$

This equation can be solved by using a first order accurate implicit finite difference scheme as

$$T_{f2}^{n+1}=\frac{T_{f2}^{n}+\theta_1 T_{f2-1}^{n+1}+\theta_2 T_1}{1+\theta_1+\theta_2} \tag{3.164}$$

where

$$\theta_1=\frac{U\Delta t}{\Delta x}, \qquad \theta_2=\frac{\Delta t}{\rho_f c_f R''_f}$$

The temperature imposed at the surface of the PCM follows as

$$T_p=\frac{R''_1 T_1+R''_2 T_f}{R''_1+R''_2} \tag{3.165}$$

where

$$R''_1=\frac{1}{h}+\frac{\delta_w}{k_w}, \qquad R''_2=\frac{\Delta y}{k_p} \tag{3.166}$$

The surface temperature given in (3.165) will then be used as the boundary condition for the solution of the phase-change problem

3.5.3 Energy conservation test

For the solution of the conjugate problem given in this section, errors mainly come from the matching conditions between the PCM and the HTF. Since experimental data are usually unavailable for comparison, the accuracy of the numerical solution developed in this section will be tested by means of an energy conservation that is based on an open-system thermodynamic analysis.

For the heat transfer of channel flow between parallel walls of phase change material without heat and work interaction with the surroundings, the first law of thermodynamics can be written as

$$\dot{E}_{in} - \dot{E}_{out} = \Delta E_{cv}/\Delta t \tag{3.167}$$

where the $\dot{E}_{in}$ refers to the energy rate associated with the fluid flow entering the channel and $\dot{E}_{out}$ refers to the energy rate associated with the fluid flow leaving the channel. The term on the right hand side represents the time rate of change of the internal energy inside the control volume. For the problem under investigation, there are energy changes in the PCM, the wall, and the fluid.

For a time period of t, the left hand side of Eq. (3.167) can be expressed as

$$E_{in} - E_{out} = \int_{\tau=0}^{t} \dot{Q}_{\beta} r_{\beta} [T_f(0,\tau) - T_f(M,\tau)] d\tau \tag{3.168}$$

while the right hand side can be expressed as

$$\begin{aligned}\Delta E_{cv} = \sum_{i=0}^{M} 2W\Bigg\{ & \int_{y=0}^{D}\int_{x=0}^{H} \rho c\left[T(x,y,t)-T_0\right]dxdy \\ & + \int_{x=0}^{H}\left[-L\rho S(x,t)\right]dx \\ & + \int_{x=0}^{H} \rho_w c_w b_w\left[T_w(x,t)-T_{w_0}\right]dx \\ & + \int_{x=0}^{H} \rho_f c_f d\left[T_f(x,t)-T_{f_0}\right]dx \Bigg\}\end{aligned} \tag{3.169}$$

Here, the energy balance in (3.167) is formulated on the basis of discharge of heat from the PCM. The PCM, the wall, and the fluid are at the same initial temperature T_0, and the channel has a width W. Each PCM plate has a thickness $2D$. Under these conditions, the first term on the right of (3.169) refers to the energy associated with the change of the sensible heat of the PCM. The second term refers to the energy associated with the phase change. The third term accounts for the energy change in the containing wall, and the last term refers to that energy associated with the change of the temperature of the HTF inside the channel. For an accurate numerical solution of the problem, the left hand side of (3.167) should be equal to the right hand side of the same equation. This energy conservation will be used to check the accuracy of a numerical experiment to be presented in Chapter 5.

3.6 Application to Encapsulated PCM TES Systems

In the preceding sections, the phase change material analyzed is in the form of a plane slab. Since the heat transfer fluid is flowing over the surfaces of the slab, the plane of symmetry can be taken to be the half thickness of the slab as shown in Figure 3.6. An alternative form of the phase change material is one that is encapsulated in spheres as shown in Figure 3.7. This section is devoted to the analysis of the phase change in packed spheres.

3.6.1 Problem formulation

The system under investigation is sketched in Figure 3.7. A tank is packed with encapsulated PCM spheres. Heat transfer fluid enters through the bottom of the tank, exchanges heat with the PCM by forced convection, and exits from the top of the tank. It is assumed that, in the HTF, the temperature only varies in the z direction while, in the capsulated spheres, the temperature only varies in the r direction as shown in Figures 3.8 and 3.9. Other assumptions that are related to the phase change analysis earlier still apply.

For the analysis of the heat transfer in the HTF, the control volume is taken to have a thickness that is equal to the diameter of the packed sphere (Figure 3.8). The energy equation for the fluid can be written in terms of the mean temperature T_f and mean velocity U as

$$\rho_f c_f V_f \left(\frac{\partial T_f}{\partial t} + U \frac{\partial T_f}{\partial z} \right) + h A_s (T_f - T_s) = 0, \quad T_f = T_f(z, t) \qquad (3.176)$$

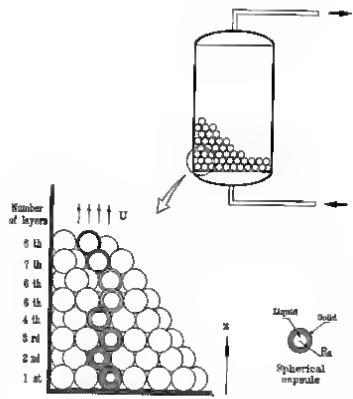

Figure 3 7 A schematic drawing for the encapsulated latent heat TES unit

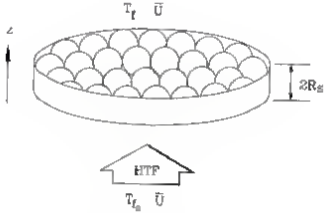

Figure 3.8 Control volume for fluid analysis

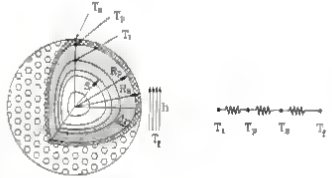

Figure 3.9 Boundary conditions for PCM/HTF analysis

where, in addition to those that have been defined previously, T_s is the surface temperature of the sphere, V_f is the volume of the free space in a packed layer, and A_s is the total surface area of the spheres that are in contact with the fluid. For a single sphere of radius R_s, the surface-to-volume ratio is given by the simple relation

$$\frac{A_s}{V_s}=\frac{3}{R_s} \tag{3.171}$$

which also holds for multiple spheres in a packed layer. Thus, by using a void fraction μ, defined as the ratio of the free volume V_f to the total volume V_s, Eq. (3.170) can be recast as

$$\frac{\partial T_f}{\partial t}+U\frac{\partial T_f}{\partial z}+\frac{3(1-\mu)h}{\mu\rho_f c_f R_s}(T_f-T_s)=0 \tag{3.172}$$

This equation is equivalent to that derived by Schumann (1929) and Rice (1978) for packed rock beds. For the present problem, the initial and boundary conditions for the fluid are given as

$$T_f(z,0)=T_{s0}, \qquad T_f(0,t)=T_{in}(t) \tag{3.173}$$

As for the spheres, the governing equation, initial, boundary, and interface conditions have been given in Section 3.3.3. These equations must be solved in conjunction with (3.172) for heat transfer analysis. As before, the solutions of the fluid and the PCM are to be matched at the surface of the spheres by the relation

$$h(T_s - T_f) = -k_f \frac{\partial T}{\partial r}\bigg|_{r=R_s} = q_w \qquad (3.174)$$

In this effort, the convective heat transfer coefficient h for the packed spheres is obtained by curve-fitting the experimental data of Chen *et al.* (1992) as

$$Nu = 11 + 0.06Pe \qquad (3.175)$$

where, Pe is the Peclet number ($Re \cdot Pr$), The Reynolds number is defined on the basis of the diameter of the sphere and the average velocity of the fluid as

$$Re = \frac{U(2R_s)}{\nu} \qquad (3.176)$$

The heat transfer coefficient can then be evaluated by means of the Nusselt number as

$$h = \frac{Nu\ k_f}{2R_s} \qquad (3.177)$$

where k_f is the conductivity of the fluid

3.6.2 Solution method

Solution of the conjugate problem for fluid flow in a packed sphere bed follows the same line described earlier for channel flow. In this case, it is assumed that the heat storage in the sphere wall is negligibly small so that the heat transfer from the fluid to the sphere can be expressed in terms of the temperature difference between the fluid and the first nodal point that is located inside the surface

of the PCM as

$$h(T_f - T_s) = \frac{T_f - T_1}{R'} \tag{3.178}$$

For the spherical PCM the total thermal resistance based on the surface area of the sphere is

$$R' = \frac{1}{h} + \frac{R_s^2}{k_w}\left(\frac{1}{R_p} - \frac{1}{R_s}\right) + \frac{R_s^2}{k}\left(\frac{1}{r_1} - \frac{1}{R_p}\right) \tag{3.179}$$

where k_w is the conductivity of the sphere wall, R_p is the radius of the PCM, and R_s is the radius of the sphere (see Figure 3.8). Equation (3.172) can then be written as

$$\frac{\partial T_f}{\partial t} + U\frac{\partial T_f}{\partial r} + \frac{3(1-\mu)}{\rho_p c_f R_s R'}(T_f - T_1) = 0 \tag{3.180}$$

As before, in the numerical solution, if the interface position S is greater than r_1, the first nodal point position that is inside the surface of the PCM, but is less than R_p, the radius of the PCM, then T_1 in Eqs (3.178)-(3.180) is replaced by T_m and r_1 is changed to S.

Equation (3.180) can be solved by using an implicit finite difference scheme as

$$T_f^{n+1} = \frac{T_f^n + \theta_1 T_{f_0}^{n+1} + \theta_2 T_1}{1 + \theta_1 + \theta_2} \tag{3.181}$$

where T_{f_0} is the temperature of the fluid at the inlet of the control

volume as shown in Figure 3.8, and

$$\theta_1=\frac{\Delta tU}{2R_p},\qquad \theta_2=\frac{3(1-\mu)\Delta t}{\mu\rho_f c_f R_p R^2} \tag{3.182}$$

The temperature at the surface of the PCM can then be evaluated as

$$T_\mu=\frac{R_1^{\prime\prime}T_1+R_2^{\prime\prime}T_f}{R_1^{\prime\prime}+R_2^{\prime\prime}} \tag{3.183}$$

where

$$R_1^{\prime\prime}=\frac{1}{h}+\frac{R_p^2}{k_p}\left(\frac{1}{R_p}-\frac{1}{R_s}\right),\qquad R_2^{\prime}=\frac{R_p^2}{k_p}\left(\frac{1}{r_1}-\frac{1}{R_p}\right), \tag{3.184}$$

This temperature is to be used as the boundary condition for the solution of the phase change in the PCM as described in Section 3.3.3.

3.6.3 Energy conservation test

As mentioned in Section 3.5.3, errors for the conjugate problem mainly come from the matching conditions between the PCM and the HTF. Since experimental data are usually unavailable for comparison, the accuracy of the numerical solution developed in this section will be tested by means of an energy conservation that is based on an open-system thermodynamic analysis.

For the heat transfer of fluid flow in packed spheres inside a tank without heat and work interactions with the surroundings, the first law of thermodynamics can be written as

$$\dot{E}_{in} - \dot{E}_{out} = \Delta E_{cv}/\Delta t \tag{3.185}$$

where the $\dot{E}_{in}$ refers to the energy rate associated with the fluid flow entering the tank and $\dot{E}_{out}$ refers to the energy rate associated with the fluid flow leaving the tank. The term on the right hand side represents the time rate of change of the internal energy inside the control volume. For the problem under investigation, there are energy changes in the PCM, the shell of the PCM sphere, and the fluid.

For a time period of t, the left hand side of Eq. (3.185) can be expressed as

$$E_{in} - E_{out} = \int_{\tau=0}^{t} Q_f \rho_f c_f [T_f(0,\tau) - T_f(H,\tau)] d\tau \tag{3.186}$$

while the right hand side can be expressed as

$$\begin{aligned} \Delta E_{cv} = \sum_{k=1}^{N} \Bigg\{ & 4\pi \int_{r=0}^{R_p} \rho c \left[T_k(r,t) - T_0 \right] r^2 dr \\ & + \frac{4\pi}{3} L \rho \left[S_k^3(t) - R_p^3 \right] \\ & + \frac{4\pi}{3} \rho_w c_w \left[R_s^3 - R_p^3 \right] \left[T_{wk}(t) - T_0 \right] \Bigg\} \\ & + \pi R_T^2 \int_{z=0}^{H} \rho_f c_f \left[T_f(z,t) - T_0 \right] dz \end{aligned} \tag{3.187}$$

Here, the energy balance is formulated on the basis of discharge of heat from the PCM. The PCM, the shell, and the fluid are at the same initial temperature T_0, and the tank has a height H and a radius R_t. The number of spheres in the tank is N which is related to the volume fraction of the PCM sphere as

$$N = (\text{volume fraction of sphere}) \frac{\text{volume of the tank}}{\text{volume of a sphere}}$$

Under these conditions, the first term on the right of (3.187) refers to the energy associated with the change of the sensible heat of the PCM. The second term refers to the energy associated with the phase change. The third term accounts for the energy change in the spherical shell of the PCM spheres, and the last term refers to that energy associated with the change of the temperature of the HTF inside the tank. It is expected that, for an accurate numerical solution of the problem, the left hand side of (3.185) should be equal to the right hand side of the same equation. This energy conservation will be used to check the accuracy of a numerical experiment to be presented in Chapter 5.

CHAPTER 4
TWO DIMENSIONAL PHASE-CHANGE EXPERIMENT

In this chapter, an experiment is described for the purpose of validating the numerical solutions described in the previous chapter. The experimental setup, method of measurements, and data reduction are discussed in detail

4.1 Objective and Basic Considerations

The objective of the experiment is to validate the numerical solutions developed in the previous chapter Since there is lack of data for two dimensional phase change, experimental measurements become necessary In this effort, the interface motion is visualized and measured The measured interface position is then compared with the predicted positions for validation of the numerical solution

It has been well established in phase-change studies that the interface position provides the best indication for the solution error Comparison of the temperature field is often inconclusive even if the interface position is conspicuously in error This is due to the fact that, for a phase change problem, the boundary and interface conditions can be satisfied exactly This leaves little error for the temperature As a result, the temperature provides little resolution for discerning the numerical solution error

To facilitate visualization of the interface position, a test cell of the configuration of a rectangular parallelepiped is constructed. Paraffin wax is chosen as the phase change material because of its very narrow melting range or nearly distinct melting point (Lane, 1986). It also possesses the desired characteristic of becoming translucent to visible light upon phase change from solid to liquid state. The interface position can then be measured by illuminating the wax with an incandescent light source and recording the interface position on photographic films by means of a camera. The thermophysical properties of the paraffin wax are summarized in Table 4.1 (source: Lane, 1983), in which, the melting point listed is the result of experimental measurements that are specifically performed for the study described in this work.

Table 4.1 Thermophysical properties of paraffin wax

Properties		Solid	Liquid
Melting point	(K)	327	-
Heat of fusion	(kJ/kg)	266	
Specific heat	$(kJ/kg\ K)$	2.51	2.95
Conductivity	$(W/m\ K)$	0.24	0.24
Density	(kg/m^3)	760	818

In the experiment, the wax is heated electrically. The apparatus is designed so that the boundary condition can be controlled precisely. Provisions are thus made to simulate the prescribed temperature at the heated side of the wax while keeping the other boundaries of the wax insulated. Since no convection has been

accounted for in the previous analysis, convection in the melted wax must be suppressed in the experiment. This activates the heating of the wax from above, effectively minimizing the free convection.

The large density difference between the solid and the liquid wax (see Table 4.1) presents another concern that is related to the expansion of the wax upon phase change. Another provision is thus made to permit the wax to overflow due to volume change. The experiment is now discussed in detail in the section that follows.

4.2 Experimental Setup and Measurement

4.2.1 The setup

The test setup is provided in a sketch given in Figure 4.1. It consists of three major components: the test cell (*e*), the light source (*f*), and a camera (*a*), as elaborated below.

The test cell is shown in an assembly drawing given in Figure 4.2 and an exploded view shown in Figure 4.3. The test cell measures 12(W)x8(H)x2(D) *cm*. It consists of a wooden frame (*e*, Figure 4.3) covered by double walled transparent lexan windows (*c*,*d*) on its front and back sides. To eliminate the convection heat loss from these windows, outer windows (*c*) are separated from the the inner windows (*d*) by a small gap (0.003*m*). A small Rayleigh number of 9i is found for the gap, providing justification of use of a two dimensional heat transfer analysis for the cell (more justifications to follow). To heat the phase change material, a heater (*f*) is provided at the top of the

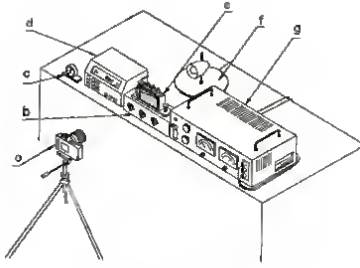

a. Camera
b. Temperature control console
c Timer
d. Digital thermometer
e. Test cell
f. Light source
g. Power supply

Figure 4.1 Test setup

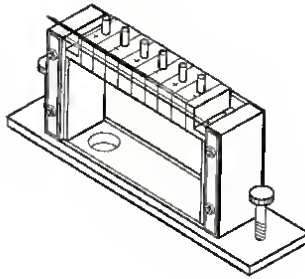

Figure 4.2 Assembly drawing of the test cell

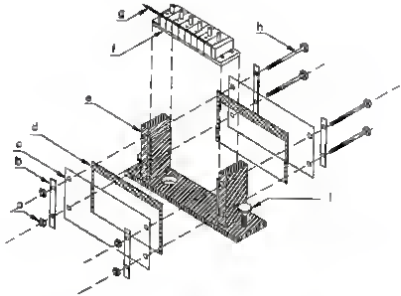

a. Nuts
b. Gaskets
c. Outer windows
d. Inner windows
e. Frame
f. Electric heater assembly
g. Thermocouple wires
h. Bolts
i. Levelling screws

Figure 4.3 Exploded view of the test cell

cell. Driven by a DC power supply (g in Figure 4.1), it is specially designed to incorporate several features as detailed below.

As shown in the drawing given in Figure 4.4, the heater is composed of three heating elements (*b*) which are individually wired to their connectors (*c*). The heater is affixed to the top of a copper plate (*a*), which keeps the temperature distribution uniform in the transverse direction while maintaining a gradual temperature variation in the other direction. Copper-constantan thermocouples (*d*) are attached to the lower side of the copper plate so that they measure the temperature imposed on the phase change material when the heater is in place in the cell. The four holes (*f*) located at the two ends of the plate are lined up with identical holes provided at the flanges of the lid (*e*). These holes are for vent purposes so that, when the phase change material expands, the material can be vented through these holes to the small recess formed between the flange and the wooden frame wall.

Paraffin wax has been used as the phase change material. It is poured into the cell through the hole at the base of the frame (*e* in Figure 4.3). The cell is placed in an upright position with the heater at the top during tests. This causes the wax to be heated from above, a position which effectively suppresses free convection circulation in the cell. As a further precaution for minimizing convection, screws (*i* in Figure 4.3) are used to adjust the interface position so that the interface is leveled at all times in the course of the experiment.

A semi-transparent grid paper is attached to the inner window facing the light source (*f* in Figure 4.1). The grid paper serves dual

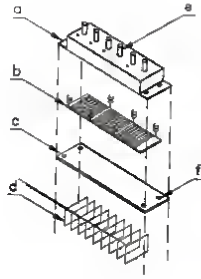

Figure 4.4 Exploded view of the heater

purposes of diffusing the light while also providing grid lines to measure the phase-change interface position. Finally, a camera (as in Figure 4.1) is used to record the images of the wax during phase change.

4.2.2 Test procedure

Prior to the experiment, the melting point of the wax is measured by using a thermometer. During the test, the digital thermometer readings are recorded once every 5 minutes and the interface positions are photographed once every 15 minutes. Because of the time delay that is unavoidable in recording temperatures from one thermocouple station to another, provision is also made to correct for the temperature variation for synchronization. During the time when the camera is not being used to record the interface position, the test cell is covered with an insulation sleeve jacket to eliminate the convection heat loss from the cell.

4.3 Sample Results and Experimental Uncertainty

Sample pictures taken for the interface positions are shown in Figure 4.5. The interface positions are clearly visible. Also, because of the temperature imposed on the wax being nonuniform, there are slight curvatures of the interface close to two ends. In this effort, the grid paper used has a scale of five divisions per centimeter. Repeated tests of reading the interface position over the background grids provides an uncertainty of position reading to be about 0.5mm.

Figure 4 5 Sample picture for interface position measurements

Since the thermocouples are highly accurate (better than ±0.5°C), errors of the experiment come primarily from the (interface) position reading

CHAPTER 5
RESULTS AND DISCUSSION

In this chapter, numerical experiments will be provided for the validation of the solution methods described in Chapter 3. Numerical solutions of one dimensional Stefan problems will be discussed first. Results for such problems will be compared with exact solutions and the results published in the literature. Solutions of two dimensional problems follow next and they will be validated by comparing them with some limiting cases and the experimental measurements described in Chapter 4. Finally, numerical results of the latent heat TES systems will be discussed.

5.1 Numerical Results of One Dimensional Problems

Eight test cases (Table 5.1) are presented for verifying the methods developed for the solution of the Stefan problem. Results are compared with analytical solutions as well as the solution methods documented in the literature. Both aluminum and paraffin wax have been tested whose property values are listed in Table 5.2. It is noted that the properties of the wax are taken to be the average of the values of the solid and the liquid state as reported in Bilek and Choi (1992a).

5.1.1 Test of accuracy and stability

Prior to the test of the stability and accuracy for the numerical solutions developed in this work, the superposition concept

Table 5 1 Cases tested for one dimensional Stefan problems

Test Case	Test Performed	Boundary and Initial Conditions (T in K, q in W/m^2 t in s)	PCM and Processes
1	Validation of the superposition method and test of stability and accuracy	T_m=363 T_i=T_m−327	wax, one-phase melting in a semi-infinite domain
2	Further validation of the superposition method	T_m=732+81^2 and q_m=6 39x10^5+3 87x10^{4}t^2, T_i=500 < T_m	aluminum two-phase melting in a semi-infinite domain
3	Further validation of the superposition method	T_m=336 7 at x=0, and q_m = 0 at x=H T_i = 317 5 < T_m	wax, two-phase melting in a finite domain
4	Stefan-number effect on interface position in finite domain	T_m= 336.7 at x=0 and q_m = 5 at x=H T_i=327 278.5 and 230	wax, two-phase melting in a finite domain
5	Test of oscillating interface for long time solution	T_m=364+20sin(πt/300) at x=0 and T_m=309 at x=H, T_i = T_m=327	wax, two-phase melting in a finite domain
6	Test of multiple interfaces in finite domain. one interface initiated from each side	T_m=732 at x=0 and T_m=315 at x=H T_i = T_m=327	aluminum, one-phase freezing in a finite domain
7	Test of multiple interfaces in finite domain. melting and freezing initiated at one side	T_m=933+0 02(100t-t^2) at x=0 and q_m=0 at x=H T_i=T_m=327	aluminum two-phase melting and freezing in a finite domain
8	Test of solution in spherical system	T_m=424 T_i=T_m=327	wax, one-phase melting of a sphere

Table 5.2 Properties of PCMs analyzed

	Aluminum	Paraffin Wax
T_m [K]	932	327
L [kJ/kg]	376.56	200
k [W/mK]	200	0.24
ρ [kg/m^3]	2.710	780
c [kJ/kgK]	1.2	2.73

is first tested by applying it to the solution of a Stefan-Neumann problem described in Test Case 1 (Ste=0.21) in Table 5.1. For this problem, the exact solution is readily available. Also, the solution of this problem is a semi-infinite domain, Eqs (3.45)-(3.49), can be treated as the solution in a finite domain, Eqs (3.52)-(3.55), if the boundary conditions at the back side of the domain is chosen properly. Thus, a uniform Δx can be used for solution. As shown in Figure 5.1, the decomposed profiles U and V can be superimposed for T. There is a distinct interface position, which does not oscillate in space. The superposition concept has thus been tested successfully.

Figure 5.2 shows the interface positions versus time for different values of Δt and Δx. In the top figure, a uniform grid of 90 points is used for the solution of U. In this effort, the time step varies from 60 to 600 s, corresponding to the Fourier modulus ($\alpha\Delta t/\Delta x^2$) from 18.5 to 185. As shown in this figure, the results converge even with a time step size as large as 600 s.

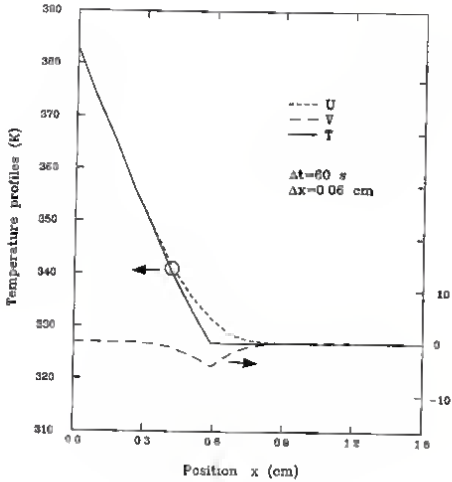

Figure 5.1 Temperature profiles of the superposition method

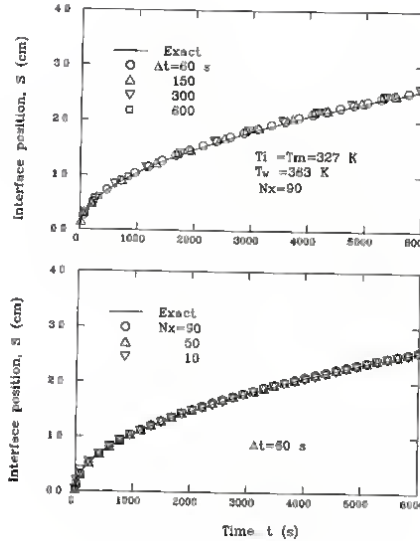

Figure 5.2 Test of accuracy and stability using different Δt and Δx

The bottom figure gives the interface positions for Δt equal 60 s. Here, the number of grid points varies from 10 to 60. Again, the results are good; in fact, they are stable in both tests. It is noted that the implicit method of solution employed here permits use of large time steps together with a coarse grid, which is not possible for explicit method of solution.

Efforts have also been made for identifying the time when the largest numerical error occurs. As shown in Figure 5-3, with Nx taken to be 90 and Δt varying from 60 to 600 s, the largest error (10%) is always found at the first time step, which is consistent with the findings for the SSM as reported by Choi and Hsieh (1992). This percentage error is diminished rapidly (less than 1%) toward large time, a distinct feature for this method.

Case 2 (Table 5-1) provides a more thorough test of the superposition method based on the development of the numerical solution given in this work. In this case, time-variant temperature and flux conditions are imposed on a semi-infinite medium (aluminum), which is initially subcooled (see Table 5-1). A two-phase melting thus occurs and the numerical results are compared with the SSM results reported by Hsieh and Choi (1992a) and Choi (1992).

For Case 2, 60 nonuniform grids are used for the solution of U, while the time step is taken to be 1 s. The interface-position-versus-time results are shown in Figures 5-4 and 5-5. In Figure 5-4, the medium is imposed with a time-variant temperature condition, while in Figure 5-5, the medium is imposed with a time-variant flux condition. Numerical results are in good agreement with the SSM results obtained

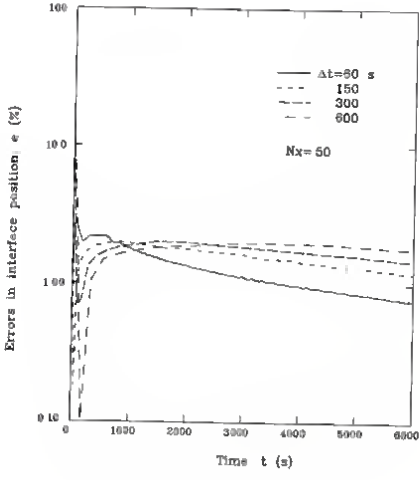

Figure 5 3 Errors in the interface positions for different Δt

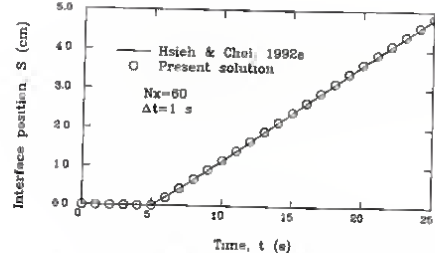

Figure 5.4 Interface positions for time-variant temperature condition

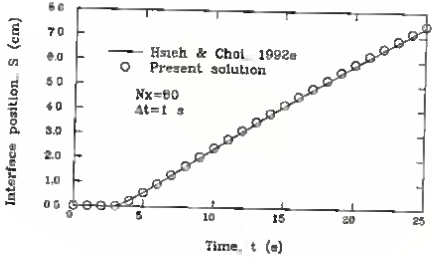

Figure 5.5 Interface positions for time-variant flux condition

by Reich and Chen (1982a), providing further assurance of the success of the superposition method.

The third test case (Case 3 in Table 5.1) deals with a problem in a finite domain. In this case, the slab is initially subcooled in a solid state with one side ($x=H$) insulated and the other side ($x=0$) imposed with a constant temperature condition. To compare the results with the published data given in the literature (Dursunkaya and Nair, 1990), the following dimensionless groups are introduced

$$Ste=\frac{c(T_w-T_m)}{L}, \qquad Sb=\frac{T_m-T_i}{T_w-T_m}$$

$$\bar{x}=\frac{x}{H}, \qquad \bar{T}=\frac{T-T_m}{T_i-T_m}, \qquad t=\frac{\alpha t}{H^2} \tag{5.1}$$

where Ste is the Stefan number and Sb is a subcooling number. Paraffin wax is again used for tests which is taken to be 1 cm thick divided into 10 grid points. The initial and boundary conditions listed in Table 5.1 are specially selected to yield a Stefan number of 0.1 and a subcooling number of 1, which have been used by Dursunkaya and Nair in their original paper. Results are shown in Figures 5.6 and 5.7. In Figure 5.6, the dimensionless interface position is plotted as a function of the dimensionless time. The present results are in good agreement with Dursunkaya and Nair's data. As shown in this figure, it takes a value of $\bar{t}$ of 5.3, which corresponds to 4600 s, for the slab to be melted completely. Figure 5.7 gives the dimensionless temperature history at the insulated side ($x=H$) of the wall. The wall temperature

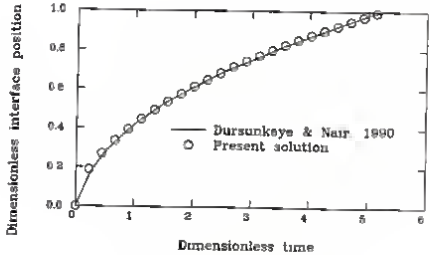

Figure 5.6 Interface positions in a finite domain

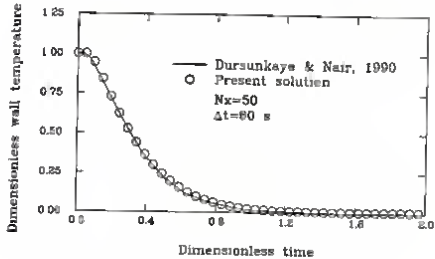

Figure 5.7 Temperature history at the insulated wall ($x=H$)

remains constant for a short while after time zero, signifying the time period when the heat has not penetrated through the depth of the wall. Then, the dimensionless temperature drops, indicating a temperature rise at the insulated side. Again, the results are in good agreement with the published data in the literature.

5.1.2 Subcooling effect on the interface position

Case 3 provides a good test for the assessment of the effect of subcooling on interface motion. The initial temperature of the wax in Case 3 is varied (230, 278.5, and 327 K) as listed in Case 4 (Table 5.1) and the results are plotted in Figure 5.8. Here, Neumann solutions in a semi-infinite domain are also attempted and their results plotted in curves for comparison. As shown in this figure, for a given subcooled condition, the interface front in a finite domain (symbols) first follows that in a semi-infinite domain. Later, they depart from each other. Eventually, all curves for the finite domain (symbols) move at same speed, which is evidenced by their identical slope at large time. These phenomena can be attributed to the fact that, since the medium is subcooled initially, it takes time for the heat supplied at $x=0$ to penetrate through the depth of the wall. Consequently, during the initial period of time to heat the wall, the heat transfer in a finite domain is equivalent to that in a semi-infinite domain with the same degree of subcooling. Once the heat penetrates through the wall and reaches the insulated boundary, the temperature at this boundary starts to rise. Then, the interface in a finite domain moves in a heated medium at a higher speed. From another

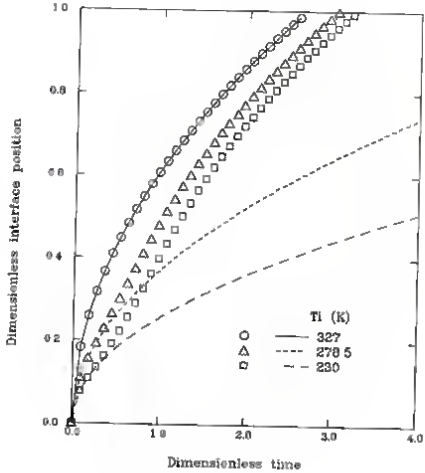

Figure 5.8 Interface positions for different subcooled conditions

perspective, the sodium in a finite domain with back side ($x = H$) insulated may be considered to be pre-heated prior to melting. Thus, for the final stage of melting, the sodium is fully pre-heated to its melting point, the problem reduces to a one-phase melting in a Stefan-Neumann problem.

5.4.3 Solution with oscillating interfaces

An interesting case arises when the wall is initially at its melting point but in solid state. For time greater than zero, the boundary at $x = 0$ is imposed with a sinusoidal temperature condition which is at a level higher than the melting point of the sodium. The boundary at $x = H$ is imposed with a constant temperature condition which is lower than the melting point of the sodium. Case 5 represents such conditions and the results are plotted in Figure 5.9, where two curves are plotted for comparison. The dashed line represents the case when the boundary at $x = 0$ is raised to a constant temperature of 354 K. The solid curve represents the boundary imposed with a sinusoidal temperature, which differs from the previous condition by that mean term (see legend). For both curves, the conditions at the other side ($x = H$) are identical. Clearly, because of the boundary conditions imposed, the interface position rapidly reaches a quasi-steady state. The solid curve fluctuates about the dashed curve, which eventually reaches the mid-phase of the sinusoidal. Using the dashed curve as a basis, there is approximately a 10 degree angle of phase delay. The interface oscillates at the same frequency as the imposed temperature cycle. The long-time cyclic solution presented here is believed to be the first

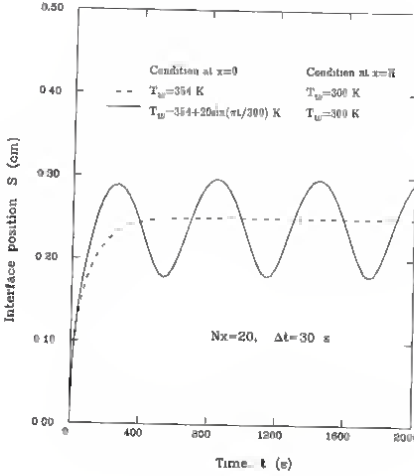

Figure 5.9 Test of oscillating interface

that addresses quasi-steady temperature variation accompanied by a phase change A more detailed follow-up study is being made by Myres and Hanch (1993)

5.1.4 Solution with multiple interfaces

Case 5 deals with a situation where the phase change is initiated from one side of the wall A variation of that is for interfaces initiated from two sides of the wall Two cases (Cases 6 and 7) are included to address such problems as listed in Table 5.1. Case 6 is for solidification of a 5 *cm* thickness slab initially in liquid state at its freezing point Both sides of this slab are exposed with constant temperature conditions which are at the levels lower than the freezing point of minimum. Phase change is thus initiated from both of the boundaries and the interfaces move toward with time as shown in Figure 5.10. Based on the Stefan number defined in (5.1), the boundary at $x=0$ is imposed with a Stefan number of 0.637, while the boundary at $x=H$ is imposed with a Stefan number of 0.319 For this problem, the interface motion can be analyzed by means of a one-phase Stefan-Neumann solution

The superposition method is tested for this case as shown in Figure 5.11 The interface positions are plotted versus time as shown in Figure 5.12, where the numerical results are compared with the Stefan-Neumann solutions. The two interface fronts move independently of each other until they merge at 2.88 *cm* The results are in good agreement with the analytical solutions

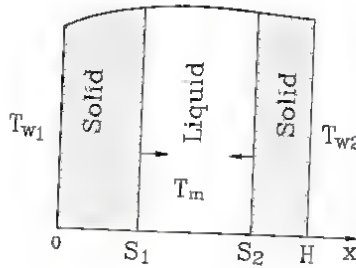

Figure 5.10 Sketch of double interfaces generated by conditions imposed on two boundaries

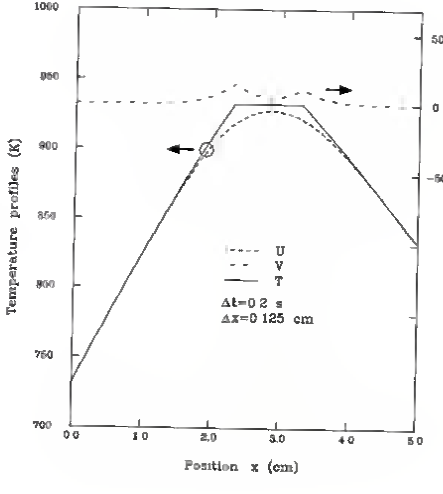

Figure 5.11 Temperature profiles for a double-interface problem

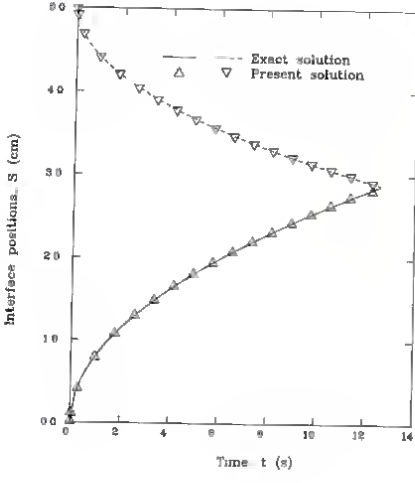

Figure 5.12 Interface positions of a double-interface problem

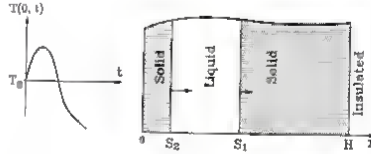

Figure 5-13 Sketch of double interfaces generated by conditions imposed on one boundary

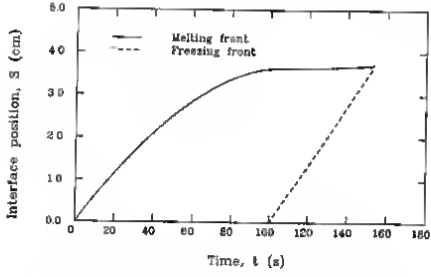

Figure 5-14 Interface positions of a melting-freezing problem

Case 7 deals with a different situation in that the phase changes are initiated from the same side of the boundaries in a plane wall. A thick aluminum wall is considered, which is initially at its melting point but in solid state. At time greater than zero, the boundary at $x=0$ is exposed with a time-variant temperature condition while the other at $x=H$ is insulated (see Table 5.1). Because of the conditions imposed, the medium first melts and then re-freezes as shown in Figure 5.13. The interface histories are plotted in Figure 5.14. Here, because of the rapid temperature drop at the boundary for time greater than 100 s, the freezing front rapidly overtakes the melting front. They eventually merge at 153 s, when the medium returns to its solid state.

5.1.5 Melting of a sphere

In all the tests performed above, the phase change has been considered in a Cartesian system. Case 8 deals with a one dimensional phase change in a sphere which is initially at its melting point but in solid state. The surface is suddenly heated to a constant temperature greater than the melting point as described for this case in Table 5.1. There is no exact solution for this problem. Hill (1987) solved this problem by an integral method, and derived the lower and upper bounds for the interface position as given by the following formulae:

$$\overline{r}^2 \geq \frac{1}{36(Ste)^2}\,(1-\overline{S})^2\left[(1+2\beta)(1+\overline{S})+2(\beta-1)\overline{S}^2\right]^2$$

$$+\frac{1}{60(Ste)}\,(1-\overline{S})^2\left[(1-\overline{S})(1+4\overline{S})+4\beta(1+3\overline{S}+\overline{S}^2)\right] \qquad (5.2)$$

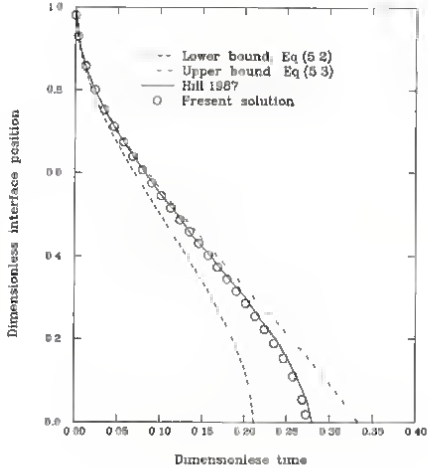

Figure 5.15 Interface positions of sphere melting

$$\leq \frac{1}{6(Ste)}\left[(1+2\beta)(1+\bar{S})+2(\beta-1)\bar{S}^2\right]$$

$$+(1-\bar{S})^2[1+2\beta+(\beta-1)\bar{S}]\Big/6[1+(\beta-1)\bar{S}] \qquad (5.3)$$

where $\beta = k/hR_x$, $\bar{S} = S/R_x$, and $t = \alpha t/R_x^2$

For the temperature condition imposed in Case 5, β in Eqs (5.2) and (5.3) are zero and Ste is unity. Numerical results are shown in Figure 5.15, where the interface position predicted by the present method is in good agreement with the approximate solution result provided by Hill (1987). Also the curve stays within the bounds predicted by using Eqs (5.2) and (5.3)

It should be mentioned that all the results presented above are solved by using a 486/33 PC. In the analytical solutions of Eqs (3.54), (3.55), and (3.57) involving infinite series, sufficient number of terms have been taken in the partial sum to ensure convergence (10^{-6}). The CPU time used in the computations of the one dimensional problems varies from a few seconds to several minutes.

5.2 Numerical Results of Two dimensional Problems

Tests of two dimensional solutions are somewhat handicapped by the lack of literature data for comparison. Reliance is thus made of some limiting cases which provide for tests of stability and accuracy of solution, in the situations when such tests are unavailable, use is made of experimental measurements for comparison of the interface position.

Table 5 3 Cases tested for two-dimensional Stefan problems

Test Case	Tests Performed	Boundary and Initial Conditions (T in K, q in W/m^2, t in s)	FCM and Processes (x and y in cm)
1	Test of stability and accuracy	T_w=397 − 100 $\lvert \frac{y}{20} \rvert$ at y=0 other boundaries insulated $T_i = T_m$ − 327	wax, one-phase melting in a finite domain of $-5 \le x \le 5,\ 0 \le y \le 4$
2	Test of long-time solution	T_w= 373 at y=0 free convection at $x = \pm \frac{W}{2}$ $T_i = T_\infty$=288 < T_m	wax, one-phase melting in a semi-infinite domain of $1.25 \le x \le 1.25$
3	Test of short-time solution by comparison with experimental data	T_w and T_i taken from experimental measurement	wax, two-phase melting in a finite domain of $0 \le x \le 12,\ 0 \le y \le 8$
4	Test of multiple and coalescing fronts	$T_w = \begin{cases} 327 + f(x,t), & t < 1800 \\ 327 - f(x,t), & t > 1800 \end{cases}$ where $f(x,t) = 8.9013^{-5}(1.5 - \frac{x}{W})(1800 - t^2)$ T_i=327 K < T_m	wax, two-phase melting and freezing in a finite domain of $0 \le x \le 10\ \ 0 \le y \le 3$

5.2.1 Test of accuracy and stability

Case 1 (Table 5.3) tests the stability and accuracy by solving the phase change in a two dimensional domain sketched in Figure 5.18. The bottom boundary is imposed with a space-variant temperature condition, while the other three sides are all insulated. Wax initially at melting point in a solid state is used for experiments.

To test the stability of solution, a 40x30 grid is used to solve the problem in x and y direction. The time step varies from 30 to 600 s, which corresponds to dimensionless time steps (Fourier modulus) of 0.5 to 10. Figure 5.17 gives the numerical results for interface position histories at $x=0$ and $x=H/2$. Two groups of curves are plotted. In each group, the solid line is an analytical solution of a Stefan-Neumann problem imposed with a uniform temperature condition. This provides for the upper bound for the interface position at $x=0$ and the lower bound for the interface position at $x=H/2$. The dashed curves give the numerical results for the two dimensional problem. These dashed curves stay within the bounds. Most importantly, all dashed curves are smooth and converge nicely irrespective of the values of the time step tested.

Figure 5.18 gives the interface position at a time equal to 3000 s. Four different time steps are tested and the curves are smooth and convergent. No instability is encountered even with the use of a time step as large as 600 s. It is thus concluded that the explicit treatment of the partial differentiation in the x direction of the V problem, Eq (3.107), does not introduce any instability in the solution. In two-dimensional problems, the time steps are determined

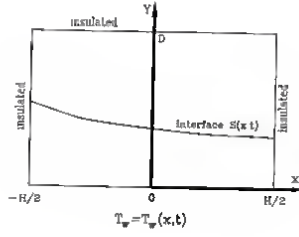

Figure 5 16 System used in two-dimensional stability test

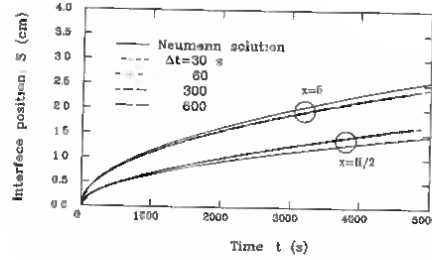

Figure 5.17 Interface positions at different times at x=0 and x=π/2

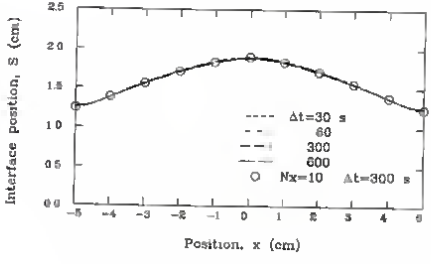

Figure 5.18 Interface position curves at t=3000s for different Δt

strictly on the basis of the accuracy rather than the stability. This also serves to verify numerically the comments made earlier at the end of Chapter 3.

It should be noted that the stability of the numerical solution demonstrated in this work is independent of the number of the grid points used in the x direction. A reduction of the number of the grids by a factor of four (N=10) and application of a time step of 300 s yield data (circles) which fall right on the curves in Figure 5.18. This also serves to demonstrate the efficiency of the method.

5.2.2 Long-time solutions

Case 2 is intended for testing the convergence of the results to a long-time solution. As summarized in Table 5.3, a column of medium of infinite height initially subcooled is used for tests. A uniform temperature is imposed at the bottom boundary while the lateral boundaries dissipate heat to ambient by convection (Figure 5.19). Heat transfer in the column is thus two dimensional. There is no exact solution of this Stefan problem. However, a steady-state solution can be derived as follows

$$\frac{T-T_m}{T_w-T_\infty}=\sum_{m=1}^{\infty}\frac{2(\beta_m^2+Bi^2)}{(\beta_m^2+Bi^2)+Bi}\,\frac{\sin\beta_m}{\beta_m}\,e^{-2y\beta_m/H}\cos(2x\beta_m/H) \qquad (5.4)$$

where $Bi=hB/2k$ is the Biot number, and β_m's are roots of

$$\beta_m\tan\beta_m=Bi, \qquad m=1,2,\ldots \qquad (5.5)$$

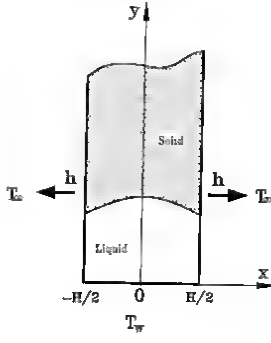

Figure 5-19 System used for long-time solution

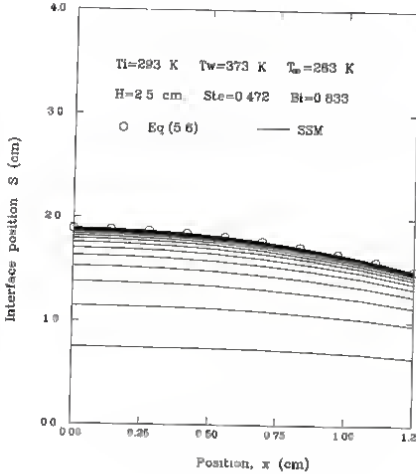

Figure 5 20 Comparison of numerical and analytical solutions for a two-dimensional problem at long time

This steady-state solution can be used for checking the interface position at long time by setting y to $S(x)$ and T to T_m in (5.4) as

$$\frac{T_m - T_{\infty}}{T_o - T_{\infty}} = \sum_{m=1}^{\infty} \frac{2(\beta_m^2 + Bi^2)}{(\beta_m^2 + Bi^2) + Bi} \frac{\sin\beta_m}{\beta_m} \cos(2x\beta_m / H) e^{-2S\beta_m / H} \qquad (5.6)$$

The interface position results are shown in Figure 5.20. Here, because of the temperature symmetry, only one half of the medium is used for presentation. As shown in this figure the interface position curves determined by the source-and-sink method (Section 3.4) move upward with time. The topmost curve, representing the steady state limit, is in close agreement with the analytical results (circles) predicted by using (5.6). In this analytical efforts, sufficient number of terms have been taken in the partial sum in the infinite series to ensure convergence (10^{-6}). The two dimensional test is thus successful at long time as shown clearly in this example.

5.2.3 Comparison with experimental results

What remains to be done is to test the two dimensional solution at short time. This is accomplished by comparing the short-time experimental results with those obtained using the numerical methods given in this work. A composite diagram is constructed as shown in Figure 5.21. Here, the data at the top refer to the imposed temperature conditions at the surface of the paraffin wax as measured

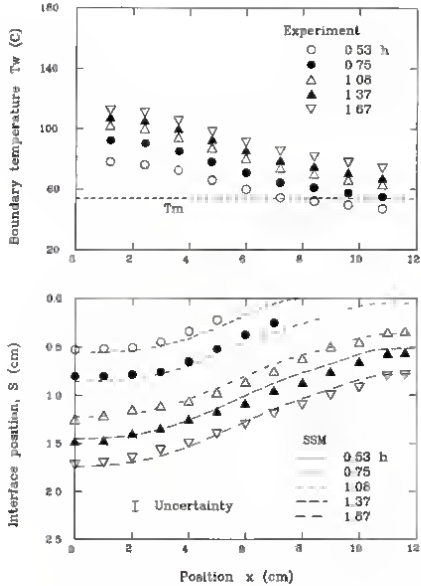

Figure 5 21 Comparison between numerical results and experimental data for two-dimensional phase change

from the experiment described in Chapter 4, while the bottom figure shows the positions of the phase-change interface. The y axis for this lower figure is intentionally drawn up-side-down so that it confirms with the analysis (Figure 3.2). It is noted that, in the computation, the z-direction is discretized into 24 elements and, once again, sufficient number of terms are taken in the Green's function to ensure convergence (10^{-6}). As shown in this lower figure, the agreement between the experiment (symbols) and the analysis (curves) is good. There are small discrepancies only in the middle section of the curve which can be attributed to the curvature of the phase-change interface position in the experiment, the leveling screws described in Section 4.2 are used to adjust the slope of the middle section of the interface curves. A leveling of this section of the curves upsets the slope at two ends. As a result, the convection can not be totally eliminated from the test cell, causing the slight disagreement between the prediction and the experiment.

5.2.4 Test for coalescing fronts

A general case of multiple coalescing fronts is tested as Case 4 (Table 5.3). Wax at melting temperature in solid state is tested which is imposed with a position- and time-varient condition at $y = 0$ (Figure 5.18) as follows:

$$T_w(z,t) = \begin{cases} 327 + 8.0\times10^{-5}(1.5 - \frac{z}{H})(1800t - t^2), & t < 1800 \text{ s} \\ 327 - 8.0\times10^{-5}(1.5 - \frac{z}{H})(1800t - t^2), & t > 1800 \text{ s} \end{cases} \tag{5.13}$$

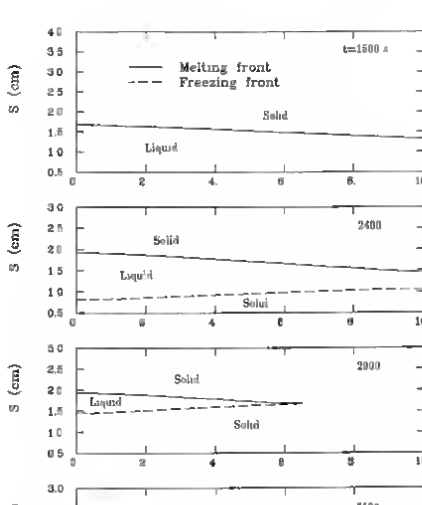

Figure 5.22 Interface position curves in a two-dimensional coalescing-front problem

Here, the sign for the second term is changed so that, for time less than 900 s, the boundary temperature decreases in the x direction yet the local boundary temperature increases with time. However, for time greater than 900 s, this local temperature decreases with time. Since the first term in both conditions refers to the melting point of the wax, $T_m(x,t)$ is greater than the melting point for time less than 1800 s while it is less than the melting point for time greater than 1800 s. The wax thus melts and re-freezes unevenly in the x direction, giving rise to a two dimensional multiple-coalescing-front problem.

The wax melts and re-solidifies as shown in Figure 5.22. No literature data have been available for comparison. Yet, the two dimensional interface motions are clearly visible due to the position-variant temperature conditions imposed.

5.3 Applications to Two Dimensional Latent Heat Thermal Energy Storage Systems

In this section, numerical results of a sample latent heat TES unit will be presented. The unit is composed of stacked rectangular PCM plates with fluid passages in between (see sketch in Figure 3.5). The input data for analysis has been compiled in Table 5.4. The unit is precharged to 80°C. Since the melting point of the PCM is 72°C, the PCM is initially in a liquid state. Cold water at 23°C is passed through the unit at three different flow rates: 1 gpm, 2gpm, and 3 gpm. The total amount of energy pre-stored in the unit is 63.5 MJ. In the numerical tests, calculations ceases as soon as the exit water temperature drops down to 40°C.

Table 5 4 Input data for TES analysis

PCM – $Na_2PO_4 \cdot 12H_2O$	
Conductivity, k $(W/m \cdot K)$	0 6
Heat capacity, c $(kJ/kg \cdot K)$	1 7
Density, ρ (kg/m^3)	1,630
Latent heat L (kJ/m^3)	110
Melting point, T_m $(°C)$	72
HTF – Water	
Conductivity, k_f $(W/m \cdot K)$	0 58
Heat capacity, c_f $(kJ/kg \cdot K)$	4 19
Density, ρ_f (kg/m^3)	1,000
Overall initial temperature, T_o $(°C)$	80
HTF inlet temperature, $T_f(0,t)$ $(°C)$	23
Volume flow rate, $\dot{Q}$ (gpm)	1,2,3
Other specifications –	
PCM length, H (m)	2
PCM width W (m)	0 5
PCM half thickness, D (m)	0 02
Channel width, $2d$ (m)	0 01
Number of PCM plates, M	4
Containing wall thickness, b_w (m)	0 0

The accuracy of the numerical simulation is tested by means of the energy conservation described in Section 3.5.3. A comparison of the left and right hand side of Eq (3.167) is shown in Figure 5.23. For all the flow rates from 1 gpm to 3 gpm, the maximum error is found to be about 3% at the end of the process, which provides a good indication of the accuracy of the present model.

The water exit temperatures during the discharge process are plotted in Figure 5.24. For a flow rate of 1 gpm, the unit runs for 170 minutes before the exit temperature drops down to 40°C. For a flow rate of 2 gpm, it works for 95 minutes, and for 3 gpm, it works for 70 minutes. Out of the 83.5 MJ energy initially stored in the unit, the energy extracted from it is 85.5, 54.3, and 52.9 MJ for the flow rate of 1, 2 and 3 gpm, respectively. It is noted that, in the temperature curves shown in Figure 5.24, the slope of the curves changes erratically. This is believed to be the result of the release of the latent heat from the PCM.

The temperature distribution in the PCM at 2-gpm flow rate is shown in Figure 5.25. It should be noted that the plots are re-scaled to make them easy to read. The topmost figure shows the positions of the isotherms in the PCM after 20 minutes of energy discharging. At that time, the lower region of the PCM is solidified where there is a large temperature gradient (see the dense temperature contours). The upper region remains in the liquid state. The solid/liquid interface can be identified by the sharp change of the density of the isotherms. At 40 minutes (second figure), the left part of the PCM is completely solidified and in uniform at phase-change temperature. The liquid

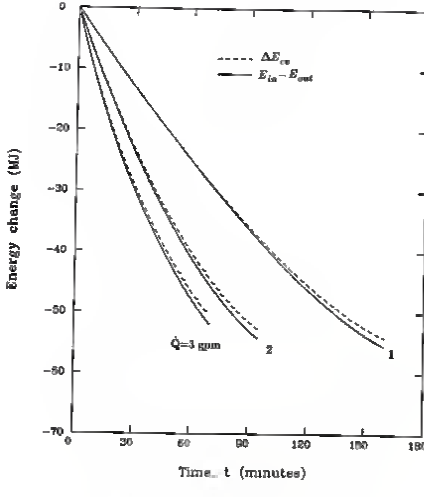

Figure 5.23 Test of energy conservation

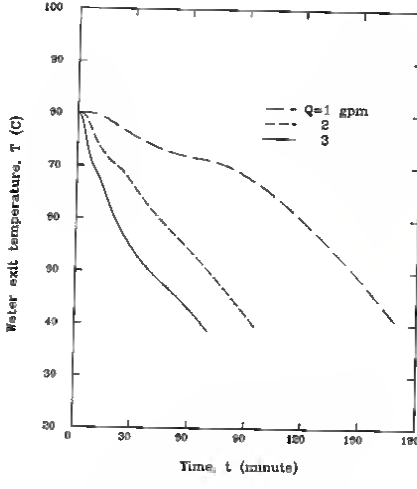

Figure 5 24 Water exit temperature at different flow rates

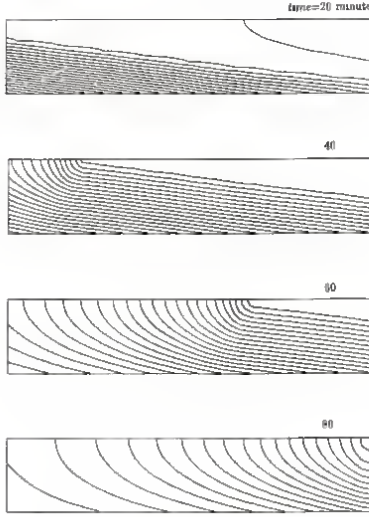

Figure 5.26 Isotherms in a half PCM plate

region diminishes in size until the PCM is completely solidified (bottom figure). After that, only sensible heat remains in the salt.

5.4 Application to Encapsulated PCM TES Systems

Numerical results for the encapsulated PCM TES system will be discussed in this section. The input data for the PCM, the HTF, and the working conditions are the same as those listed in Table 5.4. Only the specifications are different, which are listed in Table 5.5. The parametric study will include the effects of the HTF flow rate, and the diameter and the thickness of the PCM ball on the thermal performance of the TES.

Table 5.5 Specifications of encapsulated TES unit

Height of tank, H (m)	1.1
Radius of tank, R_t (m)	0.21
Overall void fraction, μ	0.4
Diameter of sphere, $2R_s$ (cm)	2, 3, 4
Shell thickness, $R_s - R_p$ (cm)	0.0, 0.2, 0.5

The accuracy of the numerical results is evaluated first by means of the energy conservation as described in Section 3.0.3. In this test, the diameter of the balls is taken as 3 cm, and the thickness of the shell is 0.2 cm. A comparison of the two calculations

of the energy change from Eqs (3 186) and (3 187) is shown in Figure 5 26 It is found that, for all the flow rates tested (1 gpm to 3 gpm), the maximum error is approximately 3% The numerical results are thus accurate

Parametric study results will be discussed next. In Figure 5 27, the water exit temperature is plotted versus time for three flow rates. As expected, for a lower flow rate the unit operates longer, for a higher flow rate, the unit operates shorter However, the total amount of energy extracted from the unit remains almost the same

The effect of the ball diameter on the water exit temperature is shown in Figure 5 28 For the three diameters tested (2 cm to 4 cm), the thickness of the shell is taken to be constant at 0 2 cm As expected, for a ball of small diameter, because of the presence of the shell, the volume fraction of the PCM is smaller As a result, less energy can be stored in and extracted from the ball As the ball diameter is increased the volume fraction of the PCM increases correspondingly However, a large ball is penalized for the smaller surface-to volume ratio The heat transfer rate is thus lower, as shown in Figure 5 28

The effect of the shell thickness is shown in Figure 5-29 It may be said that the main drawback of having a thick shell is the reduction of the volume fraction of the PCM. For example, for a ball of 3 cm diameter, when the shell thickness is increased from 0 2 cm to 0-5 cm, the volume occupied by the PCM is reduced by 54 3% This greatly reduces the energy that can be stored in the unit, as clearly shown in Figure 5 29

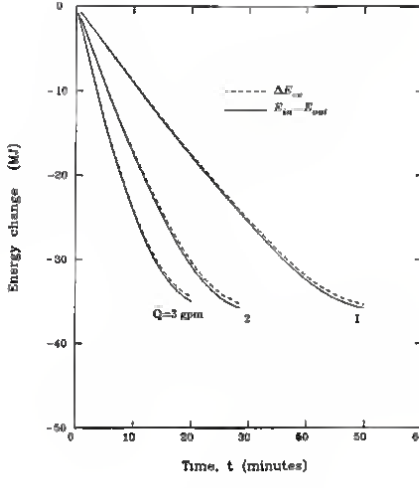

Figure 5 28 Test of energy conservation

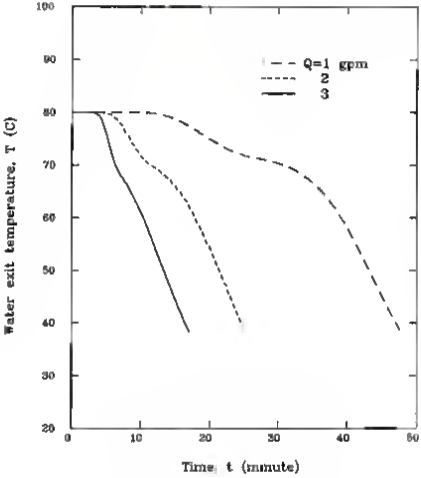

Figure 5 27 Water exit temperature at different flow rates

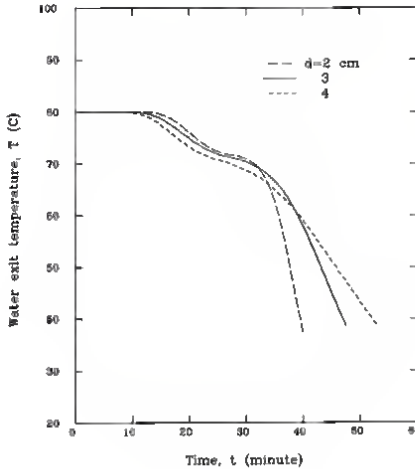

Figure 5-28 Water exit temperature for different ball diameters

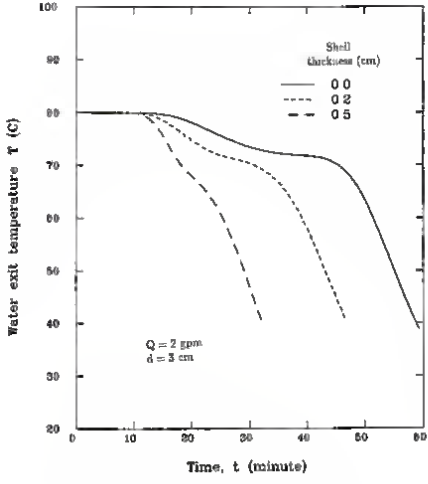

Figure 5.29 Water exit temperature for different shell thickness

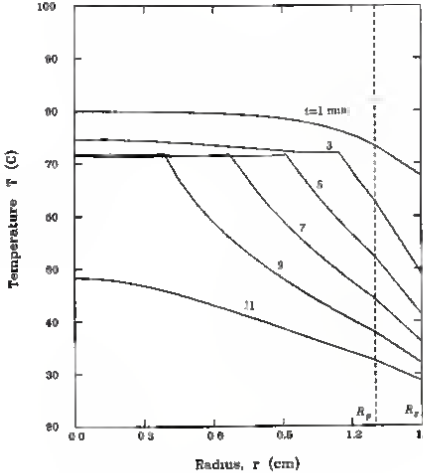

Figure 6.30 Temperature profile in the PCM and the shell

It is also informative to compare the temperature distribution in the PCM ball (see Figure 5.30). Here, the topmost curve refers to a situation when the PCM is still in the liquid state since there is no abrupt change of the temperature slope in the ball. Phase change takes place at 3 though 9 minutes. The interface moves toward with time. At 11 minutes, the PCM has completely solidified. Only sensible heat is being extracted from the ball.

5.5 Visualization of Numerical Results

To graphically visualize the operation of the latent heat TES system, two animating post-processors are developed using a QuickBASIC language. Sample outputs of the post-processors from a computer screen are shown in Figures 5.31 and 5.32. From the graphics, the interface position, the flow rate, the exit water temperature, the available energy left in the unit, and other system information can be viewed simultaneously.

Figure 5.31 Post-processor for a two dimensional TES unit

Figure 5.32 Post-processor for an encapsulated TES unit

CHAPTER 6
CONCLUSIONS AND RECOMMENDATIONS

Based on the analysis and results of the present work, the following conclusions can be drawn:

1. A source-and-sink method has been developed for the solution of multi-dimensional phase-change problems. The method has been shown to be accurate by comparison with exact analysis and experimental measurements. In the source-and-sink method, only one set of equations is required to solve for the temperatures in both liquid and solid phase regions.

2. The success of the present method relies on the use of superposition technique. The validity of the superposition method for the solution of Stefan problems with constant and equal properties in different phases has been rigorously analyzed. In the superposition method, the solution of the Stefan problem was superimposed by a finite difference method, which was used to calculate the temperature distribution due to the initial and boundary conditions, and an analytical solution, which was used to track the interface position and to update the temperature due to the motion of the interface. For multi-dimensional problems, a hybrid scheme was developed which combines an analytical solution in one direction and a finite difference method in another direction. With these efforts, a fine

marching scheme was developed with which both short time and long time solutions can be obtained.

The stability of the solution methods for one and two dimensional Stefan problems was analyzed and numerically tested. No instabilities were encountered in the tests even for very large time steps. This provides assurance of stable and converged solutions.

3. In the hybrid method of solution, the subcooling and superheating conditions can be handled conveniently. It is not necessary to divide the solution into pre-melting, melting, pre-freezing, and freezing stages. Furthermore, the initial condition can be uniform and nonuniform, and the domain of solution can be finite and semi-infinite. In this work, the effects of subcooling on the interface positions in a finite medium have been studied. Problems with oscillating interfaces resulting from time-variant boundary conditions have also been solved.

4. With the use of multiple source and sink method, multiple interfaces resulting from periodic melting and freezing are encountered in the discharging/recharging processes of a latent heat TES unit were successfully calculated. Coalescing fronts in a two dimensional melting and freezing problem with multiple phase regions were also investigated.

5. A two dimensional phase change experiment was conducted for testing the accuracy of the short-time solutions of the numerical method. An analytical solution was used for the test of accuracy for long-time solutions. In both cases, the interface positions were used

for comparison. Numerical results were in good agreement with the experimental measurements as well as the analytical solutions.

6. Applications of the solution methods to the simulation of latent heat thermal energy storage units were discussed. Two conjugate heat transfer problems were solved for the prediction of thermal performance of two TES units. The first one was composed of parallel channels formed by stacked PCM plates, and was modeled as two dimensional conjugate problems. The second was an encapsulated TES unit consisting of packed PCM spheres. In both cases, the accuracy of the numerical method was tested by means of energy conservation based on open-system thermodynamic analysis. It has been shown from the numerical results presented in Chapter 5 that the present methods were accurate and efficient.

Parametric studies of the encapsulated TES unit were also attempted. The effects of the flow rate, the diameter and the shell thickness of the PCM sphere on the thermal performance were analyzed. Two post-processors for graphical visualization of the TES system performance were also developed.

The following are recommended for further work:

1. The source-and sink method with superposition technique will be extended to the solution of three dimensional phase-change problems such as laser cutting, drilling, and surface hardening.

2. The properties of the PCM in the present analysis have been considered as constant and equal in different phase regions. In the

future work, unequal properties for different phase regions will be solved by using double sources and sinks as analyzed in Koladner (1986). The variation of the thermal conductivity with temperature will also be accounted for by using Kirchhoff transformation if convection does not appear at the boundary.

3. In the present analysis, the source-and-sink method requires the formulation of the Green's function. In the case where the Green's function can not be analytically formulated, a modification scheme that combines the source-and-sink method and the boundary element method reported recently (Heleh, 1993) can be used. In the boundary element methods, the Green's free space solutions can be used to replace the Green's functions which strongly rely on the geometry of the domain as well as the boundary conditions.

APPENDIX A
DERIVATION OF EQUATIONS (3.52) AND (3.53)

In Cartesian coordinate systems, the decomposed temperature V is given by (see Eq. (3.40))

$$V(x,t_1)=\frac{L}{k}\int_{\tau=t_0}^{t_1}\frac{dS(\tau)}{d\tau}G(x,t_1\,|\,S(\tau),\tau)d\tau \tag{A.1}$$

In a finite domain, the Green's function for a temperature condition imposed at $x=0$ is given by (see Eq. (3.50))

$$G(x,t\,|\,x\ \tau)=\sum_{n=1}^{\infty}\frac{2}{H}e^{-\alpha\beta_n^2(t-\tau)}\sin(\beta_n x)\sin(\beta_n x') \tag{A.2}$$

Here,

$$\beta_n=\begin{cases}\dfrac{n\pi}{H}, & \text{for a temperature condition at } x=H\\[2ex] \dfrac{(2n-1)\pi}{2H}, & \text{for a flux condition at } x=H\end{cases}$$

Substituting (A.2) into (A.1) yields the following formulation

$$V(x,t_1)=\frac{2L}{kC}\sum_{n=1}^{\infty}B_n(t_1)\sin(\beta_n x) \tag{A.3}$$

where

$$B_n(t_1)=\int_{\tau=t_0}^{t_1}\frac{dS(\tau)}{d\tau}\left\{e^{-\alpha\beta_n^2(t_1-\tau)}\sin(\beta_n S(\tau))\right\}d\tau \tag{A.4}$$

For a small Δt, it is assumed that the interface velocity is constant from t_0 to t_1. Thus,

$$S(\tau) = S(t_0) + v(\tau - t_0) \tag{A 5}$$

where $v = \frac{dS}{dt}$. It follows that $dS = v d\tau$, and Eq. (A.4) can be transformed as

$$B_n(t_1) = e^{-\alpha\beta_n^2 S(t_1)/v} \int_{S(t_0)}^{S(t_1)} \left\{ e^{\alpha\beta_n^2 S/v} \sin(\beta_n S) \right\} dS \tag{A 6}$$

This equation can be integrated and the result is given by

$$B_n(t_1) = e^{-\alpha\beta_n^2 S(t_1)/v} \left\{ \frac{e^{\alpha\beta_n^2 S(t_1)/v}}{(\alpha\beta_n^2/v)^2 + \beta_n^2} \left[\left(\alpha\beta_n^2/v \right) \sin(\beta_n S(t_1)) - \beta_n \cos(\beta_n S(t_1)) \right] \right.$$

$$\left. - \frac{e^{\alpha\beta_n^2 S(t_0)/v}}{(\alpha\beta_n^2/v)^2 + \beta_n^2} \left[\left(\alpha\beta_n^2/v \right) \sin(\beta_n S(t_0)) - \beta_n \cos(\beta_n S(t_0)) \right] \right\} \tag{A 7}$$

After rearrangement, Eq. (A.7) can be written as

$$B_n(t_1) = \frac{v}{(\alpha\beta_n^2)^2 + (\beta_n v)^2} \left\{ \left[\alpha\beta_n^2 \sin(\beta_n S(t_1)) - v\beta_n \cos(\beta_n S(t_1)) \right] \right.$$

$$\left. - e^{-\alpha\beta_n^2 (t_1 - t_0)/v} \left[\alpha\beta_n^2 \sin(\beta_n S(t_0)) - v\beta_n \cos(\beta_n S(t_0)) \right] \right\} \tag{A 8}$$

This completes the derivation of Eq. (3.52).

For a flux condition at $x = 0$, the Green's function is given by (see Eq. (3.51))

$$G(x,t|x',\tau) = C_o + \sum_{n=1}^{\infty} \frac{2}{H} e^{-\alpha\beta_n^2(t-\tau)} \cos(\beta_n x)\cos(\beta_n x') \tag{A.9}$$

Here,

$$C_o = \begin{cases} 0 \\ \frac{1}{H} \end{cases}, \qquad \beta_n = \begin{cases} \frac{(2n-1)\pi}{2H}, & \text{for a temperature condition at } x = H, \\ \frac{n\pi}{H}, & \text{for a flux condition at } x = H. \end{cases}$$

Substituting (A.9) into (A.1) yields the following for solution

$$V(x,t_1) = C_o \frac{L}{c}\frac{dS}{dt}\Delta t + \frac{2L}{Hc}\sum_{n=1}^{\infty} C_n(t_1)\cos(\beta_n x) \tag{A.10}$$

where

$$C_n(t_1) = \int_{\tau=t_o}^{t_1} \frac{dS(\tau)}{d\tau}\left\{e^{-\alpha\beta_n^2(t_1-\tau)}\cos(\beta_n S(\tau))\right\}d\tau \tag{A.11}$$

By following the same line as derived in (A.5)-(A.6), Eq. (A.11) can be written as

$$C_n(t_1) = e^{-\alpha\beta_n^2 S(t_1)/v} \int_{S(t_o)}^{S(t_1)} \left\{e^{\alpha\beta_n^2 S/v}\cos(\beta_n S)\right\}dS \tag{A.12}$$

This equation can be integrated and the result is given by

$$C_n(t_1) = e^{-\alpha\beta_n^2 S(t_1)/v}\left\{\frac{e^{\alpha\beta_n^2 S(t_1)/v}}{(\alpha\beta_n^2/v)^2+\beta_n^2}\left[(\alpha\beta_n^2/v)\cos(\beta_n S(t_1))+\beta_n\sin(\beta_n S(t_1))\right]\right.$$
$$\left. - \frac{e^{\alpha\beta_n^2 S(t_o)/v}}{(\alpha\beta_n^2/v)^2+\beta_n^2}\left[(\alpha\beta_n^2/v)\cos(\beta_n S(t_o))+\beta_n\sin(\beta_n S(t_o))\right]\right\} \tag{A.13}$$

After rearrangement, Eq. (A-13) can be written as

$$C_n(t_1) = \frac{n}{(\alpha\beta_n^2)^2 + (\beta_n v)^2} \left\{ \left[\alpha\beta_n^2 \cos(\beta_n S(t_1)) + v\beta_n \sin(\beta_n S(t_1)) \right] \right.$$

$$\left. - e^{-\alpha\beta_n^2(t_2 - t_1)} \left[\alpha\beta_n^2 \cos(\beta_n S(t_2)) + v\beta_n \sin(\beta_n S(t_2)) \right] \right\} \qquad (A\text{-}14)$$

This completes the derivation of Eq (3-53)

APPENDIX B
DERIVATION OF EQUATION (3.68)

In a spherical coordinate system, the decomposed temperature is given by (see Eq (3.63))

$$V(x,t_1)=\frac{L}{L}\int_{\tau=1_0}^{t_1}\frac{dS(\tau)}{d\tau}S^2(\tau)G(x,t_1|S(\tau),\tau)d\tau \qquad (B.1)$$

For a solid sphere, the Green's function for a temperature condition imposed at the sphere surface is given by (see Eq (3.64))

$$G(x,t|x',\tau)=\frac{1}{xx'}\sum_{n=1}^{\infty}\frac{2}{R_x}e^{-\alpha\beta_n^2(t-\tau)}\sin(\beta_n x)\sin(\beta_n x') \qquad (B.2)$$

Here,

$$\beta_n=\frac{n\pi}{R_x}$$

Substituting (B.2) into (B.1) yields

$$V(x,t_1)=\frac{2L}{cR_x}\sum_{n=1}^{\infty}D_n(t_1)\frac{\sin(\beta_n x)}{x} \qquad (B.3)$$

where

$$D_n(t_1)=\int_{\tau=1_0}^{t_1}S(\tau)e^{-\alpha\beta_n^2(t-\tau)}\sin(\beta_n S(\tau))d\tau \qquad (B.4)$$

Following the same line as derived in APPENDIX A, for a small time step Δt, the interface position can be written as

$$S(\tau) = S(t_o) + v(\tau - t_o) \ , \qquad dS = v d\tau \tag{B_5}$$

Then, Eq (B_4) can be transformed as

$$D_n(t_1) = \int_{S(t_o)}^{S(t_1)} S e^{-\alpha\beta_n^2 [S(t_1) - S]/v} \sin(\beta_n S) dS \tag{B 6}$$

From an integration table, one can get

$$\int x e^{ax} \sin(bx) dx = \frac{x e^{ax}}{a^2 + b^2} [a \sin(bx) - b \cos(bx)] - \frac{e^{ax}}{(a^2 + b^2)^2} [(a^2 - b^2) \sin(bx) - 2ab \cos(bx)] \tag{B 7}$$

Then, Eq-(6 B) can be integrated and rearranged as follows

$$D_n(t_1) = \frac{v}{(\alpha\beta_n^2)^2 + (\beta_n v)^2} \left\{ \alpha\beta_n^2 \left[S(t_1) \sin(\beta_n S(t_1)) - S(t_o) e^{-\alpha\beta_n^2 \Delta t} \sin(\beta_n S(t_o)) \right] - (\beta_n v) \left[S(t_1) \cos(\beta_n S(t_1)) - S(t_o) e^{-\alpha\beta_n^2 \Delta t} \cos(\beta_n S(t_o)) \right] \right\}$$
$$- \frac{v^2}{[(\alpha\beta_n^2)^2 + (\beta_n v)^2]} \left\{ \left[(\alpha\beta_n^2)^2 - (\beta_n v)^2 \right] \left[\sin(\beta_n S(t_o)) - e^{-\alpha\beta_n^2 \Delta t} \sin(\beta_n S(t_1)) \right] - 2\alpha\beta_n^2 \left[\cos(\beta_n S(t_1)) - e^{-\alpha\beta_n^2 \Delta t} \cos(\beta_n S(t_1)) \right] \right\} \tag{B 8}$$

This completes the derivation of Eq (3 68).

APPENDIX C
FORTRAN PROGRAM FOR TWO DIMENSIONAL PHASE CHANGE PROBLEMS

```
C ===========================================================C
C                                                            C
C          Numerical Solution of Phase Change Problems       C
C                                                            C
C  One/Two-dimensional phase change problems,                C
C  Combined FDM and SSM method, Time marching scheme,        C
C  Combined Newton-Raphson/Bisection for searching for S,    C
C  One/Two interfaces,                                       C
C  With/without free convection on the vertical boundaries,  C
C  Finite domain.                                            C
C  1st  kind B.C. imposed at x=0, insulated at x=b           C
C  Time/space variant boundary condition                     C
C===================    PROGRAM MAIN     ====================C
C*
      PARAMETER (MAXX=100,MAXY=50,MAXX2=MAXX*2,
     1           MAXT=MAXX*MAXY,MM2=MAXY*10)
      DIMENSION Y(MAXT),T(MAXT),TD(MAXT),TWO(MAXX),
     1          TW(MAXX),S(MAXX2),SD(MAXX2),
     2          DUM2(MM2),ITFS(MAXX2)
      COMMON /ALL/XDIM,YDIM,DX,DY,DT,CK,CP,RHO,ALPHA,HFG
      COMMON /IO/IREAD,IOUT,IREST,IDUMP
      CHARACTER*10 FREAD, FOUT, FREST, FDUMP, TITLE
C
      IREAD = 2
      IOUT  = 10
      IREST = 98
      IDUMP = 99
C
C==READ INFO
C
900   WRITE(*,*) 'Input data file ?'
      READ(*,1000) FREAD
      OPEN(IREAD,FILE=FREAD,ERR=810)
      GOTO 920
810   PRINT*,' Open error.. No file found!'
      GOTO 900
920   CONTINUE
```

```
      READ(IREAD,1000) TITLE
      READ(IREAD,*)
      READ(IREAD,1000) FOUT
      READ(IREAD,*)
      READ(IREAD,1000) FREST
      READ(IREAD,*)
      READ(IREAD,1000) FDUMP
      READ(IREAD,*)
      READ(IREAD,*) CK,CP,RHO,DFG,TINIT,TMELT
      READ(IREAD,*)
      READ(IREAD,*) HCDV, TAIR
      READ(IREAD,*)
      READ(IREAD,*) XDIM, YDIM, NX, NY
      READ(IREAD,*)
      READ(IREAD,*) DTT,TOUT,TSTOP,KREST
C
C==Initialization
      NXY = MAX(NX,NY)
      ITOUT = TOUT
      TIK = TINIT + 273
      TMK = TMELT + 273
      TINF= TAIR  + 273
      PRINT*,'======INITIALIZATION==-------
      CALL INIT(NX,NY,KBC,IBC,FREST,KREST,TSTART,TIK,Y,T,SD,S,TW)
C
C--Main solution procedure
      CALL PROCES(NX,NY,NXY,KBC,IBC,ITFS,TSTART,ITOUT,TSTOP,
     1            DTT,HCDV,TINF,TMK,TIK,Y,T,TO,S,SO,TW,TWD,
     2            DUM2(1),DUM2(NXY+1)   )
C
C==Output
      OPEN(IOUT, FILE=FOUT)
      CALL OUTPUT(NX,NY,TSTOP,Y,T)
      CLOSE (IOUT)
      CALL DUMP(NX,NY,FDUMP,TSTOP,SD,S,Y,T,TW)
1000  FORMAT(A40)
      STOP
      END
C
C==-===== SUBROUTINE INIT  -----========
C   Initialization
      ---------------------------------------------------------
      SUBROUTINE INIT(NX,NY,KBC,IBC,FREST,KREST,TS,TIK, Y,T,SD,S,TW)
      PARAMETER (MAXBC=50)
      DIMENSION SO(NX+2),S(NX+2),TW(NX),Y(NX,NY),T(NX,NY)
      COMMON /ALL/XDIM,YDIM,DX,DY,DT,CK,CP,RHO,ALPHA,HFC
      COMMON /BC/XBC(MAXBC),TBC(MAXBC,2),TIB1,TIB2
      COMMON /IO/IREAD,IOUT,IREST,IDUMP
      CHARACTER*40 FREST
C-
      SCAL  = 0.01
      XDIM = XDIM*SCAL
      YDIM = YDIM*SCAL
```

```
      IF(NX.EQ.1) THEN
      DX = 1.
      ELSE
      DX = XDIM/FLOAT(NX-1)
      END IF
      DY = YDIM/FLOAT(NY-1)
      ALPHA = CK/(RHO*CP)
      IF(KREST.EQ.1) THEN
      OPEN(IREST,FILE=FREST,FORM='UNFORMATTED',STATUS='OLD')
      CALL RESTART(NX,NY,TS,SO,S,Y,T,TW)
      CLOSE(IREST)
      PRINT*,'=== RESTART OK ! ===='
      ELSE
      TS = 0.
      DO 100 J=1,NY
      DO 100 I=1,NX
      Y(I,J)  = (J-1)*DY
      T(I,J)  = TIK
100   CONTINUE
      DO 120 I=1,NX
      SO(I,1) = 0.
      S (I,1) = 0.
      SO(I,2) = 0.
      S (I,2) = 0.
120   CONTINUE
      END IF
C- INPUT BOUNDARY CONDITIONS-
      READ(2,*)
      READ(2,*) KBC,IBC
C
C-KBC>0: Uniform T  B.C.     KBC<0: X-variant T  B.C.
C-IBC>0: Constant T  B.C.    IBC<0: time-variant T  B.C.
C-
      NBC = IABS(KBC)
      IF(NBC.GT.MAXBC) STOP 'KBC is too large'
      READ(2,*)
      READ(2,*) (XBC(I),I=1,NBC)
      READ(2,*)
      READ(2,*) TIB2
      READ(2,*) (TBC(I,2),I=1,NBC)
      TIB1 = TIB2
      DO 300 I=1,NBC
      TBC(I,1) = TBC(I,2)
300   CONTINUE
310   CONTINUE
      IF(TS.LE.TIB2) GOTO 500
      TIB1 = TIB2
      DO 320 I=1,NBC
320   TBC(I,1) = TBC(I,2)
      READ(2,*,END=500) TIB2
      READ(2,*) (TBC(I,2),I=1,NBC)
      GOTO 310
```

```
500   CONTINUE
      CALL INTBC(NX,NBC,DX,TS,TW)
      RETURN
      END
C
C========= SUBROUTINE INTBC ============
      SUBROUTINE INTBC(NX,NBC,DX,TIME,TW)
      PARAMETER (MAXBC=50)
      COMMON /BC/XBC(MAXBC),TBC(MAXBC,2),T1B1,T1B2
      DIMENSION U(MAXBC),Y2(MAXBC),TB(MAXBC),TW(NX)
C-
      DTIME = T1B2-T1B1
      DO 9 I=1,NBC
      IF(ABS(DTIME).LT.0.01) THEN
      TB(I) = 0.5*(TBC(1,I)+TBC(1,2))
      ELSE
      TB(1) = TBC(1,1) + (TBC(1,2) TBC(1,1))*(TIME-T1B1)/DTIME
      END IF
9     CONTINUE
      YP1 = 0
      YPN = 0
      Y2(1) = -0.5
      U(1) = (3./(XBC(2) XBC(1)))*((TB(2) TB(1))/
     1              (XBC(2)-XBC(1))-YP1)
      DO 10 I=2,NBC-1
      SIG = (XBC(I)-XBC(I-1))/(XBC(I+1) XBC(I-1))
      P   = SIG*Y2(I-1)+2
      Y2(I) = (SIG-1.)/P
      U(I)  = (6.*((TB(I+1)-TB(I))/(XBC(I+1)-XBC(I))-
     1          (TB(I)-TB(I-1))/(XBC(I)-XBC(I-1)))/
     2          (XBC(I+1)-XBC(I-1)) SIG*U(I-1))/P
10    CONTINUE
      QN = 0.5
      UN = (3./(XBC(NBC)-XBC(NBC-1)))*(YPN-(TB(NBC)-TB(NBC-1))/
     1              (XBC(NBC)-XBC(NBC-1)))
      Y2(NBC) = (UN-QN*U(NBC-1))/(QN*Y2(NBC-1)+1.)
      DO 20 I=NBC-1,1,-1
      Y2(I) = Y2(I)*Y2(I+1) + U(I)
20    CONTINUE
      DO 50 I=1,NX
      XX = (I-1)*DX
       IF(XX.LE.XBC(1)) THEN
       TWC = TB(1) + 273.0
         ELSE
         DO 30 J=2,NBC
            IF(XX.GE.XBC(J-1) AND XX.LE.XBC(J)) THEN
            H  = XBC(J) XBC(J-1)
            A  = (XBC(J)-XX)/H
            B = (XX-XBC(J-1))/H
            TERM1 = A*TB(J-1)+B*TB(J)
            TERM2 = ((A**3-A)*Y2(J-1)+(B**3-B)*Y2(J))*(H**2)/6
            TWC = TERM1+TERM2 + 273.0
```

```
            GOTO 40
            END IF
30        CONTINUE
          TWC - TB(NBC) + 273 0
          ENO IF
40      TW(I) = TWC
50      CONTINUE
        RETURN
        ENO
C-
C=====--- SUBROUTINE RESTART ------------
        SUBROUTINE RESTART(NX,NY,TS,SO,S,Y,T,TW)
        DIMENSION Y(NX NY) T(NX,NY), S(NX 2),SO(NX,2),TW(NX)
        COMMON /IO/IREAO,IOUT,IREST,IDUMP
        READ(IREST) TS
        READ(IREST) ((Y(I,J) T(I,J),I-1,NX),J-1,NY)
        REAO(IREST) (S(I,1),S(I,2),SO(I,1),SO(I,2),TW(I),I-1,NX)

        RETURN
        ENO
C
C------SUBROUTINE DUMP-------------------
        SUBROUTINE DUMP(NX NY,FDUMP,TS,SO S,Y,T,TW)
        DIMENSION Y(NX NY) T(NX,NY), S(NX 2),SO(NX,2),TW(NX)
        COMMON /IO/IREAO IOUT IREST,IDUMP
        CHARACTER*40 FDUMP
        OPEN(IDUMP FILE=FDUMP,FORM-'UNFORMATTED')
        WRITE(IDUMP) TS
        WRITE(IDUMP) ((Y(I,J),T(I,J),I=1,NX),J=1,NY)
        WRITE(IDUMP) (S(I,1),S(I,2),SO(I,I),SO(I,2), TW(I),I-1,NX)
        CLOSE(IDUMP)
        RETURN
        END
C
C======-- SUBROUTINE PROCES --------------
C   Main solution procedure      FDM and SSN methods.
C-----------------------------------------------------------------
       --
        SUBROUTINE PROCES(NX,NY,NXY,KBC,IBC,ITFS,TSTART,ITOUT,TSTOP,
     1               DTT,HCOV,TINF TMX,TIK Y,T,TO,S,SO,TW,TWO TW1, DUM2)
        PARAMETER (MAXBC=50)
        COMMON /BC/XBC(MAXBC),TBC(MAXBC,2),TIB1,TIB2
        DIMENSION
        S(NX 2),SO(NX,2),TW(NX),TWO(NX),Y(NX,NY),T(NX,NY),TO(NX,NY)
        DIMENSION TW1(1), DUM2(1), ITFS(NX,2)  TO(NX,NY)
        COMMON /ALL/XDIM YDIM,DX DY,DT,CK,CP RHO ALPHA HFG
        COMMON /SS/TS11,TS12,TS21,TS22
C-
        NCY  = 0
        DX2  = DX*DX
        DCP  = HFG/CP
        TIME   TSTART
```

```
      AMP  = 50
      PR10 = 30

      NBC  = IABS(KBC)
      DO 2 I=1,NX
      TW1(I) = TW(I)
      ITFS(I,1) = 0
      ITFS(I,2) = 0
2     CONTINUE
      DO 900 WHILE (TIME.LT.TSTOP)
      NCY = NCY + 1
C-Slow start
      IF(DTT.LT.0. AND. NCY.LE.10) THEN
        DT = ABS(DTT)*(0.1*NCY)**2
      ELSE
        DT = ABS(DTT)
      END IF
C-
      TIME = TIME + DT
      IF(KBC.LT.0) CALL GETTW(NX,NBC,DX,TIME,TW)
      DO 100 I=1,NX
        IF(IBC.EQ.-1) TW(I) = TW1(I) +
2                     AMP*SIN(3.1415D+(TIME-0.5*DT)/PRID)
      TWO(I) = T(I,1)
      DO 100 J=1,NY
      TO(I,J) = T(I,J)
100   CONTINUE
C
C-Solve for U-problem
      CALL FINDT1(NX,NY,NCY,HCOV,TINF,TIK,TO,T,TW,
     1            DUM2(1),DUM2(NXY+1),DUM2(2*NXY+1),DUM2(3*NXY+1))
      IF(ABS(DFG).LT.1.E-8) GOTO 600
C
C-Check for interface status
      CALL CHKS(NX,NY,ITFS,S,SO,TW,TWO,TMK,YDIM)
C-
      PRINT*
      PRINT*,'Find interface at t=',TIME
      PRINT*,'     S1(I)          S2(I)          Tw1(I)'
      DO 500 I=1,NX
      IF(ITFS(I,1).EQ.0.AND.ITFS(I,2).EQ.0) GOTO 500
      DO 200 J=1,NY
      J1 = NXY+J
      DUM2(J)  = T(I,J)
      DUM2(J1) = Y(I,J)
200   CONTINUE
      IF(ITFS(I,1).EQ.1.AND.ITFS(I,2).EQ.0) THEN
C-
C-S1  (Melting)
      HFGCP = GCP
      SS  = S(I,1)
      SSO= SO(I,1)
C
```

```
C-Search for single melting interface

        CALL FINDIS(NY,SSO,SS,HFGCP,TMK,DUM2(1),DUM2(NXY+1),
     1       DUM2(2*NXY+1),DUM2(3*NXY+1),DUM2(4*NXY+1),DUM2(5*NXY+1))
C
C-Solve for V-problem, update S and T
        CALL FINDT2(NY,TMK,HFGCP,DUM2(1),DUM2(NXY+1),SSO,SS)
       S (I,1) = SS
       SO(I,1) = SSO
       TS      = TS11 + TS12
       ELSE IF(ITFS(I,1)-EQ 0 AND ITFS(I,2)-EQ-1) THEN
C
C-S2  (Freezing)
        HFGCP = -HCP
        SS  = S(1,2)
        SSO =SO(1,2)
C
C-Search for single freezing interface
        CALL FINDIS(NY,SSO,SS,HFGCP,TMK,DUM2(1),DUM2(NXY+1),
     1       DUM2(2*NXY+1),DUM2(3*NXY+1),DUM2(4*NXY+1),DUM2(5*NXY+1))
C
C-Solve for V-problem, update S and T
        CALL FINDT2(NY,TMK,HFGCP,DUM2(1),DUM2(NXY+1),SSO,SS)
       S (1,2) = SS
       SO(1,2) = SSO
       TS      = TS11 + TS12
       ELSE IF(ITFS(1,1)-EQ 1-AND-ITFS(1,2)-EQ-1) THEN
C
C-S1 & S2   (S1-Melting, S2-Freezing)
        SS1   = S (1,1)
        SSO1  = SO(1,1)
        SS2   = S (1,2)
        SSO2  = SO(1,2)
        HFGCP = HCP
C
C-Search for double interfaces
        CALL FIND2S(NY,SSO1,SSO2,SS1,SS2,HFGCP,TMk,
     1              DUM2(1),DUM2(NXY+1),DUM2(2*NXY+1),
     2              DUM2(3*NXY+1),DUM2(4*NXY+1),DUM2(5*NXY+1) )
C
C-Solve for V-problem, update S and T
        CALL FINDTT(NY,tmk,HFGCP,SSO1,SSO2,SS1,SS2,
     1              DUM2(1),dum2(nxy+1) )
       S (1,1) = SS1
       SO(1,1) = SSO1
       S (1,2) = SS2
       SO(1,2) = SSO2
       END IF
C
      DO 300 J=1,NY
      T(1,J) = DUM2(J)
300   CONTINUE
```

```
      WRITE(*,1000) S(I,1),S(I,2),T(I,1),(I-1)*dx
500   CONTINUE

500   CONTINUE
      IP = MOD(NCY,ITOUT)
       DO 700 I=1,NX
       IF(IP EQ.0) WRITE(30,1000) (I-1)*DX,S(I,1),S(I,2),TIME
700   CONTINUE
       IC = NX/2
       WRITE(50,1000) TIME, S(1,I),S(IC,I),S(NX,1)
       WRITE(51,1000) TIME, S(1,2),S(IC,2),S(NX,2)
500   CONTINUE
1000  FORMAT(5E15.5)
      RETURN
      END
C
C---- SUBROUTINE GETTW ==========
      SUBROUTINE GETTW(NX,NBC,DX,TIME TW)
      PARAMETER (MAXBC=50)
      COMMON /BC/XBC(MAXBC),TBC(MAXBC,2),TIB1,TIB2
      DIMENSION TW(NX)
C-
310   CONTINUE
      IF(TIME.LE.TIB2) GOTO 500
      TIB1 = TIB2
      DO 320 I=1,NBC
320   TBC(I,1) = TBC(I,2)
      READ(2,*,END=400) TIB2
      READ(2,*) (TBC(I,2),I=1,NBC)
      GOTO 310
400   TIB2 = 1.E08
500   CONTINUE
      CALL INTBC(NX,NBC,DX,TIME,TW)
      RETURN
      END
C
C---- SUBROUTINE CHKS==========
      SUBROUTINE CHKS(NX,NY,ITFS,S,SO,TW,TWO,TMK,YDIM)
      DIMENSION ITFS(NX,2),S(NX,2),SO(NX,2),TWO(NX),tw(nx)
C-
      DO 10 I=1,NX
       IF(Tw(I).TMK.GT.0.5.and.TWO(I)-TMK.le.0.5) THEN
C-Tw > Tm  : Melting
        ITFS(I,1) = I
        ELSE if(tw(I).TMK.lt.0.5.and.TWO(I).TMK.ge.0.5) then
C-Tw < Tm  : Freezing
        ITFS(I,2) = I
        ENDIF
C-Interface reaches other boundary
      IF(ITFS(I,1).EQ.1.AND.S(I,1).GE.YDIM)  THEN
      ITFS(I,1) = 0
      S(I,1)    = 0
      ENDIF
```

```
      IF(ITFS(I,2) EQ 1 AND S(I,2) GE YDIM)  THEN
      ITFS(I,2) = 0

      S(I,2)       0
      END IF
C-Interface merges
      IF(S(I,1) GT 1 E-4 AND ABS(S(I,2) S(I,1)) LE 1 E-8) THEN
      ITFS(I,1) = 0
      ITFS(I,2) = 0
      S(I,1) = 0
      S(I,2) - 0
      SO(I,1) = 0
      SO(I,2) = 0
      END IF
C-
      IF(Tw(I) GT TMK AND S(I 1) GT S(I,2) AND S(I,2) GT 0 ) THEN
        S(I,1)     - 0
        SO(I,1)    = 0
        S(I,2)     = 0
        SO(I 2)    = 0
      ITFS(I,1) - 1
      ITFS(I,2) - 0
      END IF
      IF(Tw(I) LT TMK AND S(I,2) GT S(I,1) AND S(I,1) GT 0 ) THEN
        S(I,2)     = 0
        SO(I,2)    - 0
        S(I,1)     = 0
        SO(I,1)    = 0
      ITFS(I,1) = 0
      ITFS(I,2) = 1
      END IF
10    CONTINUE
      RETURN
      END
C-
C===== SUBROUTINE FINDS ===-------------
C  Find the interface position S at time = t
C-------------------------------------------
      SUBROUTINE FINDIS(NY,SD S,HFGCP,TMK,TI,YI, AA, BB, CC, DD)
      DIMENSION YI(1) TI(1) AA(I) BB(I),CC(I),DD(I)
      COMMON /ALL/XDIM,YDIM DX,DY,DT,CK,CP,RHO,ALPHA,HFG
C
      EPSS   = 1 E-06
      EPST   - 1 E-05
      DSDT - ABS(S-SO)
      SSD - S
      IF(DSDT LE 1 E-08) THEN
      DDD   - 0 025*YDIM
      ELSE
      DDD   = DMAX1(DSDT, 0 0001D0)
      END IF
      DO 100 J=1,NY
      AA(J) = 0 5
```

```
      BB(J) = 2.0
      CC(J) = 0.5

100   CONTINUE
      DD(1) = 3.*(TI(2)-TI(1))/DY
      DD(NY) = 3.*(TI(NY-1)-TI(NY))/DY
      DO 200 J=2,NY-1
      DD(J) =3.*(AA(J)*(TI(J+1)-TI(J))+CC(J)*(TI(J)-TI(J-1)))/DY
200   CONTINUE
      CALL TRID(NY,AA,BB,CC,DD)
      YL   = SSO - DDD
      RT   = SSO + DDD
        IF(YL LT.0.)   YL = 0
      IF(RT.GT.YDIM) RT=YDIM
10    CONTINUE
      YPRE  = YL
      CALL SPLINE(NY,YI,TI,DD,YL,T1)
      CALL GREFT(YL,SSO,YPRE,GINT)
      T2    = GINT*HFGCP
      FL    = T1 + T2 - TMK
      YLOC  = RT
      YPRE  = YLOC
      CALL SPLINE(NY,YI,TI,DD,RT,T1)
      CALL GREFT(YLOC,SSO,YPRE,GINT)
      T2    = GINT*HFGCP
      FH    = T1 + T2 - TMK
        IF(ABS(FH) LT EPST) GOTO 40
      IF(FH*FL GT 0.) THEN
      YL = YL - DDD
      RT = RT + DDD
          IF(YL LT 0.) YL = 0
        IF(RT.GT.YDIM) then
        RT = YDIM
        GOTO 40
        END IF
      END IF
C-
      IF(FL LT 0.) THEN
         YH = RT
         FO = FL
      ELSE
         YH = YL
         YL = RT
         FO = FH
      END IF
      RT = 0.5*(YH+YL)
      YLOC = RT
      YPRE = YLOC
      DO  = DDD
      H   = DO
      CALL SPLINE(NY,YI,TI,DD,RT,T1)
      CALL GREFT(YLOC,SSO,YPRE,GINT)
      T2    = GINT*HFGCP
```

```
      F     = T1 + T2 - TMK
            IF(ABS(F) LT EPST) GOTO 40

      DF    = (F-FL)/(RT-YL)
      RTO   = RT
      FL    = F
       IF(F.LT.0.) THEN
         YL = RT
       ELSE
         YH = RT
       END IF
C
      DO 20 L=1,200
      IF(((RT-YH)*DF-F)*((RT-YL)*DF-F) GE 0.
     I   OR ABS(2.*F) GT ABS(DO*DF)) THEN
         DO = D
         D  = 0.5*(YH-YL)
         RT = 0.5*(YH+YL)
       ELSE
         DO = D
         D  = F/DF
         RT = RT - D
       END IF
      YLOC = RT
      YPRE = YLOC
      CALL SPLINE(NY,Y1,T1,DD,RT,T1)
      CALL GREFT(YLOC,SSo,YPRE,GINT)
      T2    = GINT*WFGCP
      F     = T1 + T2 - TMK
            IF(ABS(F) LT EPST OR ABS(W) LT EPSS) GOTO 40
      DF    = (F-FL)/(RT-RTO)
      RTO   = RT
      FL    = F
       IF(F LT 0.) THEN
         YL = RT
       ELSE
         YH = RT
       END IF
20    CONTINUE
40    CONTINUE
      SO = S
      S  = RT
      RETURN
      END
C
C====- SUBROUTINE TRID -====-====-=
C   Tridiagonal solver
C-------------------------------------------------------
      SUBROUTINE TRID(M2,B,D,A,CI)
      DIMENSION A(1),B(1),D(1),C1(1)
      M1 = 1
      MP1 = M1+1
      DO 100 I=MP1,M2
```

```
      RR = D(I)/D(I-1)
      B(I) = D(I)-RR*A(I-1)

      C1(I)= C1(I)-RR*C1(I-1)
100   CONTINUE
      RR = 1./D(M2)
      C1(M2)=C1(M2)*RR
      DO 200 I=MP1,M2
      J = M2-I+M1
      RR = 1./D(J)
      C1(J)=(C1(J)-A(J)*C1(J+1))*RR
200   CONTINUE
      RETURN
      END
C
C===== SUBROUTINE SPLINE ===============
C   Spline interpolation
C------ ----- ---- ----- ---------------
      SUBROUTINE SPLINE(NY,Y,T,D,YY,TS1)
      DIMENSION Y(1),T(1),D(1)
      IF(YY.LE.Y(1)) THEN
      TS1 = T(1)
      RETURN
      END IF
      DO 10 J=2,NY
      IF(YY.GE.Y(J-1).AND.YY.LE.Y(J)) THEN
      DL = YY-Y(J-1)
      DR = Y(J)-YY
      DL2 = DL*DL
      DR2 = DR*DR
      H = Y(J)-Y(J-1)
      TERM1 = (3.*H - 2.*DR)*DR2*T(J-1)/H
      TERM2 = (3.*H - 2.*DL)*DL2*T(J  )/H
      TERM3 = (H-DR)*DR2*D(J-1)
      TERM4 = (H-DL)*DL2*D(J  )
      TS1 = (TERM1+TERM2+TERM3-TERM4)/H**2
      GOTO 20
      END IF
10    CONTINUE
      TS1 = T(NY)
20    CONTINUE
      RETURN
      END
C
C======== Subroutine GREFT ----------
C  Integration of GREEN's function over t from t0 to t1
C------ ---- --- ---------
      SUBROUTINE GREFT(YLOC,YP0,YP1,GINT)
      COMMON /ALL/XDIM,YDIM,DX,DY,DT,CK,CP,RHO,ALPHA,BFG
      EPS = 1.E-04
      IF(ABS(YLOC).LT.1.E-08) THEN
      GINT = 0
      RETURN
```

```
      ENDIF
      PI  = 3.1415927

      DR  = YP1 - YP0
      DR2 = DR*DR
        IF(ABS(DR) LT 1.E-08) THEN
        GINT = 0.
        RETURN
        ENDIF
      PIY = 0.5*PI/YDIM
      ALPHAT = ALPHA*DT
      SUM = 0.
      SUM1 = 0.
      DO 100 IY=1,50000
      BETA = (2*IY-1)*PIY
      BRQ  = BETA*YP0
      BM1  = BETA*YP1
      BXL  = BETA*XLOC
      BETA2 = BETA*BETA
      ABT   = ALPHAT*BETA2
      EPT   = EXP(-ABT)
      DEN   = ABT*ABT + BETA2*DR2
      TI    = ABT/DEN
      T2    = BETA*DR/DEN
      TERM1 = TI*SIN(BM1)
      TERM2 = T2*COS(BM1)
      TERM3 = TI*SIN(BRQ)
      TERM4 = T2*COS(BRQ)
      SUMI = TERM1-TERM2*EPT*(TERM3-TERM4)
      SUM  = SUM + SUM1*SIN(BXL)
      SUM1 = SUM1+SUMI
      TT   = TI+T2
      ERR  = ABS(TT/SUM1)
      IF(ERR.LT.EPS) GOTO 200
100   CONTINUE
      IF(ERR.GE.1.E-3) THEN
      WRITE(*,*) 'No convergence !!'
      STOP 'No convergence in GreenS fnactIon'
      ENDIF
200   CONTINUE
      GINT = 2.*DR*SUM/YDIM
      RETURN
      END
C
C-------- SUBROUTINE FINDT2 ---------
C   Find temp. correction due to interface
C ------------------------------------------------------------
      SUBROUTINE FINDT2(NY,TMP,NFGCP,YI,TI,SO,S)
      DIMENSION YI(NY),TI(NY)
      COMMON /ALL/XDIM,YDIM,DX,DY,DT,CK,CP,RHO,ALPHA,NFG
      REWIND (40)
      IF(S.GE.YDIM.OR.S.LE.0.) RETURN
      YPRE = S
```

```
      SSO   = SO
      DO 400 J=I,NY

      YLOC = YI(J)
      CALL GREFT(YLOC SSO,YPRE,GINTI)
      T2    = GINTI*REGCP
      WRITE(40,10) YLOC,TI(J)-TMK,T2,T2+TI(J)-TMK
      TI(J) = TI(J) + T2
400   CONTINUE
10    FORMAT(4F14.4)
      RETURN
      END
C
C-------- SUBROUTINE FINDTI ---------
C  FDM method for solving TI
C-----------------------------------------------------------------
      SUBROUTINE FINDTI(NX,NY,acy,RCOV,TINF,TIK,TO,T,TW,
     1                  A, C, B, Q )
      DIMENSION TO(NX,NY),T(NX,NY),TW(NX)
      DIMENSION A(1),B(1) C(1),Q(1)
      COMMON /ALL/XDIM,YDIM,DX,DY,DT,CK,CP,RHO,ALPHA,HFG
      DX2 = DX*DX
      DY2 = DY*DY
      HIB = DX*RCOV/CK
      IF(RCOV.LE.0.) BIO = 0
       COEX = 0.5*ALPHA*DT/DX2
        COEY = 0.5*ALPHA*DT/DY2
      NI=NY-1
C-SWEEP IN J-DIR-
      DO 300 I=1,NX
      DO 100 J=1,NI
      JJ=J+1
      A(J) = -COEY
      B(J) = 1 + 2.*COEY
      C(J) =  COEY
      IF(NX.EQ.1) THEN
      D2TDX2 = 0.
      ELSE
        IF(I.EQ.1) THEN
        D2TDX2 = 2.*COEX*(T(I+1,JJ)-T(I,JJ)-BIO*(T(I,JJ)-TINF))
        ELSE IF(I.EQ.NX) THEN
        D2TDX2 = 2.*COEX*(T(I,JJ)-T(I-1,JJ)+BIO*(T(I,JJ)-TINF))
        ELSE
        D2TDX2 = COEX*(T(I+1,JJ)-2.*T(I,JJ)+T(I-1,JJ))
        ENDIF
      ENDIF
      Q(J) = T(I,JJ) + D2TDX2
100   CONTINUE
      TO(I,I) = TW(I)
      B(1) = B(1) + COEY*TW(I)
      A(NI) = -2*COEY
      CALL TRIB(NI,A,B,C,Q)
      DO 200 J=1,NI
```

```
      JJ = J+1
      T0(I,JJ) = D(J)

200   CONTINUE
300   CONTINUE
C
C--SWEEP IN I-D
      J1 = 2
      DO 600 J=J1,NY
      DO 400 I=1,NX
      A(I) = -COEX
      B(I) = 1 + 2.*COEX
      C(I) = -COEX
       IF(J EQ NY) THEN
       D2T0Y2 = 2.*COEY*(T0(I,J-1)-T0(I,J))
       ELSE
       D2T0Y2 = COEY*(T0(I,J+1)-2.*T0(I,J)+T0(I,J-1))
       END IF
       D(I) = T0(I,J) + D2T0Y2
400   CONTINUE
      IF(NX GT 1) THEN
      C(1) = -2.*COEX
      B(1) = 1.+ 2.*COEX*(1.+BIO)
      D(1) = D(1) + 2.*COEX*BIO*TINF
      A(NX) = -2.*COEX
      B(NX) = 1.+2.*COEX*(1.+BIO)
      D(NX) = D(NX) + 2.*COEX*BIO*TINF
      CALL TRIO(NX,A,B,C,D)
      END IF
      DO 500 I=1,NX
      T(I,J) = D(I)
500   CONTINUE
600   CONTINUE
      DO 700 I=1,NX
      T(I,1)   T0(I)
700   CONTINUE
      RETURN
      END
C
C---- SUBROUTINE OUTPUT ----------
C----
      SUBROUTINE OUTPUT(NX,NY,TSTOP,Y,T)
      DIMENSION Y(NX,NY),T(NX,NY)
      COMMON /ALL/XDIM,YDIM,DX,DY,DT,CK,CP,RHO,ALPHA,HFG
      COMMON /IO/IREAD,IOUT,IREST,IOUMP
C=
      WRITE(IOUT,*) NX,NY,0
      DO 100 J=1,NY
      DO 100 I=1,NX
      X = (I-1)*DX
      WRITE(IOUT,1000) X Y(I,J),T(I,J)
100   CONTINUE
1000  FORMAT(3E13 8)
```

```
      RETURN
      END
C
C======= SUBROUTINE FIND2S =------------
C     Search for double interfaces
C-------------------------- - -
      SUBROUTINE FIND2S(NY,S01,S02,S1,S2,BFGCP,TMK,
     I                  TI,YI, AA, BB, CC, OD )
      DIMENSION YI(1),TI(1),AA(1),BB(1),CC(1),DD(1)
      COMMON /ALL/XDIM,YDIM,DX,DY,DT,CK,CP RHO,ALPHA,BFG
C=
      EPSS  = 1.E-06
      EPST  = 1.E-05
      SS1   = S1
      SS2   = S2
      DSDT1 = S1-S01
      DSDT2 = S2-S02
      OIRO = S01-S02
      IF(ABS(DSDT1) LE 1.E-08) THEN
      OOO1   = 0.005*YDIM
      IF(S01.LE.1.E-8) DD01=0.1*YDIM
      ELSE
      DD01  = DSDT1
      ENO IF
      IF(ABS(DSDT2) LE 1.E-08) THEN
      DDD2  = 0.005*YOIM
      IF(S02 LE 1.E 8) OOD2=0.1*YOIM
      ELSE
      ODD2  = DSDT2
      END IF
      DO 100 J=1,NY
      AA(J) = 0.5
      BB(J) = 2.0
      CC(J) = 0.5
100   CONTINUE
      DO(1)  = 3.*(TI(2)-TI(I))/DY
      DO(NY) = 3.*(TI(NY)-TI(NY-1))/DY
      DO 200 J=2,NY-1
      DD(J) =3.*(AA(J)*(TI(J+1)-TI(J))+CC(J)*(TI(J)-TI(J-1)))/DY
200   CONTINUE
      CALL TRID(NY,AA,BB,CC,OO)
      YL1   = SSI
      RT1   = SS1 - DDD1
      YL2   = SS2
      RT2   = SS2 - DDD2
      BT1   = DMAX1(YI(1),RT1)
      RT2   = DMAX1(YI(I),RT2)
      OIRI  = RT1 RT2
      IF(OIRO*OIRI.LT.0.) THEN
         IF(DIRO.GT.0.)  RT1 = BT2
         RT2 = RT1
      GOTO 40
      END IF
```

```
      YPRE1  = RT1
      YPRE2  = RT2

      YLOC   = RT1
      CALL SPLINE(NY,Y1,T1,DD,YLoc,T11)
      CALL GREFT2(YLoc,SS1,ss2,YPRE1,ypre2,GINT1,glnt2)
      T21    = HFGCP* (glnt1 - glnt2)
      FL1    = T11 + T21 - TMK
      YLOC   = RT2
      CALL SPLINE(NY,Y1,T1,DD,Yloc,T12)
      CALL GREFT2(YLoc,ss1,SS2,YPRE1,ypre2,glnt1,GINT2)
      T22    = HFGCP* (glnt1 - glnt2)
      FL2    = T12 + T22 - TMK
      RT1 = SS1 + DDD1
      RT2 = SS2 + DDD2
      1CONT=0
1D    CONTINUE
      1CONT = 1CONT + 1
      D1R1  = RT1-RT2
      IF(D1R0*D1R1 LT 0 ) THEN
        IF(D1R0 GT 0.)  RT1 = RT2
        RT2 = RT1
      GOTO 4D
      END IF
      YLOC = RT1
      YPRE1 = RT1
      YPRE2 = RT2
      CALL SPLINE(NY,Y1,T1,DD,yloc,T11)
      CALL GREFT2(YLoc,SS1,ss2,YPRE1,ypre2,GINT1,glnt2)
      T21    = HFGCP* (glnt1    glnt2)
      FH1    = T11 + T21    TMK
      YLOC = RT2
      CALL SPLINE(NY,Y1,T1,DD,yloc,T12)
      CALL GREFT2(YLoc,SS1,ss2,YPRE1,ypre2,GINT1,glnt2)
      T22    = HFGCP* (glnt1 - glnt2)
      FH2    = T12 + T22 - TMK
C-
        IF(FH2*FL2 GT 0.) THEN
          IF(1CONT GT 1D) THEN
          DDD2 = -1D*DDD2
          1CONT = 0
          END IF
          IF(RT2 GE YD1M) DDD2 =  -1D*DDD2
          IF(RT2 LE Y1(1)) DDD2 = -10.*DDD2
        IF(ABS(DDD2) GT 0.2*YD1M) DDD2=0.5*DDD2
      RT2 = RT2 + DDD2
        IF(RT2 GT YD1M) RT2 = YD1M
        IF(RT2 LT Y1(1)) RT2 = Y1(1)
      END IF
C-
      IF(ABS(YL1-RT1) LT 1.E-8) RT1 = YL1 + 1.E-05
      IF(ABS(YL2-RT2) LT 1.E-8) RT2 = YL2 + 1.E-05
      DO 20 L=1,5D
```

```
      a11 = (fh1-f11)/(rt1-y11)
      a12 = (fh1-f11)/(rt2-y12)

      a21 = (fh2-f12)/(rt1-y11)
      a22 = (fh2-f12)/(rt2-y12)
      if(abs(a11).lt.1.e-8) then
       x2 = -fh1/a12
       x1 = -(fh2+a22*x2)/a21
      else
       bj = a22-a21*a12/a11
         if(abs(bj) lt 1.e-8) then
         x1 = -fh1/a11
         x2 = -fh2/a22
       else
       x2 = (a21*fh1/a11 - fh2)/(a22 - a12*a21/a11)
       x1 = -(fh1+a12*x2)/a11
      end if
      end if
      if(abs(x1)+abs(x2) le epse) goto 40
      IF(ABS(X1) GE EPSS) THEN
      y11 = rt1
      f11 = fh1
      END IF
      IF(ABS(X2) GE EPSS) THEN
      y12 = rt2
      f12 = fh2
      END IF
      if(abs(x1) gt 0.5*ydim) x1=0.1*x1*ydim/abs(x1)
      if(abs(x2) gt 0.5*ydim) x2=0.1*x2*ydim/abs(x2)
      rt1 = rt1 + x1
      rt2 = rt2 + x2
      YLOC = RT1
      YPRE1 = RT1
      ypre2 = rt2
      CALL SPLINE(NY,Y1,T1,DD,yloc,T11)
      CALL GREFT2(YLoc,SS1,ss2,YPRE1,ypre2,G1NT1,gint2)
      T21    = BFGCP* (gint1 - gint2)
      FH1    = T11 + T21   TMK
      YLOC = RT2
      CALL SPLINE(NY,Y1,T1,DD,yloc,T12)
      CALL GREFT2(YLoc,SS1,ss2,YPRE1,ypre2,G1NT1,gint2)
      T22    = BFGCP* (gint1 - gint2)
      FH2    = T12 + T22 - TMK
20    CONTINUE
40    CONTINUE
      TS11 = T11
      TS12 = T12
      TS21 = T21
      TS22 = T22
      S01  = S1
      s02  = s2
      S1   = RT1
      s2   = rt2
```

```
      if(ABS(s1-s2) LT 1.E-6) then
      s1 = 0.5*(s1+s2)

      s2 = s1
      end if
      RETURN
      END
C=
C=======  GREEN'S FUNCTION FOR FINITE DOMAIN  ==========
      SUBROUTINE GREFT2(YLOC,YD1,yO2,Yp1,yp2,G1,g2)
      COMMON /ALL/XOIM,YOIM,DX,DY,DT,CK,CP,RHO,ALPHA,HFG
C=
      EPS = 1.E-04
      IF(ABS(YLOC) LT 1.E-08) THEN
      G1 = 0.
      g2 = 0
      RETURN
      ENE IF
      PI  = 3.1415927
      DR1  = YP1  - YD1
      DR2  = YP2  - YO2
      DR12 = DR1*DR1
      dr22 = dr2*dr2
      PIY  = 0.5*PI/YDIM
      ALPHAT = ALPHA*DT
C-
      SUMg1 = 0.
      sumg2 = 0.
      SUM1 = 0.
      sum2 = 0.
      DO 100 IT=1,50000
      BETA = (2*IT-1)*PIY
      BRO1  = BETA*YD1
      BR11  = BETA*YP1
      BRO2  = BETA*YO2
      BR12  = BETA*YP2
      BXL   = BETA*YLOC
      BETA2 = BETA*BETA
      ABT   = ALPHAT*BETA2
      EPT   = EXP(-ABT)
      DEN1  = ABT*ABT + BETA2*DR12
      DEN2  = ABT*ABT + BETA2*DR22
      T11   = ABT/DEN1
      t12   = abt/den2
      T21   = BETA*DR1/DEN1
      T22   = BETA*DR2/DEN2
      TERM11 = T11*SIN(BR11)
      TERM21 = T21*COS(BR11)
      TERM31 = T11*SIN(BRD1)
      TERM41 = T21*COS(BRO1)
      TERM12 = T12*SIN(BR12)
      TERM22 = T22*COS(BR12)
      TERM32 = T12*SIN(BRD2)
```

```
      TERM42 = T22*COS(BR02)
      SUMI1 = TERM11-TERM21-EPT*(TERM31-TERM41)

      SUMg1   = SUMg1 + SUMI1*SIN(BXL)
      SUMI2 = TERM12-TERM22-EPT*(TERM32-TERM42)
      SUMg2   = SUMg2 + SUMI2*SIN(BXL)
      SUM1  = SUM1+SUMI1
      sum2  = sum2+sumi2
      TT1     = TI1+T21
      TT2     = TI2+T22
      IF(I7 LT 20) GOTO 100
      ERR   = (ABS(TT1)+ABS(TT2))/(SUM1+SUM2)
      IF(ERR LT EPS) GOTO 200
100   CONTINUE
      IF(ERR GT 1.E-3) THEN
      WRITE(*,*) 'No convergence !'
      END IF
200   CONTINUE
      G1 = 2.*BR1*SUMg1/YDIM
      G2 = 2.*BR2*SUMg2/YDIM
      RETURN
      END
C=
C============SUBROUTINE FINDTT===========
C     Solve for V-problem for double interfaces
C---------------------------------
      SUBROUTINE FINDTT(NY,TMK,HFGCP,S01,S02,S1,S2,TI,YI)
      DIMENSION TI(1),YI(1)
      COMMON /ALL/XDIM,YDIM,DX,DY,DT,CK,CP,RHO,ALPHA,HFG
      COMMON /SS/TS11,TS12,TS21,TS22
      REWIND (40)
      YPRE1 = S1
      SS1   = S01
      YPRE2 = S2
      SS2   = S02
      DO 400 J=1,NY
      YLOC = YI(J)
      CALL GREFT2(YLOC,SS1,ss2,YPRE1,ypre2,GINT1,gint2)
      T2    = HFGCP*(gint1-gint2)
      write(40,10) yloc,tI(j)-tmk,t2,t2+TI(j)-tmk
      TI(J) = TI(J) + T2
400   CONTINUE
10    FORMAT(4F14.4)
      RETURN
      END
C=========================          END OF PROGRAM          ===============C
```

REFERENCES

Alexiades, V, and Solomon, A. D., 1993, Mathematical Modeling of Melting and Freezing Processes, Hemisphere Publishing Corporation, Washington, DC.

Allen, D. N. de G., and Severn, R. T., 1962, "The application of relaxation methods to the solution of non-elliptic partial differential equations, iii Heat conduction, with change of state, in two dimensions," *Quart J. Mech Appl Math*, Vol 15, pp. 53-92.

Anderson, D. A., Tannehill, J. C., and Fletcher, R. H., 1984, Computational Fluid Mechanics and Heat Transfer, Hemisphere Publishing Corporation, Washington, DC.

Barozzi, G. S., and Pagliarini, G., 1985, "A method to solve conjugate heat transfer problems: The case of fully developed laminar flow in a pipe," *Trans ASME, J Heat Transfer*, Vol 107, pp. 77-83.

Base, B., and Bate, W. A., 1990, "Numerical study of steady state and transient laser melting problems--i. Characteristics of flow field and heat transfer," *Int J Heat Mass Transfer*, Vol 33, pp. 1149-1163.

Bell, G. E., 1978, "A refinement of the heat balance integral method applied to a melting problem," *Int J. Heat Mass Transfer*, Vol 21, pp. 1357-1362.

Bell, G. E., 1979, "Solidification of a liquid about a cylindrical pipe," *Int J Heat Mass Transfer*, Vol 22, pp. 1681-1686.

Boley, B. A., 1974, "The embedding technique in melting and solidification problems," Moving Boundary Problems in Heat Flow and Diffusion, *Proc. Conf. Univ. Oxford*, March 25-27, pp. 150-172.

Bonnerot, R., and Jamet, P., 1974, "A second order finite element method for one-dimensional Stefan problem," *Int J Numer Meth Engrg.*, Vol 8, pp. 811-820.

Boucheron, E. A., and Smith, R. N., 1986, "An enthalpy formulation of the simple algorithm for phase change heat transfer problems," *ASME/AIChE Natl. Heat Transfer Conf.*, 23rd, Denver, August 4-7, 85-HT-7.

Budhia, H, and Kreith, F , 1973, "Heat transfer with melting and freezing in a wedge," *Int. J Heat Mass Transfer*, Vol 16, pp 195-211

Carslaw, H S , and Jaeger, J C , 1959, Conduction of Heat in Solids, Oxford Universelty Press, Oxford, U K

Choi, C Y , 1981, "Exact and numerical solution of one- and two-phase melting and solidification problems impased with constant or time-varlant temperature and flux conditions," Ph D Dissertation, Universelty of Florida

Choi, C Y., and Walch, C K , 1982, "Solution of Stefan problems imposed with cyclic temperature and flux boundary conditions," *Int J Heat Mass Transfer*, Vol 25, pp 1191-1195

Chou, F C Liaw, W Y., and Liu, S R., 1992, "Analysis and experiment of non-Darcian convection in horizontal square packed-sphere channels - I Forced convection," *Int J Heat Mass Transfer*, Vol 35, pp 195-205

Chuang, Y K , and Szekely, J , 1971, "On the use of Green's functions for solving melting or solidification problems," *Int J Heat Mass Transfer*, Vol 14, pp 1285-1294

Crank, J , 1981, "How to deal with moving boundaries in thermal problems," Numerical Method in Heat Transfer, Lewis, R W , Morgan, K., and Zienkiewicz (eds), Wiley, New York, pp 177-200

Crank, J , 1984, "Free and Moving Boundary Problems," Clarendon Press, Oxford

Dudm, J L., and Vrentas, J S , 1999, "Perturbation solutions of diffusion-controlled moving boundary problems," *Chem Eng Sci*, Vol 24, pp 461-470

Furoumkaya, Z , and Neir, S , 1990, "A moving boundary problem in a finite domain," *J Appl Mech*, Vol 57, pp 50-59

Elliot, C M and Ockendon, J R , 1982, Weak and Variational Methods for Moving Boundary Problems, Research Notes in Mathematics 59, Pitman Advanced Publishing Progrm, Boston

Furzeland, R M, 1980, "A comparative study of numerical methods for moving boundary problems", *J Inst Math Appl*, Vol 26, pp 411-429

Gmelinski, V ,1978,"New equations for heat and mass transfer in turbulent pips and channel flow," *Int. Chem Eng*, Vol 19, pp 359-370

Goodman, T R , 1958, "The heat-balance integral and its applications to problems involving a change of phase," *ASME J Heat Transfer*, Vol 80, pp 335-341

Goodman, T. R., 1964, "Application of integral methods to transient nonlinear heat transfer," *Adv. Heat Transfer*, Vol. 1, pp. 71-79.

Goodman, T. R., and Shea, J. J., 1960, "The melting of finite slabs," *ASME J. Appl. Mech.*, Vol. 27, pp. 16-24.

Goodrich, L. E., 1978, "Efficient numerical technique for one-dimensional thermal problems with phase change," *Int. J. Heat Mass Transfer*, Vol. 21, pp. 615-621.

Gupta, R. S., and Kumar, D., 1980, "A modified variable time step method for one-dimensional Stefan problem", *Comp. Meth. Appl. Mech. Eng.*, Vol. 23, pp. 101-109.

Gupta, D. S., and Kumar, D., 1981, "Variable time step methods for one-dimensional Stefan problem with mixed boundary condition," *Int. J. Heat Mass Transfer* Vol. 24, pp. 251-259.

Hantasglu, N. A., 1986, "A numerical solution to moving boundary problem - Application to melting and solidification," *Int. J. Heat Mass Transfer*, Vol. 29, pp. 485-493.

Hantasglu, N. A., and Banh, C. A., 1961 "Desublimation: A moving boundary problem and numerical solution," *Num. Heat Transfer, Part A*, Vol. 19, pp. 219-230.

Hill, J. M., 1987, One-dimensional Stefan Problems: An Introduction, Longman Scientific and Technical, Essex, England

Hong, C. P., Ueda, T., and Kimura, Y., 1984, "Numerical methods for casting solidification: Part 1, the coupling of the boundary element and finite difference methods for solidification problems," *Metallurgical Transaction B*, Vol. 15B, pp. 91-99

Holch, C. K., 1993, "Unification of source-and-sink method and boundary element for the solution of potential problems," *J. Heat Transfer*, in press

Huang, C. K., Chen, C. Y., 1992a, "Solution of one- and two-phase melting and solidification problems imposed with constant or time-variant temperature and flux boundary conditions," *J. Heat Transfer*, Vol. 114, pp. 524-528.

Huleb, C. K., Chel, C. Y., 1992b, "A general analysis of phase change energy storage for solar energy applications," *J. Solar Energy Eng.*, Vol. 114, pp. 203-209

Huleb, C. K., Chel, C. Y., and Kassab, A. J., 1992, "Solution of Stefan problems by a boundary element method," Boundary Element Technology VII, C. A. Brebbia and M. S. Ingber, eds., Computational Mechanics Publications, Southampton, UK, pp. 473-490.

Seu, C. F., Sparrow, E. M., and Patankar, S. V., 1981, "Numerical solution of moving boundary problems by boundary immobilization and a control-volume-based fleite-difference scheme," *Int J Heat Mass Transfer*, Vol. 24, pp 1335-1345

Kays, W. M., and Crawford, M. E., 1980, Convective Heat and Mass Transfer, McGraw-Hill Publishing Company, New York

Kolodner, I. I., 1956, "Free boundary problems for heat equations with application to problems of change phase," *Comm. Pure Applied Mathematics*, Vol. 9, pp. 1-31

Lacroix, M., and Voller, V. R., 1990, 'Finite different solutions of solidification phase change problems: Transformed versus fixed grids," *Numerical Heat Transfer*, B, Vol 17, pp 25-41

Lane, A. Charge, 1986, "Solar Heat Storage: Latent Heat Materials," Vol 11: Technology, CRC press, Boca Raton, Florida

Langford, D., 1973, "The heat balance integral method," *Int J Heat Mass Transfer*, Vol. 16, pp. 2424-2428

Liang, S. J., 1983, "A study of free and moving boundary problems involving thin crystal growth," Ph D. Dissertation, Univ. of Florida

Lightfoot, N. S. H., 1929,"The solidification of molten steel," *Proc. London Math. Soc.*, Vol 31, pp 97-116

Murray, W. D., and Landis, F., 1959, "Numerical and machine solution of transient heat-conduction problems involving melting and freezing, Part 1-Method of analysis and sample solutions," *J Heat Transfer*, Vol. 81, pp 106-112

Noble, B., 1975, "Heat balance method in melting problems," Moving boundary problems in heat flow and diffusion, Ockendon, J. R., and Hodgkins, W. R. eds., Clarendon Press, Oxford, pp 208-209

Nyrna, J. G., and Reich, C. K., 1983, "Combination of source-and sink method and complex-temperature method for the solution of Stefan problems imposed with cyclic temperature and flux conditions," Submitted to *J. Heat Transfer*

Oberkampf, W. L., 1978, "Domain mapping for the numerical solution of partial differential equations," *Int J. Numer Meth Engng.*, Vol 10, pp 211-223

Ockendon, J. R., 1974,"Moving boundary problems in heat flow and diffusion," *Proc. Conf Univ. Oxford*, March 25-27

O'Neill, K., 1983, "Boundary integral equation solution of moving boundary phase change problems," *Int J Numer. Meth. Engng.*, Vol 19, pp 1825-1850

Patel, P D., 1968,"Interface condition in heat conduction problems with change of phase," *AIAA J.*, Vol 8, pp 2454-2458

Phan, Q. T., 1985, "A fast, unconditionally stable finite difference scheme for heat conduction with phase change," *Int J Heat Mass Transfer*, Vol 28, pp 2079-2084

Phan, Q. T., 1986, "The use of lumped capacitance in the finite-element solution of heat condition with phase change," *Int. J Heat Mass Transfer*, Vol 29, pp 285-291

Poots, G., 1962,"An approximate treatment of heat conduction problem involving a two-dimensional solidification front," *Int J Heat Mass Transfer*, Vol 5, pp 335-348

Rathjen, K A., and Jiji, L M., 1971, "Heat conduction with melting or freezing in a corner," *J Heat Transfer*, Vol 93, pp 101-109

Riaz, M 1978,"Transient analysis of packed bed thermal storage systems," *Solar Energy*, Vol 21, pp 123-128

Rubinstein, L I., 1971, "The Stefan problem," *Am Math Soc Trans. Math Monogr* No. 27.

Saltoh, T., 1978, "Numerical method for multidimensional freezing problems in arbitrary domains," *J Heat Transfer*, Vol 100, pp 294-299.

Sadegh, A. M., Jiji, L. M., and Weinbaum, S., 1987,"Boundary integral equation technique with application to freezing around a buried pipe," *Int. J Heat Mass Transfer*, Vol 30, pp 223-232

Sarler, B., Alujevic, A., and Kuhn, G., 1991,"Solution of multidimensional Stefan problem by BEM," *Zeitschrift fur Angewandte Mathematik und Mechanik*, Vol 71, pp 811-814

Schumann, T. E. W., 1929,"Heat transfer: a liquid flowing through a porous prism," *J Franklin Inst.*, Vol 208, pp 405-416

Shyy, W., Faung, Y., Hunter, C. B., Wei, D. Y., and Chen, M. H., 1992, "Modelling of turbulent transport during continuous ingot casting," *Int J Heat Mass Transfer*, Vol 35, pp 1229-1240

Sikarskie, D. L., and Boley, B. A., 1965 "The solution of a class of two-dimensional melting and solidification problems," *Int J Solid Struct*, Vol 1, pp 207-234

Solomon, A. D., 1978, "The application and extendability of the Megerlin's method for solving parabolic free boundary problems," Moving Boundary Problems Wilson D G, Solomon, A D, and Boggs P T, eds., Academic Press, New York, pp 187-202

Tamma, K. K, and Namburu, R. R., 1990,"Recent advance, trends and new perspectives via enthalpy-based finite element formulations for applications to solidification problems," *Int J Numer Meth. Engng*, Vol. 30, pp. 803-820

Tao, L. N., 1978, "The Stefan problem with arbitrary initial and boundary conditions," *Quart. Appl. Math.*, Vol 36, pp 223-233

Tao, L. N., 1980, "The analyticity of solutions of the Stefan problem," *Arch Rational Mech Anal.*, Vol. 72, pp. 1-10

Tao, L. N., 1981,"The exact solution of some Stefan problems with prescribed heat flux," *ASME J. Appl Mech.*, Vol. 48, pp. 732-736.

Veller, V., and Crose, M., 1983, "An explicit numerical method to track a moving phase change front," *Int. J Heat Mass Transfer*, Vol 26, pp. 147-150.

Weinbaum, S., and Jiji, L. M., 1977,"Singular perturbation theory for melting or freezing in a finite domain initially not at the fusion temperature," *ASME J Appl Mech.*, Vol. 44, pp. 25-30.

Wilson, D. G., Solomon, A. D., and Boggs, P. T. (eds.), 1978, Moving Boundary Problems, Academic Press, New York

Yao, L. S., and Prusa, J., 1989, "Melting and freezing," *Adv. Heat Transfer*, Vol 20, pp. 135-143.

Yoon, W. W., 1981, "Application of the heat balance integral to melting problems with initial subcooling," *Int J Heat Mass Transfer*, Vol 23, pp. 1157-1160

Zabaras, N., and Mukherjee, S., 1987,"An analysis of solidification problem by the boundary element method," *Int. J. Numer Meth Engng.*, Vol 24, pp. 1879-1900

BIOGRAPHICAL SKETCH

Hongjoo Li was born in Beijing, China, on September 15, 1961, one hundred thirty years after the phase-change problems were first studied. He received his B.S. degree in 1982 and M.S. degree in 1985 in Aerospace Engineering from Northwestern Polytechnical University, Xian, China. He finished his Ph.D. requirements in 1988 and was assigned to fulfill an international cooperation plan in W. Germany before he could make the final step--oral defense--to get the cap.

After completing the cooperation contract, he forfeited his Ph.D. degree in China and came to the United States in 1989, where he began his new education career starting from pre-elementary education, English, in the University of Florida.

When he was 30-year old, he received his second M.S. degree in Mechanical Engineering from the University of Florida. In the same year, he had a lovely daughter Angela Y. Li. Then he was admitted to Ph.D. candidacy in 1992. H. Li married Ye Lue in 1986 in Xian, China.

I certify that I have read this study and that in my opinion it conforms to acceptable standards of scholarly presentation and is fully adequate, in scope and quality, as a dissertation for the degree of Doctor of Philosophy

Chung K. Hsieh, Chairman
Professor of Mechanical Engineering

I certify that I have read this study and that in my opinion it conforms to acceptable standards of scholarly presentation and is fully adequate, in scope and quality, as a dissertation for the degree of Doctor of Philosophy

Yogi D. Goswami, Cochairman
Professor of Mechanical Engineering

I certify that I have read this study and that in my opinion it conforms to acceptable standards of scholarly presentation and is fully adequate, in scope and quality, as a dissertation for the degree of Doctor of Philosophy

Wei Shyy
Professor of Aerospace Engineering, Mechanics and Engineering Science

I certify that I have read this study and that in my opinion it conforms to acceptable standards of scholarly presentation and is fully adequate, in scope and quality, as a dissertation for the degree of Doctor of Philosophy

James F. Klausner
Assistant Professor of Mechanical Engineering

I certify that I have read this study and that in my opinion it conforms to acceptable standards of scholarly presentation and is fully adequate, in scope and quality, as a dissertation for the degree of Doctor of Philosophy

Renwei Mei
Assistant Professor of Aerospace Engineering, Mechanics and Engineering Science

This dissertation was submitted to the Graduate Faculty of the College of Engineering and to the Graduate School and was accepted as partial fulfillment of the requirements for the degree of Doctor of Philosophy.

December 1993

Wilfred M. Phillips
Dean, College of Engineering

Karen A. Holbrook
Dean, Graduate School